Lotka-Volterra Predator-Prey Models

Analytic and Numerical Methods

by

Paul W. Draper

A thesis submitted in partial fulfillment
of the requirements for the degree of
Master of Science (M.Sc.) in Computational Sciences

The Faculty of Graduate Studies
Laurentian University
Sudbury, Ontario, Canada

THESIS DEFENCE COMMITTEE/COMITÉ DE SOUTENANCE DE THÈSE
Laurentian Université/Université Laurentienne
Faculty of Graduate Studies/Faculté des études supérieures

Title of Thesis Titre de la thèse	Lotka-Volterra Predator-Prey Models Analytic and Numerical Methods	
Name of Candidate Nom du candidat	Draper, Paul	
Degree Diplôme	Master of Science	
Department/Program Département/Programme	Computational Sciences	Date of Defence Date de la soutenance May 15, 2017

APPROVED/APPROUVÉ

Thesis Examiners/Examinateurs de thèse:

Dr. Hafida Boudjellaba
(Co-supervisor/Co-directeur(trice) de thèse)

Dr. Youssou Gningue
(Co-supervisor/Co-directeur(trice) de thèse)

Dr. Stephanie Czapor
(Committee member/Membre du comité)

Approved for the Faculty of Graduate Studies
Approuvé pour la Faculté des études supérieures
Dr. David Lesbarrères
Monsieur David Lesbarrères
Dean, Faculty of Graduate Studies
Doyen, Faculté des études supérieures

Dr. Tewfik Sari
(External Examiner/Examinateur externe)

ACCESSIBILITY CLAUSE AND PERMISSION TO USE

Abstract

The Lotka-Volterra equations are a classical model of the populations of interacting species. In the case of two interacting species, we present a closed parametric solution to a particular case of the Lotka-Volterra model. We also determine closed expressions for the branch points, bounds on the parameter, amplitude of the oscillation of the prey and predator populations, and period of this model in terms of the Lambert W function. In the case of three interacting species, under certain conditions solutions are again periodic. However, standard numerical methods often fail to preserve this periodicity, as well as other important properties of the model. The underlying geometry of the three-species predator-prey model is developed through the framework of Poisson dynamics. It is shown that the system is bi-Poisson and possesses two independent first integrals. Numerical methods for approximating solutions to the model are constructed which incorporate the underlying Poisson geometry of the continuous system. These methods preserve the periodicity of solutions, and the error in the first integrals remains bounded. Simulations are used to show that these methods produce more accurate results than standard numerical methods which do not consider the Poisson structure of the equations.

Keywords: Lotka-Volterra Model, Lambert W Function, Geometric Numerical Integration, Poisson System, Non-Standard Finite Differences, Integrable System.

Acknowledgements

First and foremost, I would like to express my sincere gratitude to my supervisor, Dr. Hafida Boudjellaba. It would be difficult to overstate the impact you've had not only on this work, but on my time at Laurentian. For your excellent advice, encouragement, ideas, and guidance, I will always be thankful.

I would also like to thank my co-supervisor, Dr. Youssou Gningue. Your insights and questions always proved to be interesting and helped extend this work in ways I could not have accomplished alone.

I am also indebted to Dr. Patrice Sawyer for his excellent review of and advice on the first part of this thesis, as well as Dr. Stephanie Czapor for her thoughtful inquiry and timely review of this project.

To Dr. Ralf Meyer, thank you for resolving some last-minute technical concerns.

I would also like to acknowledge Laurentian University as well as the Natural Sciences and Engineering Research Council of Canada for their financial support.

To my parents, your unwavering support will always be with me.

To Debbie, the last four and a half years since I've met you have been incredible. Thank you for always believing in me. For whatever comes next, I'm always excited knowing I get to share it with you.

Paul Draper,

April, 2017.

Contents

List of Figures

Chapter 1

Introduction

The Lotka-Volterra system is the most fundamental model of the population dynamics of species in a predator-prey relationship. As such, it has been studied extensively, and much is known about its properties. Nonetheless, there is still much to be discovered. In particular, despite the apparent simplicity of the equations, it appears difficult to determine analytical expressions for their solution.

In the first part of the thesis, we give an alternative derivation of an analytical formula for the solutions of the model originally developed in [5] in the case when two of its parameters are equal. Under this hypothesis, the equations permit a symmetry which can be exploited to derive a solution using only elementary techniques. We use this solution to obtain more information regarding the properties of the model. For instance, the Lotka-Volterra equations are periodic, and we obtain a closed integral formula for the period of the model. We also determine closed expressions for the branch points of the model, where each population reaches a maximum and a minimum. This gives the amplitude of each species - how widely the population numbers

vary across time. Finally, since the solutions derived are parametric, we obtain the appropriate bounds on this parameter. It will be shown that each of these values can be expressed in terms of the Lambert W function, which cannot be expressed in terms of elementary functions [12].

In its original formulation, the Lotka-Volterra predator-prey system models two interacting species. However, the equations can be naturally generalized to model three or more species. Though the three-species model is much less studied than its two-species counterpart, some of its dynamical properties have been investigated [11]. Notably, under certain hypotheses, the solutions are again periodic.

The second part of this thesis is concerned with the three-species predator-prey model. However, our approach to obtaining solutions to this model will be numerical as opposed to analytic. The main difficulty in applying numerical methods to systems with periodic solutions such as the Lotka-Volterra system is that the methods often do not preserve this periodicity. Instead, the solutions appear to spiral. Typically these methods also fail to preserve a number of other properties of the system. Yet, some numerical methods do produce qualitatively accurate simulations of solutions. In the two-species model, the problem of distinguishing methods that produce accurate solutions from those that do not has been adequately solved. Essentially, effective numerical methods must preserve the underlying geometry of the continuous system. The process of constructing numerical methods which possess a similar geometry to the continuous model has been applied to many other problems, and is a well-developed

field of study called Geometric Numerical Integration. However, in contrast to the two-species case, there is very little research on the geometric numerical integration of the three-species model. In the second part of this thesis, we are concerned with understanding the geometry of this model and constructing a class of geometric numerical integrators which produce accurate simulations of its solutions.

We begin Part I with the second chapter where we introduce the two-species Lotka-Volterra predator-prey model, as well as some other preliminary material required later.

In the third chapter, we review the literature on the analysis of the solutions and period of the two-species model, and state clearly the research problem for the first part of this thesis.

The fourth chapter contains the main results of Part I. This includes the derivation of the closed parametric solution and expressions for the branch points, bounds on the parameter, and the period. We apply these formulas to a concrete example to illustrate their efficacy.

The second part of this thesis begins in the fifth chapter, where we introduce some basic properties of numerical methods. We also introduce Hamiltonian and Poisson systems, as well as their properties, as they are used to formalize the geometry of the three-species model.

In chapter six, we review the literature on the geometric numerical integration of the two-species model and introduce the three-species predator-prey model before

clearly stating the research problem for Part II.

The seventh chapter contains the results of Part II. We begin with a development of the geometry of the three-species system through the framework of Poisson systems. Then, a class of geometric numerical integration methods is proposed which are shown to preserve several key properties of the continuous model.

The eighth and final chapter concludes the thesis with a discussion of some of the limitations of the current work as well as directions for future research.

Part I

Parametric Solution of a Predator-Prey Model

Chapter 2

Preliminaries

2.1 Introduction

The Lotka-Volterra system is a well-known elementary model of the population dynamics of two species, one predator and one prey. The model is a pair of two nonlinear differential equations

$$\begin{cases} \dfrac{dx}{dt} = ax - \alpha xy, & x(0) = x_0 \\ \dfrac{dy}{dt} = -cy + \gamma xy, & y(0) = y_0. \end{cases} \tag{2.1.1}$$

Here, x and y represent the population numbers of the prey and predator, respectively, and $x(t) \geq 0$ and $y(t) \geq 0$ for all $t \geq 0$. The parameter a is the growth rate of the prey and c is the death rate of the predator. All parameters are positive [31]. These equations were originally formulated by Alfred Lotka through the study of the dynamics of organic systems [26] and chemical reactions [27] as well as Vito Volterra in the study of fish populations in the Adriatic Sea [41].

We see from the first equation that in the absence of the predator (when $y = 0$) we have $dx/dt = ax$, meaning that the prey grows at a rate proportional to the current population. Similarly, from the second equation we see that in the absence of a prey

food source, the predator dies out at a rate proportional to the current population. The two interaction factors αxy and γxy represent the effect of consumption of prey by a predator. The factors state that the number of encounters between predator and prey is proportional to the product of the populations. These interactions decrease the prey population, as prey are consumed, and increase the predator population.

The Lotka-Volterra system is a simplistic predator-prey model, though it is still highly useful as it captures many dynamics of species interactions and can be extended in many ways to develop more sophisticated models. These models typically derive from attempts to fix assumptions made by the Lotka-Volterra equations which are sometimes unrealistic [31], such unbounded prey growth in absence of the predator, an unlimited food supply for the prey, and that the predators survival depends only on the prey species. One such example is the model of Gause [19] discussed in [17]:

$$\begin{cases} \dfrac{dx}{dt} = xg(x) - p(x)y \\ \dfrac{dy}{dt} = -cy + p(x)y. \end{cases}$$

Here, c is the death rate of the predator. In the absence of the predator, term $g(x)$ incorporates growth of the prey which is dependent upon the density of the prey population, so that this growth need not be unbounded as in the Lotka-Volterra model. The term $p(x)$, called the functional response, is the intake rate of the predator as a function of prey density. Many forms for the functional response have been proposed and are reviewed in [40].

Predator-prey systems have also been extended to model interactions between three

or more species and the effects of human harvesting of species. For example, Clark [13] considered the model of harvesting two ecologically independent populations

$$\begin{cases} \dfrac{dx}{dt} = rx\left(1 - \dfrac{x}{k}\right) - q_1 Ex \\ \dfrac{dy}{dt} = sy\left(1 - \dfrac{y}{L}\right) - q_2 Ey \\ \dfrac{dE}{dt} = \epsilon\left(p_1 q_1 x + p_2 q_2 y - c\right) E, \end{cases}$$

which was shown by Boudjellaba and Sari [9] to exhibit a delayed loss of stability. While the dynamic and qualitative behavior of these models has been studied extensively, it appears to be very difficult to obtain explicit solutions to the systems. In the next section, we review the basic dynamics of the Lotka-Volterra model.

2.2 The Lotka-Volterra Predator-Prey Model

As mentioned above, it is a difficult task to find analytical solutions to predator-prey models, and the Lotka-Volterra system is no exception to this rule. However, we can still gain an understanding of the behavior of its solutions. To begin, note that from (2.1.1) we have

$$\frac{dy}{dx} = \frac{dy/dt}{dx/dt} = \frac{y(-c + \gamma x)}{x(a - \alpha y)}.$$

This is a separable differential equation which can be solved to give

$$a \ln y - \alpha y + c \ln x - \gamma x = C, \tag{2.2.1}$$

a family of implicit curves describing the behavior of the solutions. It can be shown [4] that these trajectories are closed in the positive quadrant of the xy-plane, meaning

that the solutions are periodic. Some trajectories of the Lotka-Volterra model are shown below.

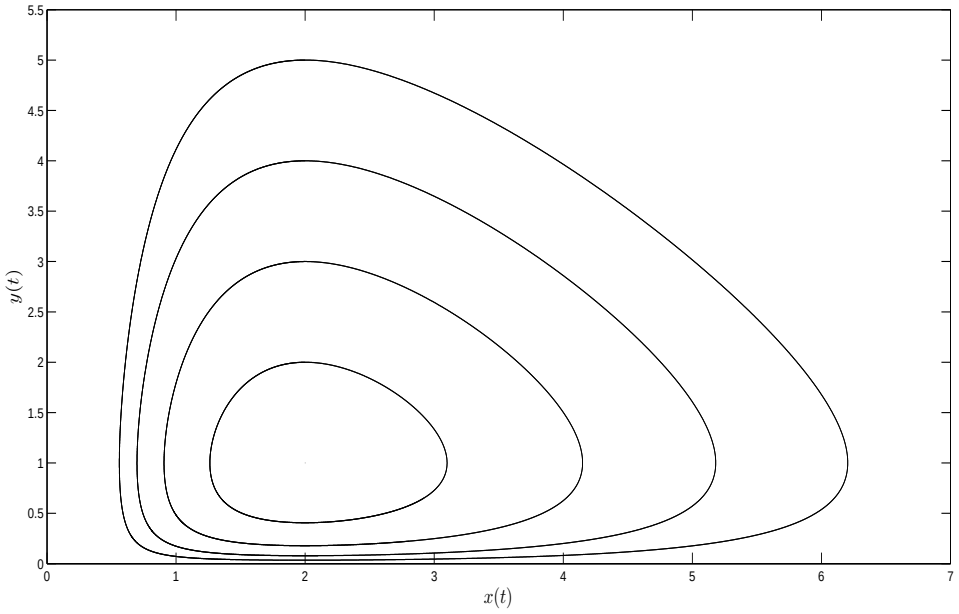

Figure 2.1: Trajectories of the Lotka-Volterra predator-prey model. $(x_0, y_0) = (2, y_0)$, where $y_0 = 2$, 3, 4, 5.

We can also study the stability of the critical points of the system, that is, solutions of

$$x(a - \alpha y) = 0, \qquad y(-c + \gamma x) = 0.$$

This gives the two critical points:

$$(0, 0) \quad \text{and} \quad \left(\frac{c}{\gamma}, \frac{a}{\alpha}\right). \tag{2.2.2}$$

We first calculate the Jacobian of (2.1.1):

$$\mathbf{J} = \begin{pmatrix} a - \alpha y & -\alpha x \\ \gamma y & -c + \gamma x \end{pmatrix}. \tag{2.2.3}$$

Evaluating the Jacobian of the system at the critical point $(0,0)$, we have

$$\mathbf{J}(0,0) = \begin{pmatrix} a & 0 \\ 0 & -c \end{pmatrix},$$

which has eigenvalues $a > 0$ and $-c < 0$. As a consequence, the origin is an unstable saddle point, repelling along the x-axis and attracting along the y-axis. An implication of this result is that extinction of the predator and prey populations can be considered highly unlikely.

Evaluating the Jacobian of the system at the critical point $(\frac{c}{\gamma}, \frac{a}{\alpha})$, we have

$$\mathbf{J}\left(\frac{c}{\gamma}, \frac{a}{\alpha}\right) = \begin{pmatrix} 0 & -\frac{\alpha}{\gamma}c \\ \frac{\gamma}{\alpha}a & 0 \end{pmatrix},$$

which has eigenvalues $\pm i\sqrt{ac}$. Hence, this equilibrium is a stable center for the linearized system. Since the trajectories (2.2.1) are closed curves in the x, y-plane, the equilibrium is a center for the nonlinear system (2.1.1) as well.

2.3 The Lambert W Function

A number of the results of this thesis require the use of the Lambert W function, which we briefly introduce in this section.

The function $W(x)$ which satisfies

$$x = W(x)e^{W(x)}, \quad x \geq -\frac{1}{e} \tag{2.3.1}$$

is called the Lambert W function. That is, the Lambert W function is the inverse function of $f(x) = xe^x$. The function is composed of two branches: $W_0(x)$ with domain

$D_0 = \left[-\frac{1}{e}, \infty\right)$ and range $R_0 = [-1, \infty)$, and $W_{-1}(x)$ with domain $D_{-1} = \left(-\frac{1}{e}, 0\right)$ and range $R_{-1} = (-\infty, -1)$. Note that for all $x \in D_{-1}$, we have

$$W_{-1}(x) < W_0(x). \tag{2.3.2}$$

For more information on the Lambert W function, refer to [14].

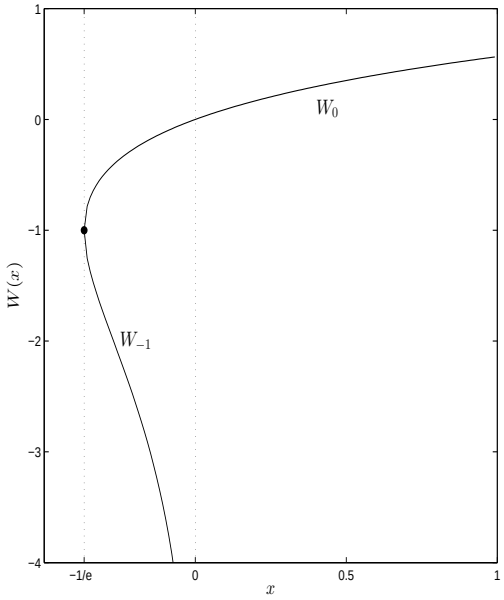

Figure 2.2: Main branches of the Lambert W function.

Chapter 3

Analytical Methods Applied to the Lotka-Volterra Model

In this chapter, we review the existing literature on two topics on the analysis of the Lotka-Volterra model. First, we discuss results on explicit solutions to the system (2.1.1). Second, we examine research into analytic expressions for the period of the Lotka-Volterra system.

3.1 Solutions to the Model

While the qualitative behavior of the solutions of system (2.1.1) was relatively easy to obtain, finding any formal explicit expression for these solutions appears to be a difficult problem, despite the apparent simplicity of the equations. For the related competitive Lotka-Volterra equations, Abdelkader [1] has given exact solutions when some of the parameters are interrelated. For the case of the basic Lotka-Volterra predator-prey model (2.1.1), normalized so that $a = \alpha = c = \gamma = 1$, Arrigoni and Steiner [5] gave a parametric solution to the model. By a parametric solution, we mean a set of points $(x(u), y(u))$ whose image is identical to $(x(t), y(t))$ in the x, y-plane.

Arrigoni and Steiner give the expressions

$$\begin{cases} x(u) = \frac{1}{2}\left(u \pm \sqrt{u^2 + 4Ke^u}\right) \\ y(u) = \frac{1}{2}\left(u \mp \sqrt{u^2 + 4Ke^u}\right), \end{cases} \tag{3.1.1}$$

where

$$K = -x_0 y_0 e^{-(x_0+y_0)} \tag{3.1.2}$$

and

$$u = x(t) + y(t). \tag{3.1.3}$$

The solution was obtained by converting the original system to a single differential equation through a series of algebraic transformations. This single equation could be solved, and using the transformations, expressions for $x(u)$ and $y(u)$ were recovered. Through a suitable change of variables [31], this normalized case is equivalent to the hypothesis that $a = c$.

3.2 The Period of the Model

The study of the period of (2.1.1) is as old as the study of the Lotka-Volterra model itself. Volterra [41] gave the first expression for the period as the sum of four absolutely convergent integrals over segments of a closed orbit. Since Volterra's original work, a number of other integral representations for the period have been developed using a variety of techniques. Hsu [22] nondimensionalizes the model, and then uses a transformed set of differential equations to arrive at the following theorem:

Theorem 3.2.1 *The period of the periodic solution for the system*

$$u'(t) = u(t)[a - v(t)]; \qquad v'(t) = v(t)[u(t) - 1]$$

subject to $u(0) = u_0 > 0$ *and* $v(0) = v_0 > 0$ *is represented as*

$$T = \int_{\log(u_*)}^{\log(u^*)} \left\{ \frac{1}{F_1^{-1}(G(z))} - \frac{1}{F_2^{-1}(G(z))} \right\} dz,$$

where u_*, u^* *are two roots of* $u - 1 - \log(u) = C_0$ *satisfying* $u_* < u^*$, $C_0 = u_0 - 1 - \log(u_0) + v_0 - a - a\log(v_0/a)$, $G(z) = \exp(z) - z - 1 - C_0$, *and* $F_2(w)$, $F_1(w)$ *are the restrictions of* $F(w) = w + a\log(1 - w/a)$ *on* $(-\infty, 0]$, $[0, a)$, *respectively.*

Other authors have first transformed the Lotka-Volterra model into a Hamiltonian system $x'(t) = \partial H/\partial y$, $y'(t) = -\partial H/\partial x$. Waldvogel [42, 43] introduces several functions and coordinates to represent the period as an integral over the period of a periodic continuously differentiable function. In contrast, Rothe [36] invokes the theory of thermodynamics and defines the state sum of the Hamiltonian system

$$Z(\beta) = \int_{-\infty}^{\infty} \int_{-\infty}^{\infty} \exp[-\beta H(x, y)] dx dy$$

for the inverse absolute temperature $\beta \in (0, \infty)$. Using this state sum, the period of the Lotka-Volterra model can be written as a convolution integral.

Using only elementary techniques, another integral representation for the period was given by Shih [39] which depends on the initial conditions and energy of the Hamiltonian. Despite the variety of integrals and methods used to arrive at them, Shih also demonstrated the equivalence of each of these integrals.

3.3 Research Problem

The goals of this part of the thesis are two-fold. The first is to present an explicit parametric solution to the Lotka-Volterra system in the case when the growth rate of the prey equals the death rate of the predator. That is, we derive a parametric solution to the system

$$\begin{cases} \dfrac{dx}{dt} = ax - \alpha xy, & x(0) = x_0 \\ \dfrac{dy}{dt} = -ay + \gamma xy, & y(0) = y_0 \end{cases} \tag{3.3.1}$$

for the nontrivial case when neither species is extinct so that $x(t) > 0$ and $y(t) > 0$ for all $t \geq 0$. Our new method is elementary, requiring nothing more sophisticated than basic algebra and calculus, hence, we give an alternative derivation of the result of Arrigoni and Steiner in [5]. The second is to determine closed expressions for the branch points of the phase curves, bounds on the parameter, amplitude of the oscillation of the prey and predator populations, and the period of the predator-prey system (3.1.1) in terms of the Lambert W function.

Chapter 4

A Closed Parametric Solution to a Class of Lotka-Volterra Models

In this chapter, we give the main results of Part I of this thesis, beginning with an elementary derivation of a parametric solution to the Lotka-Volterra system under the condition $a = c$. Using this solution, we obtain the branch points, parameter bounds, population amplitudes, and period in terms of the Lambert W function. The expressions will be illustrated with numerical examples.

4.1 Results

4.1.1 Parametric Solution of a Predator-Prey System

The first result gives a closed parametric solution in the xy-phase plane to the system (3.3.1). Recall that by a parametric solution, we mean a set of points $(x(v), y(v))$ whose image is identical to $(x(t), y(t))$ in the xy-phase plane.

Theorem 4.1.1 *A parametric solution in the xy-phase plane of the predator-prey*

system (3.3.1) is given by

$$\begin{cases} x(v) = \dfrac{a}{2\gamma}\left((av) \pm \sqrt{(av)^2 + 4Ke^{av}}\right) \\ y(v) = \dfrac{a}{2\alpha}\left((av) \mp \sqrt{(av)^2 + 4Ke^{av}}\right) \end{cases} \tag{4.1.1}$$

where

$$K = -\frac{\alpha\gamma}{a^2}x_0y_0 \exp\left(-\frac{1}{a}(\gamma x_0 + \alpha y_0)\right). \tag{4.1.2}$$

Proof:

Beginning with the well-known change of variables [31],

$$X(T) = \frac{\gamma}{a}x(t); \quad Y(T) = \frac{\alpha}{a}y(t); \quad T = at, \tag{4.1.3}$$

system (3.3.1) becomes

$$\begin{cases} \dfrac{dX}{dT} = X(1-Y), & X(0) = \dfrac{\gamma}{a}x_0 \\ \dfrac{dY}{dT} = Y(X-1), & Y(0) = \dfrac{\alpha}{a}y_0. \end{cases} \tag{4.1.4}$$

Note that we have

$$\begin{cases} \dfrac{dX}{dT}Y = XY - XY^2 \\ \dfrac{dY}{dT}X = -XY + X^2Y. \end{cases}$$

Summing these two equations gives

$$\frac{dX}{dT}Y + \frac{dY}{dT}X = X^2Y - XY^2.$$

Since $XY \neq 0$,

$$\frac{1}{XY}\left(\frac{dX}{dT}Y + \frac{dY}{dT}X\right) = X - Y = \frac{dX}{dT} + \frac{dY}{dT}.$$

This can be written as

$$\frac{1}{XY}\frac{d}{dT}(XY) = \frac{d}{dT}\ln(XY) = \frac{d}{dT}(X+Y).$$

Integrating both sides of this equation with respect to T, we obtain

$$\ln(XY) = X + Y + K_1$$

so that

$$XY = K_2 e^{(X+Y)} = -Ke^{(X+Y)}. \tag{4.1.5}$$

Now, make the substitution $u = X + Y$ so that $-XY - Ke^u = 0$. Adding and subtracting X^2 to this expression, we obtain

$$X^2 - uX - Ke^u = 0,$$

from which the quadratic formula gives

$$X(u) = \frac{1}{2}\left(u \pm \sqrt{u^2 + 4Ke^u}\right).$$

If we instead add and subtract Y^2, we obtain

$$(-Y)^2 - Y^2 - XY - Ke^u = 0.$$

Putting $\widehat{Y} = -Y$, we rewrite this expression as

$$\widehat{Y}^2 + Y\widehat{Y} + X\widehat{Y} - Ke^u = \widehat{Y}^2 + u\widehat{Y} - Ke^u = 0,$$

from which the quadratic formula gives

$$\widehat{Y}(u) = \frac{1}{2}\left(-u \pm \sqrt{u^2 + 4Ke^u}\right)$$

so that

$$Y(u) = \frac{1}{2}\left(u \mp \sqrt{u^2 + 4Ke^u}\right),$$

where from the initial conditions and (4.1.5) we have $K = -X_0Y_0e^{-(X_0+Y_0)}$. Let $v = (1/a)u$. From (4.1.3) we obtain

$$\begin{cases} x(v) = \dfrac{a}{\gamma}X(av) = \dfrac{a}{2\gamma}\left((av) \pm \sqrt{(av)^2 + 4Ke^{av}}\right) \\ y(v) = \dfrac{a}{\alpha}Y(av) = \dfrac{a}{2\alpha}\left((av) \mp \sqrt{(av)^2 + 4Ke^{av}}\right) \end{cases}$$

with

$$K = -X_0Y_0e^{-(X_0+Y_0)} = -\frac{\alpha\gamma}{a^2}x_0y_0\exp\left(-\frac{1}{a}(\gamma x_0 + \alpha y_0)\right)$$

by the initial conditions in (4.1.4). ■

Observe that the solution (4.1.1) obtained above can be written as the union of two curves in the xy-plane. We call them the upper curve U (where $\alpha y \geq \gamma x$) defined by

$$\begin{cases} x_U(v) = \dfrac{a}{2\gamma}\left((av) - \sqrt{(av)^2 + 4Ke^{av}}\right) \\ y_U(v) = \dfrac{a}{2\alpha}\left((av) + \sqrt{(av)^2 + 4Ke^{av}}\right) \end{cases} \tag{4.1.6}$$

and lower curve L (where $\alpha y \leq \gamma x$) defined by

$$\begin{cases} x_L(v) = \dfrac{a}{2\gamma}\left((av) + \sqrt{(av)^2 + 4Ke^{av}}\right) \\ y_L(v) = \dfrac{a}{2\alpha}\left((av) - \sqrt{(av)^2 + 4Ke^{av}}\right) \end{cases} \tag{4.1.7}$$

so that $x(v) = x_U(v) \cup x_L(v)$ and $y(v) = y_U(v) \cup y_L(v)$. Note that when $\alpha = \gamma$, we have

$$x_U(v) = y_L(v) \quad \text{and} \quad x_L(v) = y_U(v) \tag{4.1.8}$$

so that the upper and lower curves are inverses of each other. In general, the upper and lower curves meet along the line $y = (\gamma/\alpha)x$ in the first quadrant of $\mathbb{R}^2$. Note that we recover the expressions (3.1.1) of Arrigoni and Steiner by setting $a = \alpha = \gamma = 1$ in expressions (4.1.1).

There is a natural biological interpretation for the parameter $v = \frac{1}{a}(X+Y) = \frac{1}{a^2}(\alpha y + \gamma x)$. From the first equation of (3.3.1), we have $\frac{dx}{dt} = ax - (\alpha y)\,x$ so that αy represents the rate of decrease of the prey population due to predation. Similarly, from the second equation of (3.3.1), we have $\frac{dy}{dt} = -cy + (\gamma x)\,y$, so that γx represents the rate of growth of the predator population due to predation. The parameter v can therefore be interpreted as a predation factor, since the sum $\alpha y + \gamma x$ represents the net impact of the predators.

In the following sections, we will use the explicit solution derived in Theorem 4.1.1 to obtain closed formulas for the critical points of the phase trajectories of system (3.3.1). Additionally, we derive bounds on v so that (4.1.1) defines a complete trajectory in phase space, as well as closed formulas for several other values including the amplitude of oscillation of the populations and the period of (3.3.1).

4.1.2 Branch Points of the Phase Curves

If we treat y as a function of x, then in the xy-plane the upper and lower curves are multivalued functions. Proposition 4.1.3 gives the location of the branch points of these curves, but we first require the following lemma.

Lemma 4.1.2 *The constant K defined in (4.1.2) satisfies $K \in \left[-\frac{1}{e^2}, 0\right)$.*

Proof:

Since K is always negative, we need only verify that $-\frac{1}{e^2} \leq K$. Using $K = -X_0 Y_0 e^{-(X_0+Y_0)}$

and rearranging, this is equivalent to

$$X_0 Y_0 e^{2-X_0-Y_0} \leq 1.$$

Taking the natural logarithm of both sides and rearranging gives

$$(\ln(X_0) - X_0) + (\ln(Y_0) - Y_0) \leq -2,$$

which holds if

$$\ln(X_0) - X_0 \leq -1 \quad \text{and} \quad \ln(Y_0) - Y_0 \leq -1.$$

But these hold by the inequality [2]

$$\ln(z) \leq z - 1; \quad z \in \mathbb{R}, z > 0$$

since X_0 and Y_0 are strictly positive. ■

We now give the locations of the branch points.

Proposition 4.1.3 *Suppose $y = y(x)$. Let v_U and v_L denote the values of the parameter determining the points at which the upper and lower curves exhibit a branch point, respectively. Then*

$$v_U = \left(\frac{1}{a}\right)(1 - W_0(Ke)) \quad \textit{and} \quad v_L = \left(\frac{1}{a}\right)(1 - W_{-1}(Ke))$$

where W_0 and W_{-1} are the two branches of the Lambert W function.

Proof:

The branch points will occur when $\frac{dx}{dy} = \frac{dx/dv}{dy/dv} = 0$; that is, when $\frac{dx}{dv} = 0$. Since

$$\frac{dx}{dv} = \frac{a}{\gamma}\frac{dX(u)}{dv} = \frac{a}{\gamma}\frac{du}{dv}\frac{dX}{du} = \frac{a^2}{\gamma}\frac{dX}{du},$$

we require

$$0 = \frac{dX}{du} = \frac{1}{2}\left(1 \pm \frac{u + 2Ke^u}{\sqrt{u^2 + 4Ke^u}}\right),$$

where the choice for the $\pm$ sign depends on the use of either the lower or upper curve. In any case, rearranging and squaring the equation gives

$$0 = 4Ke^u(1 - u - Ke^u), \tag{4.1.9}$$

hence

$$e^u = (-1/K)u + (1/K).$$

Putting $u = 1 - s$, we obtain $se^s = Ke$ so that $s = W(Ke)$, and thus $u = 1 - W(Ke)$, giving

$$v = \left(\frac{1}{a}\right)(1 - W(Ke)).$$

Note that $s = W(Ke)$ is defined since by Lemma 4.1.2, $Ke \in \left[-\frac{1}{e}, 0\right)$. It remains to choose the appropriate branch of W for the upper and lower curve branch points. From $u = X + Y$, we see that $u = \left(\frac{1}{a}\right)(\gamma x + \alpha y)$ by (4.1.3). It follows that u increases as x and y increase. Since $x(u_U) < x(u_L)$ (while $y(u_U) = y(u_L)$), we have $u_U < u_L$, and so $s_U > s_L$. For this to be true we must have both branches of W defined and hence $Ke \in \left(-\frac{1}{e}, 0\right)$. By (2.3.2), we have $s_U = W_0(Ke)$ and $s_L = W_{-1}(Ke)$. The result follows from $v = \left(\frac{1}{a}\right)(1 - s)$. ■

The previous computation also gives an expression for the branch points if x is treated as a function of y.

Corollary 4.1.4 *Suppose that $x = x(y)$. Let v_U^* and v_L^* denote the values of the*

parameter determining the points at which the upper and lower curves exhibit a branch point, respectively. Then

$$v_U^* = v_L = \left(\frac{1}{a}\right)(1 - W_{-1}(Ke)) \quad \textit{and} \quad v_L^* = v_U = \left(\frac{1}{a}\right)(1 - W_0(Ke)).$$

Proof:

In this case, we require $\frac{dy}{dx} = \frac{dy/dv}{dx/dv} = 0$, so that $\frac{dy}{dv} = 0$. Since $\frac{dy}{dv} = \frac{a^2}{\alpha}\frac{dY}{du}$, we require

$$0 = \frac{dY}{du} = \frac{1}{2}\left(1 \mp \frac{u + 2Ke^u}{\sqrt{u^2 + 4Ke^u}}\right).$$

Squaring and rearranging results in equation (4.1.9) with solution $u = 1 - s = 1 - W(Ke)$. To choose the appropriate branch of W in this case, note that $y(u_L^*) < y(u_U^*)$ (while $x(u_L^*) = x(u_U^*)$), so that $u_L^* < u_U^*$. This gives $s_U^* < s_L^*$, so we must have $s_L^* = W_0(Ke)$ and $s_U^* = W_{-1}(Ke)$. The result follows. ■

From the results of Proposition 4.1.3 and Corollary 4.1.4, we can easily obtain closed expressions for the amplitudes of the prey and predator populations. We first note that the maximum and minimum of $x(v)$ are the same as those of $x(t)$, and similarly for $y(v)$ and $y(t)$.

Lemma 4.1.5 *We have*

$$\max_v x(v) = \max_t x(t) = x_L(v_L) \quad \textit{and} \quad \max_v y(v) = \max_t y(t) = y_U(v_U^*) \tag{4.1.10}$$

$$\min_v x(v) = \min_t x(t) = x_U(v_U) \quad \textit{and} \quad \min_v y(v) = \min_t y(t) = y_L(v_L^*). \tag{4.1.11}$$

Proof:

The maximum and minimum of $x(t)$ occur when $\frac{dx}{dt} = 0$. Since $\frac{dx}{dy} = \frac{dx}{dt}\frac{dt}{dy}$ and $\frac{dt}{dy} \neq 0$,

we have $\frac{dx}{dt} = 0 \Leftrightarrow \frac{dx}{dy} = 0$. But as seen before, $\frac{dx}{dy} = 0 \Leftrightarrow \frac{dx}{dv} = 0$, which defines the maximum and minimum of $x(v)$, and so (4.1.10) follows using Proposition 4.1.3. The proof is analogous for y using Corollary 4.1.4. ■

We can now give closed expressions for the amplitude of the oscillation of both the prey and predator populations.

Proposition 4.1.6 *Let A_x and A_y be the amplitudes of the prey and predator populations, respectively. Then*

$$A_x = x_L(v_L) - x_U(v_U) \tag{4.1.12}$$

and

$$A_y = y_U(v_U^*) - y_L(v_L^*). \tag{4.1.13}$$

Proof:

Using Lemma 4.1.5, we have

$$A_x = \max_t x(t) - \min_t x(t) = \max_v x(v) - \min_v x(v) = x_L(v_L) - x_U(v_U)$$

and

$$A_y = \max_t y(t) - \min_t y(t) = \max_v y(v) - \min_v y(v) = y_U(v_U^*) - y_L(v_L^*).$$

■

We also note the following observation about the coordinates of the branch points.

Proposition 4.1.7 *$y_U(v_U) = y_L(v_L) = \frac{a}{\alpha}$, and $x_U(v_U^*) = x_L(v_L^*) = \frac{a}{\gamma}$.*

Proof:

First, note that since

$$\frac{du}{dT} = \frac{d(X+Y)}{dT} = X - Y = \frac{\gamma x - \alpha y}{a}, \tag{4.1.14}$$

we see that $\frac{du}{dT} = 0$ only for points lying on the line $y = \frac{\gamma}{\alpha}x$. Clearly, the branch points do not lie on this line for any nontrivial solution trajectory (that is, where the trajectory is not solely the interior equilibrium). Hence, we are concerned only with the situation in which $\frac{du}{dT} \neq 0$.

Now, at the X-nullcline where $Y = 1$, we have

$$0 = \frac{dX}{dT} = \frac{dX}{du}\frac{du}{dT} \Rightarrow \frac{dX}{du} = 0$$

and at the Y-nullcline where $X = 1$, we have

$$0 = \frac{dY}{dT} = \frac{dY}{du}\frac{du}{dT} \Rightarrow \frac{dY}{du} = 0.$$

But from Proposition (4.1.3) and Corollary (4.1.4) we see that $dX/du = 0$ and $dY/du = 0$ determine the branch points when $Y = Y(X)$ and $X = X(Y)$, respectively. Additionally, note that since

$$\frac{dX}{du} = \frac{a^2}{\gamma}\frac{dx}{dv} \quad \text{and} \quad \frac{dY}{du} = \frac{a^2}{\alpha}\frac{dy}{dv},$$

we see

$$\frac{dX}{du} = 0 \Leftrightarrow \frac{dx}{dv} = 0 \quad \text{and} \quad \frac{dY}{du} = 0 \Leftrightarrow \frac{dy}{dv} = 0,$$

so that $dX/du = 0$ and $dY/du = 0$ determine the branch points when $y = y(x)$ and $x = x(y)$. That is, $Y = 1$ at the branch points determined by v_U and v_L, while

$X = 1$ at the branch points determined by v_U^* and v_L^*. Since $Y = 1 \Rightarrow y = \frac{a}{\alpha}$ and $X = 1 \Rightarrow x = \frac{a}{\gamma}$, the proof is complete. ■

4.1.3 Bounds on v

In this section, we determine the minimum and maximum value of the parameter v.

Proposition 4.1.8 *Let v_{min} and v_{max} denote the minimum and maximum value of the parameter v, respectively. Then*

$$v_{min} = -\frac{2}{a} W_0\left(-\sqrt{-K}\right) \quad \textit{and} \quad v_{max} = -\frac{2}{a} W_{-1}\left(-\sqrt{-K}\right).$$

Proof:

The minimum and maximum value of v will occur where $dv/dt = 0$. Since $v = \frac{1}{a}u$, we have

$$\frac{dv}{dt} = \frac{d\left(\frac{1}{a}u\right)}{dt} = \frac{1}{a}\frac{dT}{dt}\frac{du}{dT} = \frac{1}{a} \cdot a \cdot \frac{du}{dT} = \frac{du}{dT}. \tag{4.1.15}$$

Hence, we require $\frac{du}{dT} = 0$, which by (4.1.14) occurs where $Y = X$. This gives

$$\frac{1}{2}\left(u - \sqrt{u^2 + 4Ke^u}\right) = \frac{1}{2}\left(u + \sqrt{u^2 + 4Ke^u}\right).$$

Rearranging and squaring both sides, we obtain

$$0 = u^2 + 4Ke^u$$

so that

$$-K = \left(\frac{1}{4}\right) u^2 e^{-u} = \left[\left(-\frac{u}{2}\right) e^{-\frac{u}{2}}\right]^2.$$

Since $K < 0$ for all (X_0, Y_0) in the first quadrant of $\mathbb{R}^2$, we can write

$$\pm\sqrt{-K} = \left(-\frac{u}{2}\right) e^{-\frac{u}{2}},$$

so that the Lambert W function gives

$$u = -2W\left(\pm\sqrt{-K}\right).$$

Now $u = X + Y > 0$ so that $W\left(\pm\sqrt{-K}\right) < 0$. Choosing the positive sign would give $W\left(\sqrt{-K}\right)$ which is positive since $\sqrt{-K}$ is positive. Hence, we choose only the negative sign so that

$$u = -2W\left(-\sqrt{-K}\right).$$

Note that by Lemma (4.1.2), we have $-\sqrt{-K} \in \left[-\frac{1}{e}, 0\right)$, so that $W\left(-\sqrt{-K}\right)$ is defined. It remains to determine which branch of the Lambert W function corresponds to each intersection point. Since $u_{min} < u_{max}$, both branches of W must be defined, and so $-\sqrt{-K} \in \left(-\frac{1}{e}, 0\right)$. By (2.3.2) we have $u_{min} = -2W_0\left(-\sqrt{-K}\right)$ and $u_{max} = -2W_{-1}\left(-\sqrt{-K}\right)$. Since $v_{min} = \frac{1}{a}u_{min}$ and $v_{max} = \frac{1}{a}u_{max}$, we obtain the result. ■

The above calculation immediately gives the following result:

Corollary 4.1.9 *The curves $x(v)$ and $y(v)$ are closed in the vx-plane and vy-plane, respectively.*

Proof:

If we let $x_L(v) = x_U(v)$, then from the previous calculation, we see that $x_L(v)$ and $x_U(v)$ intersect at the points $(v_{min}, x(v_{min}))$ and $(v_{max}, x(v_{max}))$. Additionally, both

$x_L(v)$ and $x_U(v)$ are continuous for $v \in (v_{min}, v_{max})$, hence, $x(v)$ defines a closed curve in the vx-plane. The proof is similar for $y(v)$. ■

To summarize, we have determined exact expressions for the following key points on the phase curves of the Lotka-Volterra system (3.3.1):

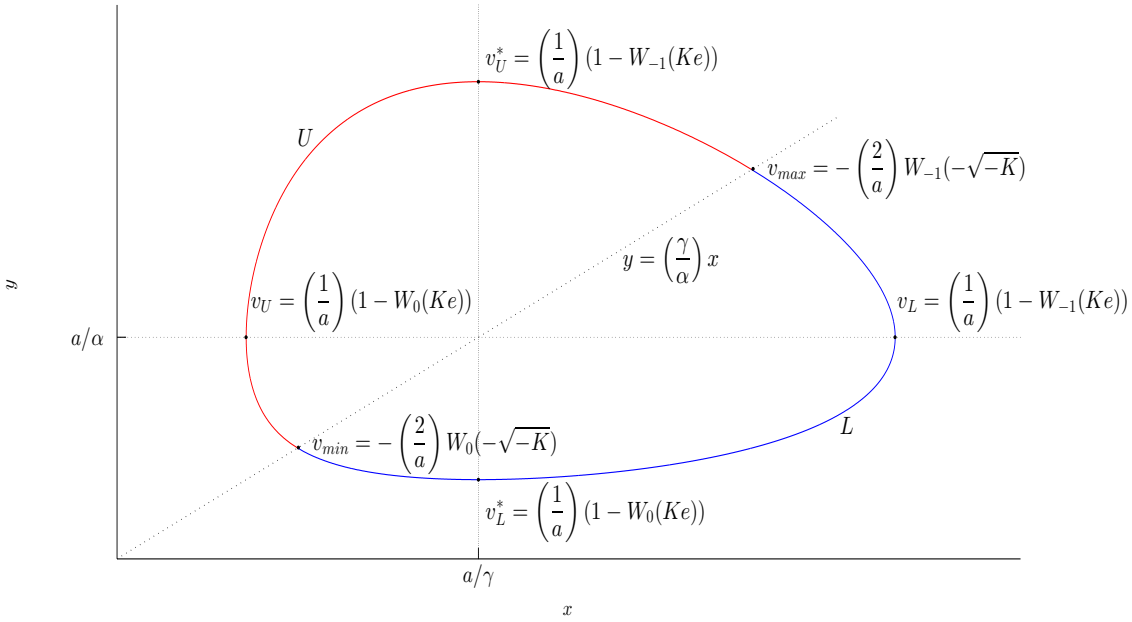

Figure 4.1: Exact trajectory of the Lotka-Volterra system (3.3.1).

4.1.4 The Period of the Lotka-Volterra Equations

Recall that the period of the Lotka-Volterra equations is the least positive value P such that $(x(t+P), y(t+P)) = (x(t), y(t))$ for all $t \in \mathbb{R}^+$. The next result gives an integral formula for the period of the Lotka-Volterra model (3.3.1) which has the advantages of having a relatively condensed expression and being simple to evaluate numerically.

Theorem 4.1.10 *The period of the Lotka-Volterra system (3.3.1) is given by*

$$P = 2\int_{-\frac{2}{a}W_0\left(-\sqrt{-K}\right)}^{-\frac{2}{a}W_{-1}\left(-\sqrt{-K}\right)} \frac{ds}{\sqrt{(as)^2 + 4Ke^{as}}}. \tag{4.1.16}$$

Proof:

By (4.1.5), $XY = -Ke^{X+Y}$, so $4XY = -4Ke^{X+Y}$. Write this as

$$2XY + 4Ke^{X+Y} = -2XY$$

then add $X^2 + Y^2$ to both sides and factor to obtain

$$(X+Y)^2 + 4Ke^{X+Y} = (X-Y)^2.$$

Note that $X + Y = u$ and $X - Y = \frac{du}{dT}$, so we have

$$u^2 + 4Ke^u = \left(\frac{du}{dT}\right)^2.$$

This gives

$$\frac{du}{dT} = \pm\sqrt{u^2 + 4Ke^u}.$$

By (4.1.15) we have

$$\frac{du}{dT} = \frac{dv}{dt},$$

so we obtain

$$\frac{dv}{dt} = \pm\sqrt{(av)^2 + 4Ke^{av}}.$$

Rearranging for dt and integrating gives

$$t(v) = \int_{v_{min}}^{v} \frac{ds}{\sqrt{(as)^2 + 4Ke^{as}}}$$

where we choose the + sign to ensure time is positive. Since $t(v_{max}) = \int_{v_{min}}^{v_{max}} \frac{ds}{\sqrt{(as)^2+4Ke^{as}}}$ for both the upper and lower curves, we have $P = 2t(v_{max})$, and the result follows. ■

In the next section, we will use the results obtained above to compute the branch points, bounds on v, amplitudes of oscillation, and period for a specific set of parameters and initial conditions.

4.2 Numerical Simulations

As an example, consider the case in which

$$a = 6, \quad \alpha = 3, \quad \gamma = 2, \quad x_0 = 0.3, \quad y_0 = 0.8. \tag{4.2.1}$$

This gives $K = -\left(\frac{1}{25}\right) e^{-\frac{1}{2}}$. Treating y as a function of x, the values of the parameters determining the branch points are

$$v_U = \left(\frac{1}{6}\right)(1 - W_0(Ke)) \approx 0.1785$$
$$v_L = \left(\frac{1}{6}\right)(1 - W_{-1}(Ke)) \approx 0.8566.$$

Then the coordinates of the upper and lower branch points, respectively, are

$$(x_U(v_U), y_U(v_U)) \approx (0.2124, 2)$$

$$(x_L(v_L), y_L(v_L)) \approx (12.4183, 2).$$

Note that we have $y_U(v_U) = y_L(v_L) = \frac{a}{\alpha} = 2$.

If instead we treat x as a function of y, then the coordinates of the upper and lower branch points, respectively, are $(3, 8.2789)$ and $(3, 0.1416)$. As expected, we have $x_U(v_U^*) = x_L(v_L^*) = \frac{a}{\gamma} = 3$. Using Proposition 4.1.6, we have the amplitude of

the prey population to be

$$A_x = x_L(v_L) - x_U(v_U) \approx 12.4183 - 0.2124 = 12.2059$$

and the amplitude of the predator population to be

$$A_y = y_U(v_U^*) - y_L(v_L^*) \approx 8.2789 - 0.1416 = 8.1373.$$

The minimum and maximum values of the parameter are

$$v_{min} = -\frac{1}{3}W_0\left(-\sqrt{-K}\right) \approx 0.0627$$
$$v_{max} = -\frac{1}{3}W_{-1}\left(-\sqrt{-K}\right) \approx 0.9789$$

and the points determined by these two values are

$$(x(v_{min}), y(v_{min})) \approx (0.5639, 0.3759)$$

$$(x(v_{max}), y(v_{max})) \approx (8.8102, 5.8735),$$

which lie on the line $y = \frac{\gamma}{\alpha}x = \frac{2}{3}x$. We plot the solution generated by equations (4.1.1) and compare it to that generated by a numerical integration of system (3.3.1) using an explicit Runge-Kutta (4,5) scheme [16]. We see that the curves appear identical and confirm the values calculated above.

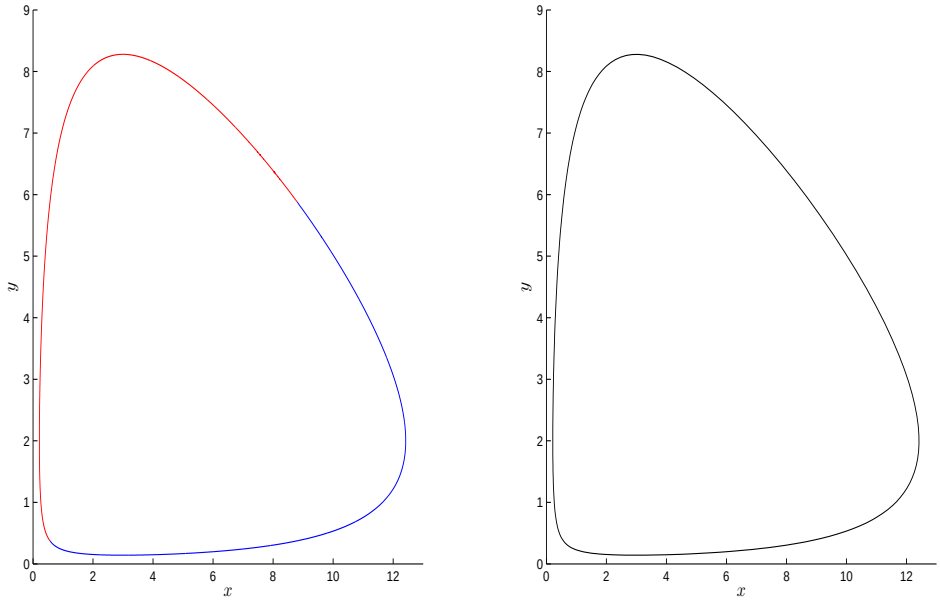

Figure 4.2: Phase curves for system (3.3.1) plotted using expressions (4.1.1) (left) vs. a numerical integration scheme (right).

We also plot $x(v)$ and $y(v)$ and see that they are closed as guaranteed by Corollary 4.1.9.

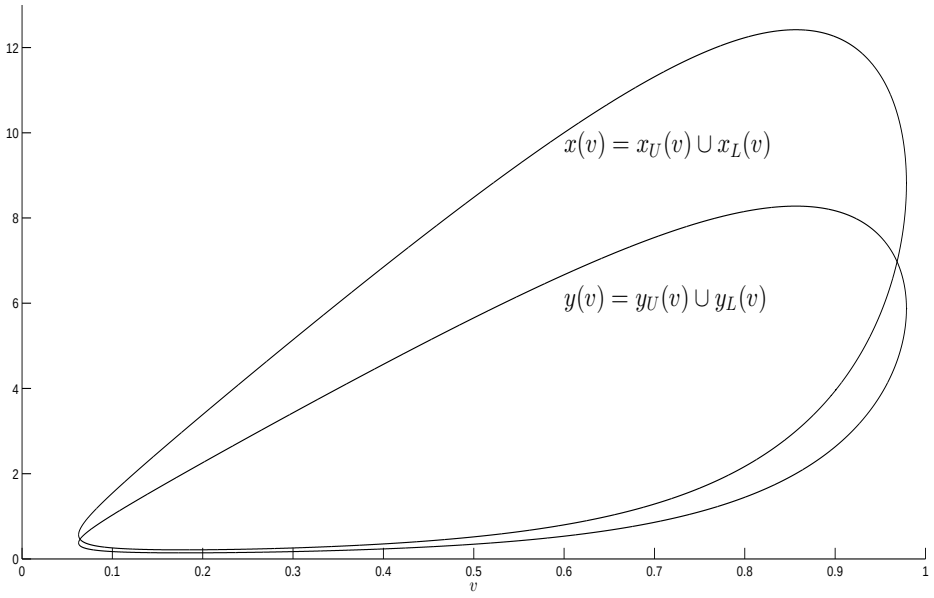

Figure 4.3: Plot of $x(v)$ and $y(v)$ using expressions (4.1.1).

While we know of no closed form expression for the integral in (4.1.16), we can approximate the period numerically with ease. Using global adaptive quadrature, we evaluate the period for the example system defined by (4.2.1), which results in $P \approx 1.364300901863$, to 12 decimal places of accuracy.

4.3 Concluding Remarks

In this part of the thesis, we have given a new derivation of a closed parametric formula for the trajectories of the classic Lotka-Volterra predator-prey system in the case where the growth rate of the prey equals the death rate of the predator. We also obtained expressions for the branch points, bounds on the parameter, amplitude of the oscillation of the prey and predator populations, and period of this model in terms of

the Lambert W function.

The main result of this section of the thesis is to demonstrate that, at least in particular cases, solutions to Lotka-Volterra equations can be understood using analytical techniques. This research adds to our understanding of the exact nature of the solutions of the model, and their important connection to the Lambert W function. In summary, while the results obtained have the benefit of allowing numerical calculations which are simple to perform to a high degree of precision, the main benefit is simply a further understanding of the Lotka-Volterra model itself.

Part II

Geometric Numerical Integration of a Three-Dimensional Lotka-Volterra System

Chapter 5

Preliminaries

5.1 Introduction

The main focus of Part I of this thesis was the application of analytical techniques to understand the solutions of the Lotka-Volterra model. To contrast, in Part II we examine numerical methods to approximate solutions. While basic numerical methods date back much further than the formulation of the Lotka-Volterra equations, as we will see, the application of some of these methods can lead to problems. In particular, the behavior of the approximate numerical solutions does not align with the behavior we expect based on an analysis of the dynamics of the model. For example, we saw in Part I that trajectories of the model are closed curves so that solutions are periodic with respect to time. However, many numerical methods do not preserve this behavior, producing approximations which instead spiral away from the initial conditions. This is problematic, especially if they are conducted over long time intervals.

Progress on this problem began in 1956, when Devogelaere [15] gave the numerical

method

$$\begin{cases} x_{n+1} = x_n + hf(u_{n+1}, v_n) \\ \\ y_{n+1} = y_n + hg(u_{n+1}, v_n) \end{cases}$$

for the system

$$\dot{x} = f(x, y); \qquad \dot{y} = g(x, y).$$

He proved that a region of points mapped by this method will have constant area, assuming that the continuous system is Hamiltonian. In 1993, Kahan [23] applied this method to the Lotka-Volterra system and found that it maintained the periodicity of the solutions, despite the fact that the system is not Hamiltonian. Sanz-Serna [37] clarified that the reason for this is that although the system is not Hamiltonian, it can be transformed into one which is Hamiltonian through a change of coordinates. Such systems are called Poisson systems, which are a natural generalization of Hamiltonian systems that possess many similar properties.

After Sanz-Serna clarified that the periodicity of solutions of the Lotka-Volterra equations could be described by the underlying Poisson geometry, many numerical methods were developed which preserve this geometry and thereby create qualitatively accurate simulations. These methods are typically referred to as non-standard finite difference methods. While similar to typical finite difference methods, they differ in several key respects which will be discussed later. As discussed previously, the process of developing numerical methods which preserve the geometry of the differential system has been applied to many systems besides the Lotka-Volterra model. This field is well developed, and has been termed Geometric Numerical Integration. Currently, there

are a number of texts dealing with the topic, the most extensive being [20].

Though the theory of Geometric Numerical Integration is well-studied, there is very little research into applying it to natural generalizations of the Lotka-Volterra model containing three or more species. In particular, the dynamics of the three-species predator-prey model have been thoroughly studied in [11]. Despite this, there is little work on developing numerical methods which produce correct solution behavior, or clarifying the underlying geometry which they must preserve. This is the motivation for Part II of this thesis. Our main goal is to describe this geometry and produce a class of numerical methods which preserve the main properties of the continuous three-species Lotka-Volterra predator-prey model. To begin, we review some basic notions regarding numerical methods and Poisson systems.

5.2 Numerical Integration of Ordinary Differential Equations

We begin with a brief introduction to some basic numerical methods for the initial value problem

$$\frac{du}{dt} = u'(t) = \dot{u} = f(t,u), \qquad u(0) = u_0 \in \mathcal{D} \subset \mathbb{R}^d. \tag{5.2.1}$$

Supposing the solution to this problem exists and is unique, it would be ideal to derive a closed expression for this solution. Unfortunately, such an expression cannot typically be found, and so numerical techniques are relied upon to obtain an approximation.

This process is called numerical integration, and the basic approach is to subdivide

the time interval of integration $[t_0, t_f]$ into a collection of mesh points $\{t_0 < t_1 < \cdots < t_N = t_f\}$ where $t_n = t_0 + nh$ for $n = 0, 1, \ldots, N$. Here, $N \in \mathbb{Z}^+$ and $h = \frac{1}{N}(t_f - t_0)$ is called the step-size of integration. Then, the exact solution $u(t_n)$ is approximated by u_n, which is specified by the particular numerical method. The values u_n are calculated successively for $n = 1, \ldots, N$. We will only consider methods in which h is held constant along the interval of integration. Before introducing some standard methods, a number of basic terms will be defined.

5.2.1 Basic Definitions

We will only be concerned with *one-step* numerical methods, in which u_{n+1} is expressed in terms of the previous u_n only. Such methods may be either explicit or implicit.

Definition 5.2.1 *For a given function ϕ, a one-step numerical method is called **explicit** if it can be expressed as*

$$u_{n+1} = u_n + h\phi\left(t_n, u_n; h\right), \quad n = 0, 1, \ldots, N-1, \quad u(t_0) = u_0 \tag{5.2.2}$$

*and is called **implicit** if it can be expressed as*

$$u_{n+1} = u_n + h\phi\left(t_{n+1}, t_n, u_{n+1}, u_n; h\right), \quad n = 0, 1, \ldots, N-1, \quad u(t_0) = u_0. \tag{5.2.3}$$

The accuracy of these methods can be investigated after introducing two measures for error.

Definition 5.2.2 *For a given explicit numerical method (5.2.2), the* ***global error*** e_n *is defined to be*

$$e_n = u(t_n) - u_n \tag{5.2.4}$$

and the ***truncation error*** T_n *is defined to be*

$$T_n = \frac{u(t_{n+1}) - u(t_n)}{h} - \phi\left(t_n, u(t_n); h\right). \tag{5.2.5}$$

For an implicit method (5.2.3), the ***global error*** *is defined as in (5.2.4), while the* ***truncation error*** *is*

$$T_n = \frac{u(t_{n+1}) - u(t_n)}{h} - \phi\left(t_{n+1}, t_n, u(t_{n+1}), u(t_n); h\right). \tag{5.2.6}$$

This truncation error is used to define the accuracy of a method.

Definition 5.2.3 *A numerical method is of* ***order of accuracy r*** *if there exist constants* K *and* h_0 *such that*

$$|T_n| \leq Kh^r \quad \text{for} \quad 0 < h \leq h_0. \tag{5.2.7}$$

If the step-size is taken to be zero, then the numerical discrete solution should be identical to the true solution. This notion is formalized with the following definition.

Definition 5.2.4 *A numerical method is said to be* ***consistent*** *if* $\phi(t, u; 0) = f(t, u)$.

Moreover, the numerical solution should approach the exact solution as the step-size approaches zero. If a few extra constraints on ϕ and f are assumed, then this notion of convergence can be made precise.

Definition 5.2.5 *A numerical method is said to be* ***convergent*** *if*

$$\lim_{n\to\infty} u_n = u(t) \quad \text{as} \quad t_n \to t \in [t_0, t_f] \quad \text{when} \quad h \to 0 \quad \text{and} \quad n \to \infty. \tag{5.2.8}$$

5.2.2 First-Order Accurate Methods

We first introduce two basic numerical methods for the initial value problem (5.2.1) which are first-order accurate. The simplest such method is explicit Euler method.

Definition 5.2.6 *The* ***explicit Euler method*** *is given by*

$$u_{n+1} = u_n + hf\left(t_n, u_n\right), \quad n = 0, 1, \ldots, N-1, \quad u(t_0) = u_0. \tag{5.2.9}$$

Note that this method is explicit in that the approximation u_{n+1} is obtained from only the previous approximation u_n. A related method is the implicit Euler method.

Definition 5.2.7 *The* ***implicit Euler method*** *is given by*

$$u_{n+1} = u_n + hf\left(t_{n+1}, u_{n+1}\right), \quad n = 0, 1, \ldots, N-1, \quad u(t_0) = u_0. \tag{5.2.10}$$

In general, this method is implicit since (5.2.9) is often a nonlinear equation which must be solved to obtain the approximation u_{n+1}. In some cases, it is possible to isolate the term u_{n+1}, avoiding the need to solve a nonlinear equation.

5.2.3 Second-Order Accurate Methods

In some cases, a numerical method with a higher order of accuracy than those of the previous section is required. Two such methods are the trapezoidal rule and the midpoint rule, which have both explicit and implicit formulations. We begin with the explicit trapezoidal rule.

Definition 5.2.8 *The **explicit trapezoidal rule**, also known as **Heun's method**, is given by*

$$u_{n+1} = u_n + \frac{h}{2}\left[f\left(t_n, u_n\right) + f\left(t_{n+1}, u_n + hf\left(t_n, u_n\right)\right)\right], \quad n = 0, 1, \ldots, N-1, \quad u(t_0) = u_0. \tag{5.2.11}$$

The related implicit trapezoidal rule is defined similarly.

Definition 5.2.9 *The **implicit trapezoidal rule**, also known as the **Crank-Nicolson method**, is given by*

$$u_{n+1} = u_n + \frac{h}{2}\left[f\left(t_n, u_n\right) + f\left(t_{n+1}, u_{n+1}\right)\right], \quad n = 0, 1, \ldots, N-1, \quad u(t_0) = u_0. \tag{5.2.12}$$

A commonly used alternative to the trapezoidal rule is the midpoint method.

Definition 5.2.10 *The **explicit midpoint method** is given by*

$$u_{n+1} = u_n + hf\left(u_n + \frac{h}{2}, u_n + \frac{h}{2}f\left(t_n, u_n\right)\right), \quad n = 0, 1, \ldots, N-1, \quad u(t_0) = u_0. \tag{5.2.13}$$

Again, the related implicit midpoint method is defined similarly.

Definition 5.2.11 *The **implicit midpoint method** is given by*

$$u_{n+1} = u_n + hf\left(u_n + \frac{h}{2}, \frac{1}{2}\left(u_n + u_{n+1}\right)\right), \quad n = 0, 1, \ldots, N-1, \quad u(t_0) = u_0. \tag{5.2.14}$$

5.3 Hamiltonian and Poisson Dynamics

In the previous section, we reviewed the classical approach to numerical integration, in which a numerical method is chosen and applied to a given initial value problem. However, this approach does not take into account any of the underlying geometric structure of the differential equation to be solved. In contrast, geometric numerical integrators oftentimes exhibit improved qualitative behaviour, in that they model the true solution more accurately, and also provide more accurate long-time simulations [8]. A large class of geometric numerical integrators have been developed which incorporate the properties of Hamiltonian and Poisson systems. We review these systems and their dynamics in this section.

Let $d > 0$ be an integer and suppose $u = (q, p)^T = (q_1, \ldots, q_d, p_1, \ldots, p_d)^T$.

Definition 5.3.1 *A **Hamiltonian system** is a system of ordinary differential equations which can be written as*

$$\frac{dq_i}{dt} = \frac{\partial H}{\partial p_i}, \quad \frac{dp_i}{dt} = -\frac{\partial H}{\partial q_i}; \quad i = 1, \ldots, d, \tag{5.3.1}$$

*where $H(q, p)$ is the **Hamiltonian function** defined on $\mathcal{D} \subset \mathbb{R}^d \times \mathbb{R}^d$. The value of the Hamiltonian function is called the **energy**.*

We can write this more compactly as

$$u'(t) = J \nabla_u H(u), \tag{5.3.2}$$

where

$$J = \begin{pmatrix} 0_d & I_d \\ -I_d & 0_d \end{pmatrix}. \tag{5.3.3}$$

Here, I_d is the $d\times d$ identity matrix, 0_d is the $d\times d$ zero matrix, and $\nabla_u = \left(\frac{\partial}{\partial u_1}, \ldots, \frac{\partial}{\partial u_d}\right)^T$ is the gradient operator. Hamiltonian systems possess a number of interesting properties, but before they are introduced we define the flow of the system.

Definition 5.3.2 *The **flow** over time t is the map φ_t defined by*

$$\varphi_t(u_0) = u(t) \quad \text{if} \quad u(0) = u_0. \tag{5.3.4}$$

In the case of autonomous Hamiltonian systems, we have the following property.

Theorem 5.3.3 *If the Hamiltonian function does not depend explicitly on t, then the energy is constant.*

Proof:

If we differentiate H along a trajectory, we obtain

$$\frac{dH}{dt} = \sum_{i=1}^{d}\left(\frac{\partial H}{\partial q_i}\frac{dq_i}{dt} + \frac{\partial H}{\partial p_i}\frac{dp_i}{dt}\right) = 0 \tag{5.3.5}$$

by (5.3.1). ■

As a result, we have $H(q(t), p(t)) = H(q(0), p(0))$ for all t.

Hamiltonian systems are also divergence-free. Recall that the divergence of a vector field $f = [f_1, \ldots, f_n]^T$ is

$$\mathrm{div} f = \frac{\partial f_1}{\partial x_1} + \cdots + \frac{\partial f_n}{\partial x_n} \tag{5.3.6}$$

By (5.3.1), we have

$$\mathrm{div} f = \frac{\partial}{\partial q}\left(\frac{\partial H}{\partial p}\right) + \frac{\partial}{\partial p}\left(-\frac{\partial H}{\partial q}\right) = 0, \tag{5.3.7}$$

as required. The significance of this result follows from Liouville's Theorem, which is proven in [3]:

Theorem 5.3.4 *(Liouville's Theorem) Let f be a divergence-free vector field. Then its flow map φ_t is volume-preserving for all t. That is, for $A \subset \mathbb{R}^n$, we have $v(\varphi_t(A)) = v(A)$, where $v(X)$ denotes the volume of X.*

As a consequence, Hamiltonian flows preserve volume in phase-space.

We next define the notion of a symplectic map.

Definition 5.3.5 *A differentiable map $g : U \to \mathbb{R}^{2d}$, where $U \subset \mathbb{R}^{2d}$ is an open set, is called* ***symplectic*** *if the Jacobian matrix $g'(q,p)$ satisfies*

$$g'(q,p)\, J g'(q,p)^T = J, \tag{5.3.8}$$

where J is defined in (5.3.3).

This allows us to state the following important result, the proof of which can be found in [20]:

Theorem 5.3.6 *If the Hamiltonian function $H(q,p)$ is twice continuously differentiable on $U \subset \mathbb{R}^{2d}$, then the flow φ_t of the Hamiltonian system is a symplectic map. That is,*

$$\varphi_t'(u)\, J \varphi_t'(u)^T = J. \tag{5.3.9}$$

This gives us an alternative way to see that Hamiltonian flows preserve volume. Note that taking the determinant of both sides of expression (5.3.9) and using the fact that

$\det J = 1$ gives

$$\det\left(\varphi_t'(u)\right) = 1. \tag{5.3.10}$$

The result follows from the Change of Variables Theorem, which states that if we are given a map $\Omega : \mathbb{R}^n \to \mathbb{R}^n$ and domain $V \subset \mathbb{R}^n$, then

$$v(V) = \int_V du \quad \text{and} \quad v(\Omega(V)) = \int_V \left|\det \frac{\partial \Omega}{\partial u}\right| du,$$

where $\frac{\partial \Omega}{\partial u}$ is the Jacobian of Ω. In the case where $d = 1$, this is equivalent to preservation of area, so that symplectic maps can be regarded as area-preserving maps. We can also use (5.3.8) above to motivate the definition of a symplectic numerical method. We will consider only the case where $d = 1$ for simplicity.

Definition 5.3.7 *A numerical method $u_{n+1} = \vartheta(u_n)$ is **symplectic** if and only if*

$$\left(\frac{\partial\left(q_{n+1}, p_{n+1}\right)}{\partial\left(q_n, p_n\right)}\right) J \left(\frac{\partial\left(q_{n+1}, p_{n+1}\right)}{\partial\left(q_n, p_n\right)}\right)^T = J \tag{5.3.11}$$

whenever it is applied to the Hamiltonian system (5.3.1).

In fact, as shown in [10], there is a simpler characterization of symplecticity of a numerical method. Since Hamiltonian systems are volume-preserving, they must preserve the differential volume-form $dq \wedge dp$ [7]. Analogously, the method $u_{n+1} = \vartheta(u_n)$ is symplectic if an only if

$$dq_{n+1} \wedge dp_{n+1} = dq_n \wedge dp_n \quad \text{for all} \quad (q_n, p_n), \tag{5.3.12}$$

where $\wedge$ denotes the exterior product of differential forms.

One of the drawbacks of Hamiltonian systems is that they are only defined for even-dimensional systems. However, a generalization called Poisson systems exist for both even and odd dimension. In a Poisson system, the matrix J defined in (5.3.3) is replaced by a nonconstant matrix $B(u)$. To define a Poisson system, we must also introduce the Poisson bracket.

Definition 5.3.8 *If an $n \times n$ matrix $B(u)$ is skew-symmetric and satisfies*

$$\sum_{i=1}^{n} \left(\frac{\partial b_{ij}(u)}{\partial u_l} b_{lk}(u) + \frac{\partial b_{jk}(u)}{\partial u_l} b_{li}(u) + \frac{\partial b_{ki}(u)}{\partial u_l} b_{lj}(u) \right) = 0 \quad \text{for all} \quad i, j, k, \tag{5.3.13}$$

*then the **Poisson bracket** of two smooth functions F and G is given by*

$$\{F, G\}(u) = \sum_{i,j=1}^{n} \frac{\partial F(u)}{\partial u_i} b_{ij}(u) \frac{\partial G(u)}{\partial u_j}. \tag{5.3.14}$$

This can be written more compactly as

$$\{F, G\}(u) = \nabla F(u)^T B(u) \nabla G(u). \tag{5.3.15}$$

The corresponding differential system

$$\dot{u} = B(u) \nabla H(u) \tag{5.3.16}$$

*is called a **Poisson system**. The function H will continue to be called the **Hamiltonian**.*

The Poisson bracket satisfies a number of algebraic identities. In particular, it is antisymmetric so that

$$\{F, G\} = -\{G, F\},$$

and satisfies the Jacobi identity

$$\{F,\{G,H\}\}+\{G,\{H,F\}\}+\{H,\{F,G\}\}=0.$$

Note that the equations (5.3.1) can be written simply in terms of the Poisson bracket as

$$\dot{u}_i=\{u_i,H\},\quad i=1,\ldots,d.$$

We next introduce several terms and results which are related to Poisson systems.

Definition 5.3.9 *A function $I(u)$ is called a **first integral** or **invariant** of the system (5.2.1) if*

$$\frac{d}{dt}I(u(t))=0 \tag{5.3.17}$$

whenever $u(t)$ is a solution to (5.2.1).

By the chain rule, we have

$$\nabla I(u(t))\cdot\frac{du}{dt}=\nabla I(u(t))\cdot f(u)=0$$

so that I is a first integral of (5.2.1) if

$$\nabla I\cdot f(u)=(\nabla I)^T f(u)=0. \tag{5.3.18}$$

We can also say that I is an invariant of the Poisson system (5.3.16) if

$$\{H,I\}=0, \tag{5.3.19}$$

since

$$\begin{aligned}\{H, I\} &= \nabla H^T B \nabla I \\ &= -\nabla H^T B^T \nabla I \\ &= -\left(B \nabla H\right)^T \nabla I \\ &= -\dot{u}^T \nabla I \\ &= -f\left(u\right)^T \nabla I \\ &= -\left(\nabla I^T f\left(u\right)\right)^T \\ &= 0.\end{aligned}$$

Note that by the antisymmetric property of the Poisson bracket, $\{H, H\} = -\{H, H\}$, and so $\{H, H\} = 0$. Hence, the Hamiltonian itself is a first integral if the system is autonomous. We also introduce to concept of a Casimir function.

Definition 5.3.10 *A function $C\left(u\right)$ is a **Casimir function** of the Poisson system (5.3.16) if*

$$\nabla C\left(u\right)^T B\left(u\right) = 0 \quad \text{for all} \quad u. \tag{5.3.20}$$

A Casimir function is always a first integral for any Poisson system with matrix $B\left(u\right)$ since

$$\nabla C^T f\left(u\right) = \nabla C^T B \nabla H = 0\left(\nabla H\right) = 0.$$

Moreover, we have the following result, which is proven in [20].

Theorem 5.3.11 *If the structure matrix $B\left(u\right)$ is of constant rank $n - q = 2m$ in a neighbourhood of $u_0 \in \mathbb{R}^n$, then there exist functions $P_1\left(u\right), \ldots, P_m\left(u\right), Q_1\left(u\right), \ldots, Q_m\left(u\right)$,*

and Casimir functions $C_1(u), \ldots, C_q(u)$ *on a neighbourhood of* u_0 *such that the gradients of* P_i, Q_j, *and* C_k *are linearly independent.*

Recall that the symplectic maps defined earlier only exist for even-dimensional systems. There is a similar notion which exist for Poisson systems.

Definition 5.3.12 *A transformation* $\varphi : U \to \mathbb{R}^n$ *(where* U *is an open set in* $\mathbb{R}^n$*) is called a* ***Poisson map*** *with respect to the Poisson bracket (5.3.14) if its Jacobian matrix satisfies*

$$\varphi'(u) B(u) \varphi'(u)^T = B(\varphi(u)). \tag{5.3.21}$$

The following theorem regarding Poisson maps is proven in [20].

Theorem 5.3.13 *The flow* $\varphi_t(u)$ *of a Poisson system is a Poisson map.*

One goal of geometric numerical integration is to develop numerical methods which are consistent with some of the geometric properties of the flow of the system. In this setting, such numerical methods are called Poisson integrators. Since the flow of a Poisson system respects the Casimirs in that $C_i(\varphi_t(u))$ is constant [20], this motivates the following definition.

Definition 5.3.14 *A numerical method* $u_1 = \phi_h(u_0)$ *is a* ***Poisson integrator*** *for the structure matrix* $B(u)$ *if the transformation* $u_0 \to u_1$ *respects the Casimirs and if it is a Poisson map whenever the method is applied to the corresponding system (5.3.16).*

Chapter 6

The Numerical Integration of Lotka-Volterra Models

In this chapter, we begin with a review of the geometry of the two-species Lotka-Volterra model. In particular, the system is Poisson, and this has certain consequences for the flow of the solutions. We then review the literature on discretizations of this model, comparing those that preserve the underlying geometry with those that do not. As expected, integrators which preserve the Poisson structure tend to produce more accurate simulations. Finally, research on the generalized three-species Lotka-Volterra predator-prey model is introduced, which motivates the research problem of Part II of this thesis.

6.1 Poisson Structure of the Two-Dimensional Lotka-Volterra Predator-Prey Model

Recall that in Part I, the two-dimensional Lotka-Volterra predator-prey model was introduced, along with some of its properties. This model can also be analyzed through the framework of Poisson dynamics. In [10], it is proven that the system of differential

equations

$$\begin{cases} \dfrac{dx}{dt} = f(x,y) \\ \dfrac{dy}{dt} = g(x,y) \end{cases}$$

is Hamiltonian if and only if the vector field (f,g) is divergence-free; that is, if and only if

$$\frac{\partial f}{\partial x} + \frac{\partial g}{\partial y} = 0.$$

This is not satisfied by the Lotka-Volterra model, since

$$\frac{\partial f}{\partial x} + \frac{\partial g}{\partial y} = (a - c) + (\gamma x - \alpha y) \neq 0$$

in general. However, noticing that

$$\begin{cases} \dfrac{1}{x}\dot{x} = \dfrac{d}{dt}(\ln x) = a - \alpha y \\ \dfrac{1}{y}\dot{y} = \dfrac{d}{dt}(\ln y) = -c + \gamma x \end{cases} \tag{6.1.1}$$

suggests the change of variables

$$w = \ln x; \quad v = \ln y. \tag{6.1.2}$$

In these new coordinates, the Lotka-Volterra system becomes

$$\begin{cases} \dot{w} = a - \alpha e^{v} & = \widetilde{f}(w,v) \\ \dot{v} = -c + \gamma e^{w} & = \widetilde{g}(w,v), \end{cases} \tag{6.1.3}$$

which is divergence-free. Hence, the transformed system is Hamiltonian, with the Hamiltonian function given by

$$\widetilde{H}(w,v) = av - \alpha e^{v} + cw - \gamma e^{w} \tag{6.1.4}$$

so that we have

$$\begin{aligned} \frac{\partial \widetilde{H}}{\partial v} &= \widetilde{f}(w,v) \\ -\frac{\partial \widetilde{H}}{\partial w} &= \widetilde{g}(w,v). \end{aligned} \tag{6.1.5}$$

By Theorem 5.3.6, the flow of this system is symplectic, so that it preserves the differential form $dw \wedge dv$.

Now, as noted by Sanz-Serna in [37], if a two-dimensional system becomes Hamiltonian after a change of variables, then the system can be written as

$$\begin{cases} \dfrac{dx}{dt} = \dfrac{1}{\sigma(x,y)} \dfrac{\partial H}{\partial y} \\ \dfrac{dy}{dt} = -\dfrac{1}{\sigma(x,y)} \dfrac{\partial H}{\partial x}, \end{cases} \tag{6.1.6}$$

where

$$\sigma(x,y) = \det \frac{\partial(w,v)}{\partial(x,y)}. \tag{6.1.7}$$

In the case of the Lotka-Volterra model,

$$\sigma(x,y) = \det \begin{pmatrix} 1/x & 0 \\ 0 & 1/y \end{pmatrix} = \frac{1}{xy}. \tag{6.1.8}$$

This is of course a Poisson system

$$\dot{u} = \begin{pmatrix} \dot{x} \\ \dot{y} \end{pmatrix} = \begin{pmatrix} 0 & xy \\ -xy & 0 \end{pmatrix} \begin{pmatrix} \frac{c}{x} - \gamma \\ \frac{a}{y} - \alpha \end{pmatrix} = B(u) \nabla_u H(u). \tag{6.1.9}$$

Moreover, we can see that

$$\begin{aligned} dw \wedge dv &= d(\ln x) \wedge d(\ln y) \\ &= \frac{1}{x} dx \wedge \frac{1}{y} dy \qquad \text{(exterior differentiation)} \\ &= \frac{1}{xy}(dx \wedge dy) \qquad \text{(linearity)} \end{aligned} \tag{6.1.10}$$

so that the flow of the Lotka-Volterra system preserves the differential form

$$\frac{1}{xy}(dx \wedge dy). \tag{6.1.11}$$

6.2 Discretizations of the Two-Dimensional Lotka-Volterra Predator-Prey Model

Numerical methods which are not designed to incorporate this geometric structure of the Lotka-Volterra system can produce simulations with behavior that differs qualitatively from that expected based on analytical results. In particular, as discussed in Part I, solutions to the Lotka-Volterra model are periodic in the x, y-plane. However, if the flow of the numerical method does not map areas in the same way as the flow of the differential system, it will likely produce a result which is qualitatively inaccurate. In the case of the Lotka-Volterra model, the form (6.1.11) must be preserved by the numerical method. Introducing the notation

$$\begin{aligned} x &= x(t) = x(k) \\ y &= y(t) = y(k) \\ X &= x(t+h) = x(k+1) \\ Y &= y(t+h) = y(k+1), \end{aligned} \tag{6.2.1}$$

this means that a numerical method should satisfy

$$\frac{1}{XY}(dX \wedge dY) = \frac{1}{xy}(dx \wedge dy). \tag{6.2.2}$$

However many standard methods, when applied to the Lotka-Volterra system, do not preserve this structure. One example is the basic explicit Euler method (5.2.9). We will consider the normalized system, with all parameters equal to one for simplicity.

When applied to the Lotka-Volterra equations, the method reads

$$\begin{aligned} X &= x\left(h - hy + 1\right) \\ Y &= y\left(-h + hx + 1\right). \end{aligned} \tag{6.2.3}$$

Plotting the solutions obtained by this method gives the following:

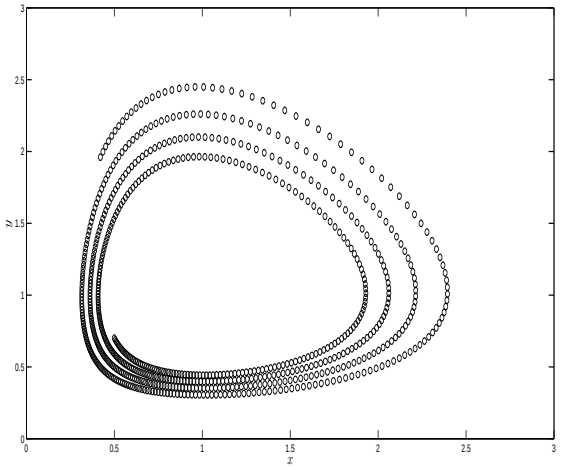

Figure 6.1: Explicit Euler method applied to the Lotka-Volterra system. $x_0 = 0.5$, $y_0 = 0.7$, and $h = \frac{1}{30}$.

This method does not preserve the periodicity of the solutions; instead, the simulation spirals outward from the initial conditions. The Implicit Euler method (5.2.10) also fails to preserve the periodicity. Typically, this method requires the solution of a nonlinear equation; however, in the case of the Lotka-Volterra equations, it is possible to obtain expressions for X and Y directly. The method reads

$$\begin{aligned} X &= x + h\left(X - XY\right) \\ Y &= y + h\left(-Y + XY\right). \end{aligned} \tag{6.2.4}$$

which can be solved for X and Y to give

$$X = \frac{x}{1-h+hY}$$
$$Y = \frac{1}{2(1+h)}\left(x+y+h-\frac{1}{h}+\sqrt{\left(\frac{1}{h}-h-x-y\right)^2+4(1+h)\,y\left(\frac{1}{h}-1\right)}\right). \tag{6.2.5}$$

Plotting the solutions obtained by this method gives the following:

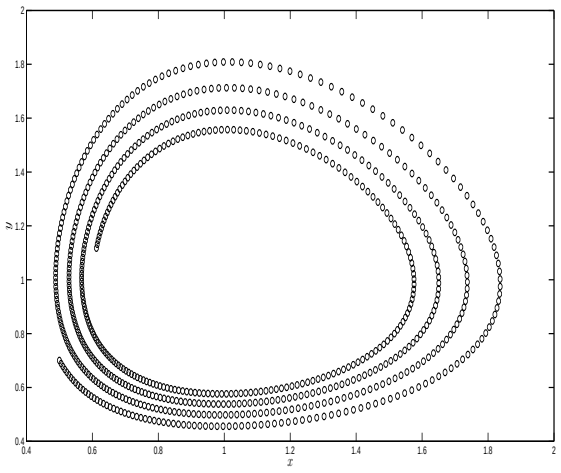

Figure 6.2: Implicit Euler method applied to the Lotka-Volterra system. $x_0 = 0.5$, $y_0 = 0.7$, and $h = \frac{1}{30}$.

In this case, the simulation spirals inward from the initial conditions.

To date, many numerical methods which do preserve the periodicity of the Lotka-Volterra equations have been developed. These methods are typically called Non-Standard Finite Difference (NSFD) Methods. This term is difficult to define precisely, but is instead defined by the following characteristics adapted from Mickens [29]:

Definition 6.2.1 *A **Non-Standard Finite Difference Method** is a finite-difference method which possesses the following characteristics:*

- *The orders of the discrete derivative approximations* $\left(i.e., \frac{dx}{dt} \approx \frac{X-x}{h}\right)$ *should be the same as the orders of the corresponding continuous derivatives.*

- *Discrete approximations to derivatives may require replacing the denominator function* h *with a non-trivial function* $\phi(h) = h + \mathcal{O}(h^2)$.

- *Nonlinear terms, in general, should be replaced by nonlocal discrete representations.*

- *The discrete scheme should be dynamically consistent with the continuous model.*

An early NSFD method for the Lotka-Volterra equations is Kahan's method [23], given by

$$\begin{aligned} \frac{X-x}{h} &= \frac{X+x}{2} - \frac{Xy+xY}{2} \\ \frac{Y-y}{h} &= -\frac{Y+y}{2} + \frac{Xy+xY}{2}. \end{aligned} \tag{6.2.6}$$

Sanz-Serna [37] showed that this method preserves the periodicity of solutions of the Lotka-Volterra model, as it satisfies the equality (6.2.2). Gander and Meyer-Spasche [18] showed that the modified forward Euler method

$$\begin{aligned} X &= x(1 + h - hy) \\ Y &= y(1 - h + hX) \end{aligned} \tag{6.2.7}$$

also produces periodic solutions as it satisfies (6.2.2). Mickens [28] introduced a NSFD method which uses a non-trivial denominator function:

$$\begin{aligned} \frac{X-x}{\phi(h)} &= (2x - X) - Xy \\ \frac{Y-y}{\phi(h)} &= -Y + (2Xy - XY), \end{aligned} \tag{6.2.8}$$

where $\phi(h) = h + \mathcal{O}(h^2)$. Isolating X and Y gives

$$\begin{aligned} X &= \frac{x(1+2\phi(h))}{1+\phi(h)+y\phi(h)} \\ Y &= \frac{y(1+2X\phi(h))}{1+\phi(h)+X\phi(h)}, \end{aligned} \tag{6.2.9}$$

from which it is clear that this method also preserves the property that $x(t) > 0$ and $y(t) > 0$ for all $t \geq 0$.

Mounim and de Dormale [30] improved on this scheme by noting that the normalized Lotka-Volterra equations possess the symmetry $f(y,x) = -g(x,y)$ and $g(y,x) = -f(x,y)$. They suggested analogously that the right-hand side of either equation in the discrete scheme should transform into the opposite of the other after the interchanges $x \leftrightarrow Y$ and $y \leftrightarrow X$. Using this principle, they formulated two schemes. The first is

$$\begin{aligned} \frac{X-x}{h} &= x - (2Xy - xy) \\ \frac{Y-y}{h} &= -Y + (2Xy - XY), \end{aligned} \tag{6.2.10}$$

which after rearranging gives

$$\begin{aligned} X &= \frac{x(1+h+hy)}{1+2hy} \\ Y &= \frac{y(1+2hX)}{1+h+hX}. \end{aligned} \tag{6.2.11}$$

Their second scheme is

$$\begin{aligned} \frac{X-x}{h} &= (2x - X) - Xy \\ \frac{Y-y}{h} &= -(2Y - y) + Xy, \end{aligned} \tag{6.2.12}$$

which after rearranging gives

$$\begin{aligned} X &= \frac{x(1+2h)}{1+h+hy} \\ Y &= \frac{y(1+h+hX)}{1+2h}. \end{aligned} \tag{6.2.13}$$

As with Mickens's method , these two schemes also preserve the positivity of solutions of the Lotka-Volterra model. Plots of solutions obtained by these schemes are below. In each case, the simulated solution is compared to the true solution.

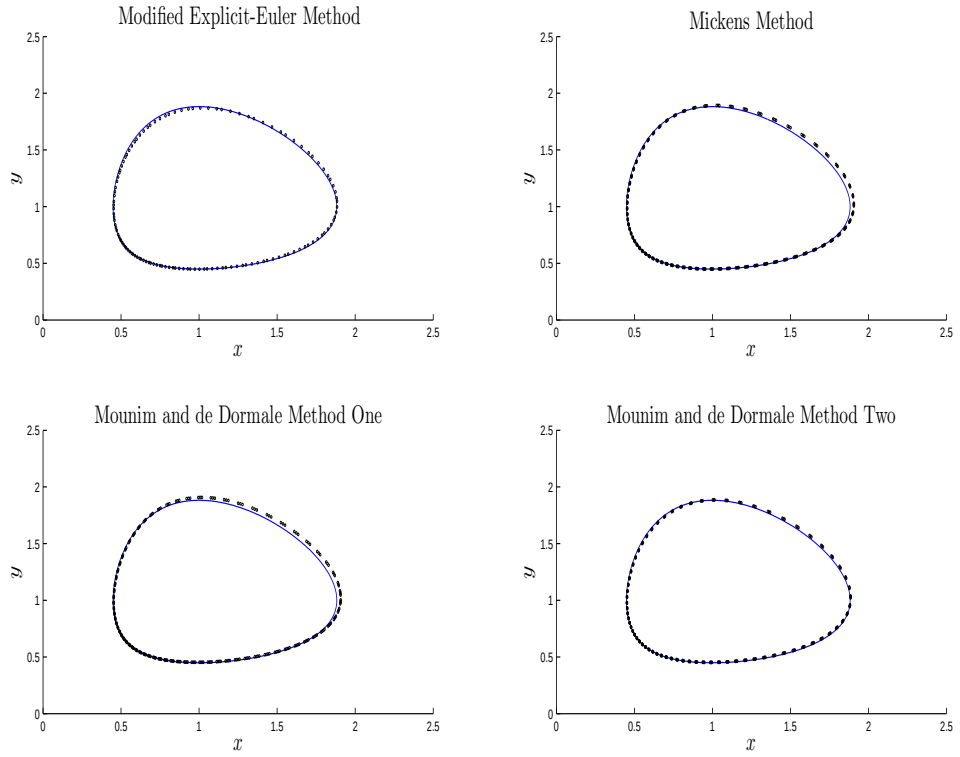

Figure 6.3: Comparison of four NSFD methods applied to the Lotka-Volterra system. In each case, the true solution is plotted as a solid line. $x_0 = 0.5$, $y_0 = 0.7$, and $h = 0.05$.

Clearly these methods preserve the periodicity of the solutions of the Lotka-Volterra model, and despite using a larger step-size h than in Figures 6.1 and 6.2, give a qualitatively more accurate simulation.

In 2006, Reoger [35] derived a general class of schemes preserving the form $\frac{1}{xy}dx \wedge dy$. Recall the observation of Mounim and de Dormale [30] that the right-hand side of either

equation in the discrete scheme should transform into the opposite of the other after the interchanges $x \leftrightarrow Y$ and $y \leftrightarrow X$. Writing the Lotka-Volterra equations as

$$\begin{cases} \dfrac{dx}{dt} = Ax + Bxy \\ \dfrac{dy}{dt} = Cy + Dxy \end{cases} \tag{6.2.14}$$

and applying this rule, Roeger suggested the scheme

$$\begin{aligned} \frac{X - x}{h} &= A\left(\epsilon_1 x + \epsilon_2 X\right) + B\left(\delta_1 xy + \delta_2 Xy + \delta_3 xY + \delta_4 XY\right) \\ \frac{Y - y}{h} &= C\left(\epsilon_1 Y + \epsilon_2 y\right) + D\left(\delta_1 XY + \delta_2 Xy + \delta_3 xY + \delta_4 xy\right), \end{aligned} \tag{6.2.15}$$

where $\epsilon_1 + \epsilon_2 = 1$ and $\delta_1 + \delta_2 + \delta_3 + \delta_4 = 1$. Roeger was able to give conditions on the coefficients so that the scheme (6.2.15) preserves the form $\frac{1}{xy} dx \wedge dy$.

Theorem 6.2.2 *If A, B, C, D, ϵ_i, and δ_i are real constants, and*

$$\delta_1\delta_3 = \delta_1\delta_4 = \delta_2\delta_4 = 0, \tag{6.2.16}$$

then the scheme (6.2.14) preserves the form $\frac{1}{xy} dx \wedge dy$.

The proof follows the methodology used by Sanz-Serna in [37]. The conditions of this theorem give a total of 65 methods which preserve the differential-form out of a total 110 possible combinations. Appropriate choices for the ϵ_i and δ_i can recover Kahan's method and Mounim and de Dormale's two methods:

$$(\epsilon_1,\ \epsilon_2,\ \delta_1,\ \delta_2,\ \delta_3,\ \delta_4) = \begin{cases} \left(\frac{1}{2},\ \frac{1}{2},\ 0,\ \frac{1}{2},\ \frac{1}{2},\ 0\right) & \text{(Kahan's Method)} \\ (1,\ 0,\ -1,\ 2,\ 0,\ 0) & \text{(Mounim and de Dormale, one)} \\ (2,\ -1,\ 0,\ 1,\ 0,\ 0) & \text{(Mounim and de Dormale, two)} \end{cases} \tag{6.2.17}$$

Note that the modified Explicit Euler method and Mickens' Method can not be classified according to this scheme. However, by removing the symmetry requirement under

the interchanges $x \leftrightarrow Y$ and $y \leftrightarrow X$, a more general scheme was developed using the same principles as above which could also classify the modified Explicit Euler method and Mickens' Method.

6.3 The Three-Dimensional Lotka-Volterra Predator-Prey Model

While the dynamics and numerical discretization of the two-dimensional Lotka-Volterra predator-prey model have been extensively investigated, there is substantially less research on the three-dimensional predator-prey model. These equations model the populations of three species in a food-chain, where each species is prey only to the species one step above it in the hierarchy. Formally, the model can be written as

$$\begin{cases} \dfrac{dx}{dt} = Ax - Bxy \\ \dfrac{dy}{dt} = -Cy + Dxy - Eyz \\ \dfrac{dz}{dt} = -Fz + Gyz, \end{cases} \tag{6.3.1}$$

where all parameters are positive. Here, x, y, and z represent the populations of the three species, where x is the bottom-level species and z is the top-level species. Also, $x(t)$, $y(t)$, and $z(t) \geq 0$ for all $t \geq 0$. The parameters A, B, C, and D are as in the two-dimensional model. The parameter F is the death rate of the species z, and in the absence of species y, the population of species z decreases exponentially. Also, there are two additional interaction factors Eyz and Gyz which account for the effect of consumption of species y by species z.

Chauvet et al. [11] proved that if $AG = BF$, then trajectories in x, y, z-phase-space

are closed curves so that the solutions are periodic. An example of such a trajectory is displayed below.

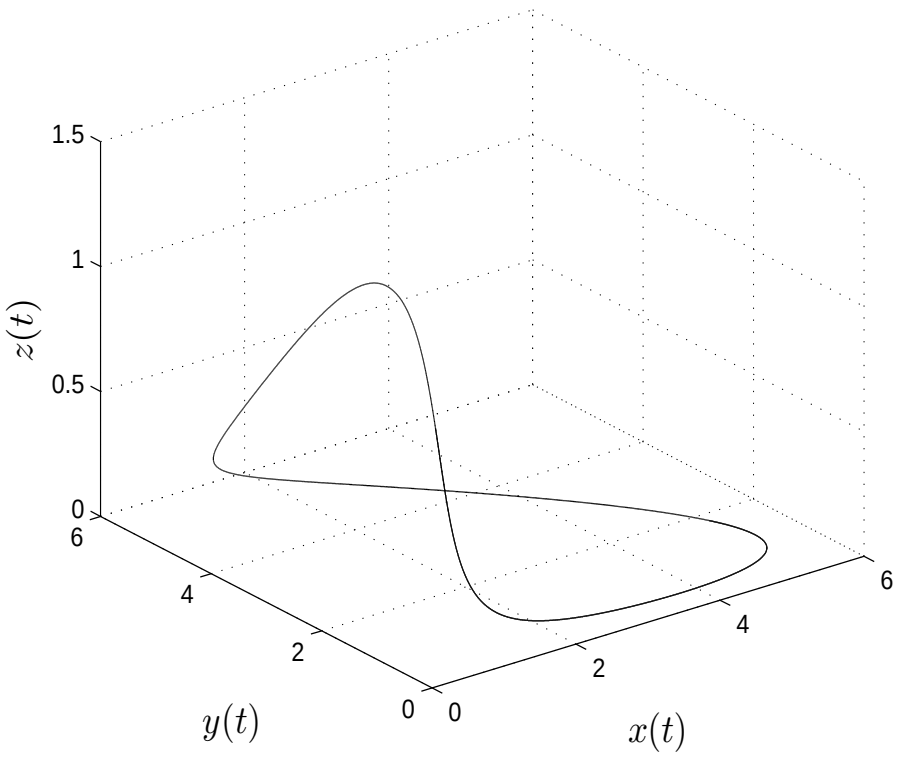

Figure 6.4: Phase-space diagram of a trajectory of the three-dimensional predator-prey model. $x_0 = 0.2$, $y_0 = 0.2$, $z_0 = 1$.

We can also see this periodicity when solutions are plotted as a function of time.

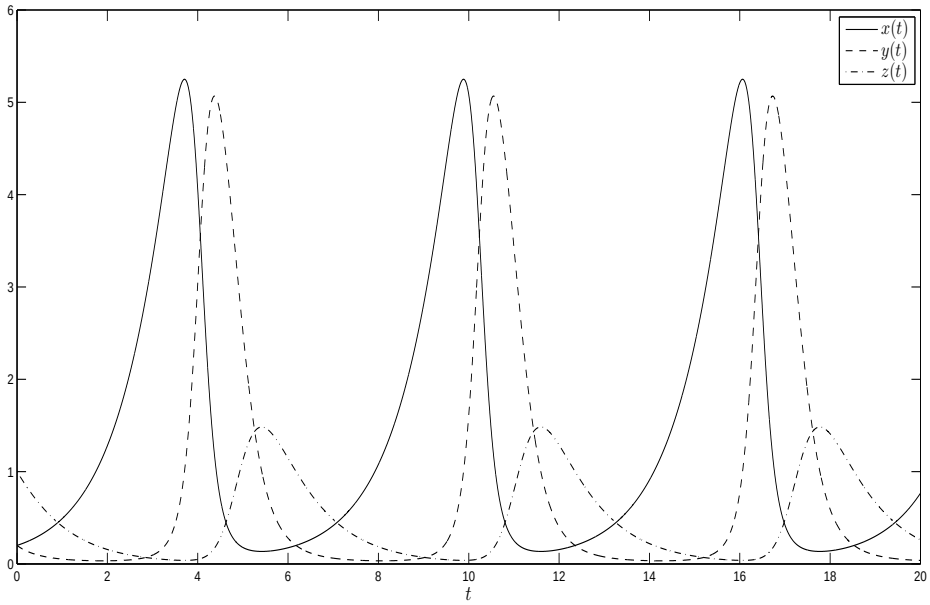

Figure 6.5: Plot of the populations of each species as a function of time. $x_0 = 0.2$, $y_0 = 0.2$, $z_0 = 1$.

Based on the above discussion, it is clear that any discretization of the three-dimensional Lotka-Volterra model should preserve the periodicity in x, y, z-space. However, standard finite-difference discretizations of the three-dimensional system exhibit problems similar to those exhibited in the two-dimensional case. For instance, the following figure displays solutions simulated with the explicit Euler method. As in the two-species model, the method produces spiralling instead of closed trajectories.

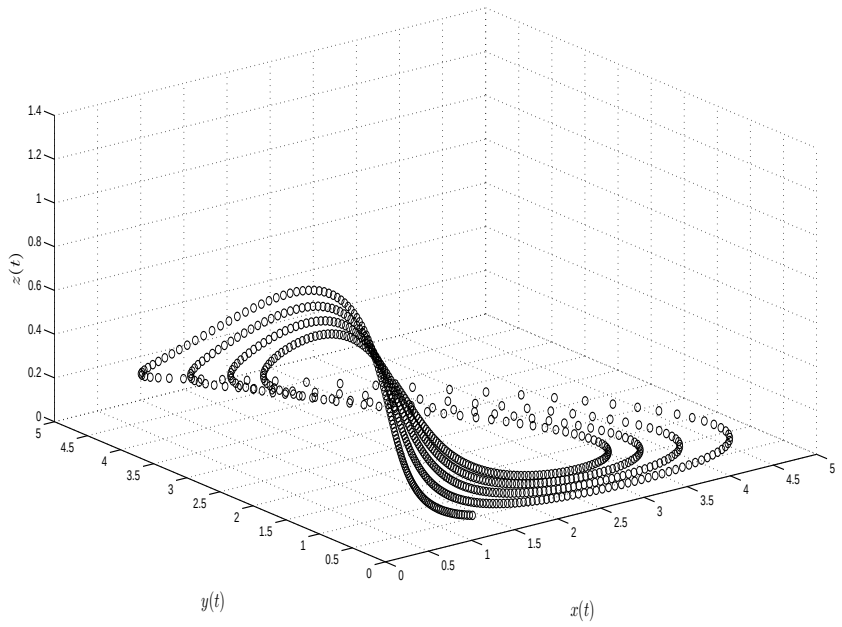

Figure 6.6: Simulation of a trajectory in phase-space using the explicit Euler method. $x_0 = 0.5$, $y_0 = 0.5$, $z_0 = 0.7, h = \frac{1}{30}$.

While there exist many NSFD methods which produce dynamically consistent discretizations for the two-dimensional Lotka-Volterra model, there is very little research on this topic for the three-dimensional case. It appears that the only published NSFD schemes which give periodicity-preserving simulations for the three-dimensional model are due to Bhowmik [6], who gave three particular discretizations and numerical demonstrations of these schemes. The lack of research on the three-dimensional Lotka-Volterra predator-prey model, both in the continuous and discrete setting, motivates the topic of Part II of this thesis.

6.4 Research Problem

The development of dynamically consistent discretizations for the two-dimensional Lotka-Volterra predator-prey model was facilitated by an understanding of the underlying Poisson structure of the equations. It is natural to suspect the same holds true for the three-dimensional case. As such, we first give a description of the geometry of the system through the framework of Poisson dynamics. Then, extending the method of Roeger [35], we develop a general class of NSFD schemes for the model. We show these schemes are dynamically consistent with the continuous model, in that they preserve the periodicity, Poisson bracket, and first integrals of the model. These propositions are supported with numerical simulations.

Chapter 7

Analysis and Numerical Integration of the Three-Species Lotka-Volterra Predator-Prey Model

In this chapter, we give the main results of Part II of this thesis, beginning with an analysis of the Poisson structure of the three-species predator-prey model. It is shown that this model is bi-Poisson; roughly speaking, this means that it has two distinct representations as a Poisson system. Similar to the two-species case, this has consequences for the geometry of the flow of solutions. Next, a general class of numerical integrators for the three-species model is proposed, and conditions are given so that the flow of the discrete methods preserves the geometry of the continuous model. It is demonstrated that the integrators developed are dynamically consistent with the continuous equations in several key respects: the integrators preserve the periodicity, first integrals, and Poisson bracket of the continuous system. This is demonstrated through a series of numerical simulations.

7.1 Continuous Dynamics of a Three-Dimensional Lotka-Volterra Predator-Prey Model

In this section, we study the Poisson structure of the three-dimensional Lotka-Volterra predator-prey model (6.3.1). As in the two-dimensional case, we will consider the normalized equations with $A = \ldots = G = 1$, so that our model is

$$\begin{cases} \dfrac{dx}{dt} = x - xy \\ \dfrac{dy}{dt} = -y + xy - yz \\ \dfrac{dz}{dt} = -z + yz. \end{cases} \tag{7.1.1}$$

Prior to stating the first result, we give the following definitions, adapted from [34].

Definition 7.1.1 *Let $\frac{du}{dt} = f(u)$ be a smooth differential equation defined on some open subset of $\mathbb{R}^n$. The system is called a **bi-Poisson system** if it can be written in two distinct ways as a Poisson system, i.e.,*

$$\frac{du}{dt} = B_1(u)\nabla H_1(u) = B_2(u)\nabla H_2(u), \tag{7.1.2}$$

where

1. *B_1 and B_2 are not constant multiples of each other, and the matrix $\alpha B_1 + \beta B_2$ is skew-symmetric and satisfies the Jacobi identity (5.3.13) for all $\alpha, \beta \in \mathbb{R}$.*

2. *H_1 and H_2 are functionally independent for all non-singular points of the vector field.*

Definition 7.1.2 *A **Poisson matrix** is a square matrix that can be written as the product of a skew-symmetric matrix and a symmetric matrix.*

The following theorem regarding Poisson matrices is proven in [33]:

Theorem 7.1.3 *An $n \times n$ matrix M is a Poisson matrix if and only if $M \sim -M$, i.e., there exists an invertible matrix T such that $M = -T^{-1}MT$.*

In the case of a three-dimensional differential system, there is an equivalent characterization of a bi-Poisson system due to Plank [34] which we will use.

Theorem 7.1.4 *A three-dimensional differential equation $\frac{du}{dt} = f(u)$ is a bi-Poisson system if and only if it admits two first integrals H_1 and H_2 such that ∇H_1 and ∇H_2 are (almost everywhere) linearly independent, and the Jacobian at every fixed point is a Poisson matrix.*

We are now in a position to state our first result.

Proposition 7.1.5 *The three-dimensional Lotka-Volterra predator-prey model (7.1.1) is a bi-Poisson system.*

Proof:

We use Theorem 7.1.4. Define

$$\begin{aligned} H_1 &= \ln x + \ln z \\ H_2 &= x + y + z - \ln x - \ln y. \end{aligned} \tag{7.1.3}$$

By (5.3.18), these are first integrals of $\frac{du}{dt} = f(u)$, since

$$\begin{aligned} (\nabla H_1)^T f(u) &= \begin{pmatrix} \frac{1}{x} & 0 & \frac{1}{z} \end{pmatrix} \begin{pmatrix} x - xy \\ -y + xy - yz \\ -z + yz \end{pmatrix} = 0, \quad \text{and} \\ (\nabla H_2)^T f(u) &= \begin{pmatrix} 1 - \frac{1}{x} & 1 - \frac{1}{y} & 1 \end{pmatrix} \begin{pmatrix} x - xy \\ -y + xy - yz \\ -z + yz \end{pmatrix} = 0. \end{aligned}$$

Moreover, we can show that ∇H_1 and ∇H_2 are linearly independent. Writing $c_1 \nabla H_1 + c_2 \nabla H_2 = 0$ as a linear system, we have

$$\begin{pmatrix} \frac{1}{x} & 1 - \frac{1}{x} \\ 0 & 1 - \frac{1}{y} \\ \frac{1}{z} & 1 \end{pmatrix} \begin{pmatrix} c_1 \\ c_2 \end{pmatrix} = \begin{pmatrix} 0 \\ 0 \\ 0 \end{pmatrix}. \tag{7.1.4}$$

After performing row operations, we obtain

$$\begin{pmatrix} 1 & 0 \\ 0 & 1 \\ 0 & 0 \end{pmatrix} \begin{pmatrix} c_1 \\ c_2 \end{pmatrix} = \begin{pmatrix} 0 \\ 0 \\ 0 \end{pmatrix},$$

so that $c_1 = c_2 = 0$, and hence ∇H_1 and ∇H_2 are linearly independent. We must now show that the Jacobian at every fixed point is a Poisson matrix. According to Chauvet et al. [11], in the region where $x(t)$, $y(t)$, $z(t) > 0$, the system (7.1.1) has a ray of fixed points parametrized by $\mu(s) = (s, 1, s-1)$ where $s > 1$. The Jacobian $\mathcal{J}(u)$ of (7.1.1) is

$$\mathcal{J}(u) = \begin{pmatrix} 1 - y & -x & 0 \\ y & x - 1 - z & -y \\ 0 & z & y - 1 \end{pmatrix}, \tag{7.1.5}$$

and evaluated at a fixed point $\mu(s)$ we have

$$\mathcal{J}(\mu(s)) = \begin{pmatrix} 0 & -s & 0 \\ 1 & 0 & -1 \\ 0 & s - 1 & 0 \end{pmatrix}.$$

We require an invertible matrix T so that $\mathcal{J}(\mu(s)) = -T^{-1} \mathcal{J}(\mu(s)) T$ for all $s > 1$

Define the matrix T by

$$T = \begin{pmatrix} -\frac{1}{s} & 1 & 1 \\ \frac{1}{s} & 1 & -\frac{1}{s} \\ 1 - \frac{1}{s} & \frac{1}{s} - 1 & 0 \end{pmatrix} \tag{7.1.6}$$

Note that

$$\det T = -1 - \frac{1}{s^3} + \frac{3}{s^2} - \frac{1}{s} = 0 \Rightarrow s = 1, -1 \pm \sqrt{2}$$

so that T is invertible when $s > 1$. By direct computation, for any $s > 1$ we have

$$-T^{-1}\mathcal{J}(\mu(s))T = -\begin{pmatrix} \frac{s}{s(s+2)-1} & \frac{s^2}{s(s+2)-1} & \frac{s^2(1+s)}{s(s^2+s-3)+1} \\ \frac{s}{s(s+2)-1} & \frac{s^2}{s(s+2)-1} & -\frac{s}{s(s+2)-1} \\ \frac{s(s+1)}{s(s+2)-1} & -\frac{s(s-1)}{s(s+2)-1} & \frac{2s^2}{s(s^2+s-3)+1} \end{pmatrix} \begin{pmatrix} 0 & -s & 0 \\ 1 & 0 & -1 \\ 0 & s-1 & 0 \end{pmatrix} \begin{pmatrix} -\frac{1}{s} & 1 & 1 \\ \frac{1}{s} & 1 & -\frac{1}{s} \\ 1-\frac{1}{s} & \frac{1}{s}-1 & 0 \end{pmatrix}$$
$$= \mathcal{J}(\mu(s))$$

and so by Theorem 7.1.3, The Jacobian at every fixed point is a Poisson matrix. Hence, by Theorem 7.1.4, system (7.1.1) is bi-Poisson. ■

While we have shown that (7.1.1) is bi-Poisson, we have not given the actual two distinct representations of $\frac{du}{dt}$ as a Poisson system. This is given in the following theorem.

Theorem 7.1.6 *Define the Poisson structure matrices*

$$B_1(u) = \begin{pmatrix} 0 & -xy & 0 \\ xy & 0 & -yz \\ 0 & yz & 0 \end{pmatrix} \tag{7.1.7}$$

and

$$B_2(u) = \begin{pmatrix} 0 & xy(1+z) & xz(1-y) \\ -xy(1+z) & 0 & xyz \\ -xz(1-y) & -xyz & 0 \end{pmatrix} \tag{7.1.8}$$

which are skew-symmetric and satisfy the Jacobi identity (5.3.13). Then we have

$$\frac{du}{dt} = B_1 \nabla H_2 = B_2 \nabla H_1, \tag{7.1.9}$$

where H_1 and H_2 are defined in (7.1.3).

Proof:

The equalities can be verified by direct calculation. ■

Given that the system (7.1.1) is bi-Poisson, we can define the two Poisson brackets of two functions υ and ω by

$$\begin{aligned} \{\upsilon, \omega\}_1 &= \nabla \upsilon^T B_1 \nabla \omega \\ \{\upsilon, \omega\}_2 &= \nabla \upsilon^T B_2 \nabla \omega. \end{aligned} \tag{7.1.10}$$

Doing so, we can write (7.1.1) in terms of the Poisson brackets as

$$\begin{cases} \dfrac{dx}{dt} = \{x, H_2\}_1 \\ \dfrac{dy}{dt} = \{y, H_2\}_1 \\ \dfrac{dz}{dt} = \{z, H_2\}_1 \end{cases} \tag{7.1.11}$$

or

$$\begin{cases} \dfrac{dx}{dt} = \{x, H_1\}_2 \\ \dfrac{dy}{dt} = \{y, H_1\}_2 \\ \dfrac{dz}{dt} = \{z, H_1\}_2 . \end{cases} \tag{7.1.12}$$

Note that due to the existence of two first integrals, solution trajectories of (7.1.1) must lie along the intersection of the two surfaces $H_1(x, y, z) = constant$ and $H_2(x, y, z) = constant$ [21]. For example, taking

$$H_1(x, y, z) = \ln(x) + \ln(z) = -1.5$$

$$H_2(x, y, z) = x + y + z - \ln(x) - \ln(y) = 3,$$

we obtain the following:

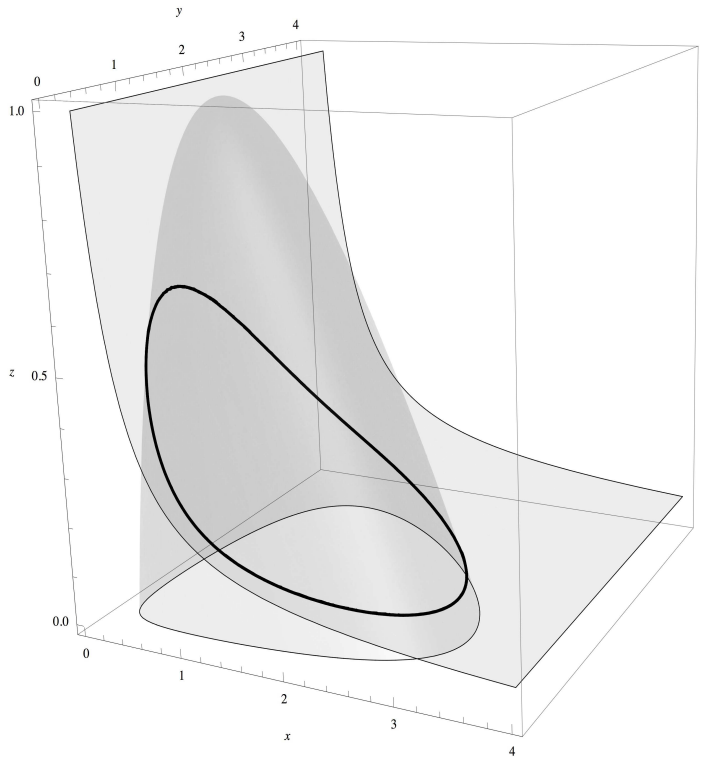

Figure 7.1: Plot of the surfaces $H_1(x, y, z) = \ln(x) + \ln(z) = -1.5$ and $H_2(x, y, z) = x + y + z - \ln(x) - \ln(y) = 3$. The solution trajectory is their intersection, highlighted in black.

As expected based on [11], the trajectory is a closed curve in phase-space.

The occurrence of periodic solutions to (7.1.1) as well as the existence of two first integrals suggests that the system may be integrable, as it is well-known that integrable systems typically exhibit more regular behavior as compared to non-integrable systems. More formally, we have the following definition from [24].

Definition 7.1.7 *For an n-dimensional Poisson system* $\frac{du}{dt} = B(u)\nabla H(u)$*, suppose the structure matrix* $B(u)$ *has constant rank* $2r$*. Then the system is* ***integrable*** *if it possesses* $n - r$ *independent involutive first integrals,* $n - 2r$ *of which are Casimir*

functions.

With this definition, we can show the following result:

Theorem 7.1.8 *The system (7.1.1) is integrable.*

Proof:

Calculating the row-echelon form of matrices B_1 and B_2, we obtain $\widetilde{B_1}$ and $\widetilde{B_2}$:

$$\widetilde{B_1} = \begin{pmatrix} 1 & 0 & -\frac{z}{x} \\ 0 & 1 & 0 \\ 0 & 0 & 0 \end{pmatrix}, \quad \widetilde{B_2} = \begin{pmatrix} 1 & 0 & -\frac{z}{z+1} \\ 0 & 1 & -\frac{z(y-1)}{y(z+1)} \\ 0 & 0 & 0 \end{pmatrix}.$$

This gives $\text{rank}(B_1) = \text{rank}(B_2) = 2$, so that $r = 1$. As shown in the proof of Proposition 7.1.5, system (7.1.1) possesses $n-r = 3-1 = 2$ independent first integrals, H_1 and H_2. We must show that these integrals are involutive, that is, $\{H_1, H_2\} = 0$. For completeness, we show this for both Poisson brackets defined in (7.1.10). By direct computation,

$$\begin{aligned} \{H_1, H_2\}_1 &= \nabla H_1^T B_1 \nabla H_2 \\ &= \begin{pmatrix} \frac{1}{x} & 0 & \frac{1}{z} \end{pmatrix} \begin{pmatrix} 0 & -xy & 0 \\ xy & 0 & -yz \\ 0 & yz & 0 \end{pmatrix} \begin{pmatrix} 1-\frac{1}{x} \\ 1-\frac{1}{y} \\ 1 \end{pmatrix} \\ &= 0 \end{aligned}$$

and

$$\begin{aligned} \{H_1, H_2\}_2 &= \nabla H_1^T B_2 \nabla H_2 \\ &= \begin{pmatrix} \frac{1}{x} & 0 & \frac{1}{z} \end{pmatrix} \begin{pmatrix} 0 & xy(1+z) & xz(1-y) \\ -xy(1+z) & 0 & xyz \\ -xz(1-y) & -xyz & 0 \end{pmatrix} \begin{pmatrix} 1-\frac{1}{x} \\ 1-\frac{1}{y} \\ 1 \end{pmatrix} \\ &= 0 \end{aligned}$$

Finally, $n - 2r = 3 - 2(1) = 1$, so by Theorem 5.3.11, we require one of the first integrals to be a Casimir function. By (5.3.20), H_1 is a Casimir of the system (7.1.1)

since

$$\nabla H_1^T B_1 = \begin{pmatrix} \frac{1}{x} & 0 & \frac{1}{z} \end{pmatrix} \begin{pmatrix} 0 & -xy & 0 \\ xy & 0 & -yz \\ 0 & yz & 0 \end{pmatrix} = \begin{pmatrix} 0 & 0 & 0 \end{pmatrix},$$

so that the three-dimensional Lotka-Volterra predator-prey system is integrable. ■

The occurrence of two first integrals also suggests that system (7.1.1) may possess not only a Poisson structure, but also a Nambu structure. Nambu dynamics, introduced in [32], are a generalization of Hamiltonian dynamics to the case when there exist multiple Hamiltonian functions. More formally, we have the following definition:

Definition 7.1.9 *Let $u \in U$ and let H_1, $H_2 : U \to \mathbb{R}$ be two functions, where $U \subset \mathbb{R}^n$. A **Nambu system** is one which can be written in the form*

$$\frac{du}{dt} = \nabla H_1(u) \times \nabla H_2(u). \tag{7.1.13}$$

Before investigating the Nambu structure of system (7.1.1), we state the following theorem from [20].

Theorem 7.1.10 *Let $\frac{du}{dt} = B(u)\nabla H(u)$ be a Poisson system, and let $w = \upsilon(u)$ be a change of coordinates. Then in the new coordinates, the Poisson system can be written in the form $\frac{dw}{dt} = \widetilde{B}(w)\nabla K(w)$, where $\widetilde{B}(w) = \upsilon'(u)B(u)\upsilon'(u)^T$, $K(w) = H(u)$, and $\upsilon'(u)$ is the Jacobian matrix of the coordinate transformation, $\frac{\partial w}{\partial u}$.*

For the bi-Poisson system (7.1.9), suppose we make the coordinate transformation

$$w = \begin{pmatrix} \alpha \\ \beta \\ \gamma \end{pmatrix} = \begin{pmatrix} \ln x \\ \ln y \\ \ln z \end{pmatrix} = \upsilon(u). \tag{7.1.14}$$

By the previous theorem, we obtain the new structure matrices

$$\begin{aligned}\widetilde{B_1}(w) &= v'(u)B_1(u)v'(u)^T \\ &= \begin{pmatrix} \frac{1}{x} & 0 & 0 \\ 0 & \frac{1}{y} & 0 \\ 0 & 0 & \frac{1}{z} \end{pmatrix} \begin{pmatrix} 0 & -xy & 0 \\ xy & 0 & -yz \\ 0 & yz & 0 \end{pmatrix} \begin{pmatrix} \frac{1}{x} & 0 & 0 \\ 0 & \frac{1}{y} & 0 \\ 0 & 0 & \frac{1}{z} \end{pmatrix} \\ &= \begin{pmatrix} 0 & -1 & 0 \\ 1 & 0 & -1 \\ 0 & 1 & 0 \end{pmatrix}\end{aligned} \tag{7.1.15}$$

and

$$\begin{aligned}\widetilde{B_2}(w) &= v'(u)B_2(u)v'(u)^T \\ &= \begin{pmatrix} \frac{1}{x} & 0 & 0 \\ 0 & \frac{1}{y} & 0 \\ 0 & 0 & \frac{1}{z} \end{pmatrix} \begin{pmatrix} 0 & xy(1+z) & xz(1-y) \\ -xy(1+z) & 0 & xyz \\ -xz(1-y) & -xyz & 0 \end{pmatrix} \begin{pmatrix} \frac{1}{x} & 0 & 0 \\ 0 & \frac{1}{y} & 0 \\ 0 & 0 & \frac{1}{z} \end{pmatrix} \\ &= \begin{pmatrix} 0 & z+1 & -(y-1) \\ -(z+1) & 0 & x \\ y-1 & -x & 0 \end{pmatrix} \\ &= \begin{pmatrix} 0 & e^{\alpha}+1 & -(e^{\beta}-1) \\ -(e^{\alpha}+1) & 0 & e^{\alpha} \\ e^{\beta}-1 & -e^{\alpha} & 0 \end{pmatrix},\end{aligned} \tag{7.1.16}$$

as well as the new Hamiltonian functions

$$\begin{aligned}K_1(w) &= K_1(\alpha,\beta,\gamma) = \alpha+\gamma, \\ K_2(w) &= K_2(\alpha,\beta,\gamma) = e^{\alpha}-\alpha+e^{\beta}-\beta+e^{\gamma}.\end{aligned} \tag{7.1.17}$$

Hence, we can write the system in the new coordinates as

$$\frac{dw}{dt} = \begin{pmatrix} \frac{d\alpha}{dt} \\ \frac{d\beta}{dt} \\ \frac{d\gamma}{dt} \end{pmatrix} = \widetilde{B_1}(w)\nabla K_2(w) = \widetilde{B_2}(w)\nabla K_1(w) = \begin{pmatrix} 1-e^{\beta} \\ e^{\alpha}-e^{\gamma}-1 \\ e^{\beta}-1 \end{pmatrix}. \tag{7.1.18}$$

In this new coordinate system, we have the following theorem.

Theorem 7.1.11 *The system (7.1.18) is a Nambu system.*

Proof:

By direct calculation,

$$\nabla K_1(w) \times \nabla K_2(w) = \begin{pmatrix} 1 \\ 0 \\ 1 \end{pmatrix} \times \begin{pmatrix} e^{\alpha}-1 \\ e^{\beta}-1 \\ e^{\gamma} \end{pmatrix} = \begin{pmatrix} 1-e^{\beta} \\ e^{\alpha}-e^{\gamma}-1 \\ e^{\beta}-1 \end{pmatrix} = \frac{dw}{dt},$$

where $w = (\alpha, \beta, \gamma)^T$. Hence, by definition (7.1.9), the system is Nambu. ■

Note that the goal is to understand the underlying geometry of the flow of the three-dimensional Lotka-Volterra predator-prey model. Given that this system becomes Nambu after a coordinate change allows us to obtain the following result regarding the flow of the model, which bears obvious resemblence to (6.1.11).

Theorem 7.1.12 *The system (7.1.1) preserves the weighted volume-form*

$$\frac{1}{xyz} dx \wedge dy \wedge dz. \tag{7.1.19}$$

Proof:

Taking the divergence of the Nambu system (7.1.18), we have

$$\begin{aligned} \nabla \cdot (\nabla K_1 \times \nabla K_2) &= \nabla K_2 \cdot (\nabla \times (\nabla K_1)) - \nabla K_1 \cdot (\nabla \times (\nabla K_2)) \\ &= \nabla K_2 \cdot (\operatorname{curl}(\nabla K_1)) - \nabla K_1 \cdot (\operatorname{curl}(\nabla K_2)) \\ &= 0, \end{aligned}$$

as the curl of the gradient is zero. Since the system is divergence-free, by Liouville's Theorem, the field (7.1.18) is volume-preserving. That is, the system preserves the volume-form $d\alpha \wedge d\beta \wedge d\gamma$. By the properties of differential forms [7], we have

$$\begin{aligned} d\alpha \wedge d\beta \wedge d\gamma &= d(\ln x) \wedge d(\ln y) \wedge d(\ln z) \\ &= \frac{1}{x} dx \wedge \frac{1}{y} dy \wedge \frac{1}{z} dz && \text{(exterior differentiation)} \\ &= \frac{1}{xyz} (dx \wedge dy \wedge dz) && \text{(linearity)}, \end{aligned}$$

so that the system (7.1.1) preserves the form

$$\frac{1}{xyz} dx \wedge dy \wedge dz. \quad ■ \tag{7.1.20}$$

To summarize, we have identified a number of important properties regarding system (7.1.1):

- Solutions are periodic.
- The system preserves the weighted differential-form (7.1.20).
- The system is Poisson, so that by Theorem 5.3.13, its flow is a Poisson map.
- The system possesses two first integrals, H_1 and H_2, defined in (7.1.3).

Any discretization of the system should aim to preserve these properties.

7.2 A Class of Integrators for the Model

In this section, we derive a class of NSFD schemes for the numerical integration of the three-dimensional Lotka-Volterra system (6.3.1). These schemes will later be shown to be dynamically consistent with the continuous model, thus providing more accurate simulations. To do so, we adapt the methods of Roeger [35] to the three-dimensional case to construct a class of integrators which preserve the same weighted differential-form (7.1.20) which is preserved by the flow of the continuous system. As evidence of the importance of requiring a scheme to preserve this form, consider the explicit Euler method, which was shown in Figure 6.6 to produce inaccurate solutions for (6.3.1) that spiral from the initial conditions. We show that this method does not preserve (7.1.20), meaning that its flow does not behave similarly to the flow of (6.3.1). As a consequence, the periodicity of the solutions is not preserved.

Proposition 7.2.1 *The explicit Euler method applied to the system (6.3.1) produces a discretization which does not preserve the weighted differential-form (7.1.20).*

Proof:

Suppose for contradiction that (7.1.20) is preserved so that

$$\frac{1}{xyz}dx \wedge dy \wedge dz = \frac{1}{XYZ}dX \wedge dY \wedge dZ. \tag{7.2.1}$$

By (5.2.9), the discrete scheme is given by

$$\begin{cases} X = (1 + h - hy)x \\ \\ Y = (1 - h + hx - hz)y \\ \\ Z = (1 - h - hy)z. \end{cases} \tag{7.2.2}$$

Differentiating each equation, we obtain

$$\begin{cases} dX = (1 + h - hy)dx + (-hx)dy \\ \\ dY = (hy)dx + (1 - h + hx - hz)dy + (-hy)dz \\ \\ dZ = (hz)dy + (1 - h + hy)dz. \end{cases} \tag{7.2.3}$$

Equivalently, we can write this as

$$\begin{pmatrix} 1 & 0 & 0 \\ 0 & 1 & 0 \\ 0 & 0 & 1 \end{pmatrix} \begin{pmatrix} dX \\ dY \\ dZ \end{pmatrix} = \begin{pmatrix} 1 + h - hy & -hx & 0 \\ hy & 1 - h + hx - hz & -hy \\ 0 & hz & 1 - h + hy \end{pmatrix} \begin{pmatrix} dx \\ dy \\ dz \end{pmatrix}.$$

Now, taking the wedge product of these three equations, we obtain

$$\begin{vmatrix} 1 & 0 & 0 \\ 0 & 1 & 0 \\ 0 & 0 & 1 \end{vmatrix} dX \wedge dY \wedge dZ = \begin{vmatrix} 1 + h - hy & -hx & 0 \\ hy & 1 - h + hx - hz & -hy \\ 0 & hz & 1 - h + hy \end{vmatrix} dx \wedge dy \wedge dz,$$

which reduces to

$$\begin{aligned} dX \wedge dY \wedge dZ = \big(&h^2xy(1 - h + hy) \\ &+ (1 + h - hy)\left[(1 - h + hx - hz)(1 - h + hy) + h^2yz\right]\big) dx \wedge dy \wedge dz. \end{aligned} \tag{7.2.4}$$

Alternatively, multiplying the three equations (7.2.2) gives

$$XYZ = (1 + h - hy)(1 - h + hx - hz)(1 - h + hy)xyz. \tag{7.2.5}$$

Now, multiplying (7.2.4) and (7.2.5), we see that the form (7.1.20) is preserved if for any $x, y, z, h > 0$, we have

$$\begin{aligned} &\left(h^2xy(1 - h + hy) + (1 + h - hy)\left[(1 - h + hx - hz)(1 - h + hy) + h^2yz\right]\right) \\ &\quad = (1 + h - hy)(1 - h + hx - hz)(1 - h + hy), \end{aligned} \tag{7.2.6}$$

or equivalently,

$$h^2\left[xy(1 - h + hy) + yz(1 + h - hy)\right] = 0. \tag{7.2.7}$$

However, this is clearly not true ($x = y = z = 1$ serves as a counter-example), and the proposition is proven. ■

To begin constructing a class of more accurate discretizations, we note the symmetry in the equations of the normalized Lotka-Volterra system

$$\begin{cases} \dfrac{dx}{dt} = x - xy & = p(x, y, z) \\ \dfrac{dy}{dt} = -y + xy - yz & = q(x, y, z) \\ \dfrac{dz}{dt} = -z + yz & = r(x, y, z). \end{cases}$$

In particular, the first and third equation satisfy

$$p(z, y, x) = -r(x, y, z) \quad \text{and} \quad r(z, y, x) = -p(x, y, z).$$

Analogous to the two-dimensional case, the right-hand side of the first and third equation in our normalized discretization should transform into the opposite of the other under the interchanges $x \leftrightarrow Z$ and $z \leftrightarrow X$.

This symmetry is preserved by our proposed scheme for the three-dimensional Lotka-Volterra model:

$$\begin{cases} \dfrac{X-x}{h} = A(a_1x + a_2X) - B(b_1xy + b_2Xy + b_3xY + b_4XY) \\ \dfrac{Y-y}{h} = -C(c_1y + c_2Y) + D(d_1xy + d_2Xy + d_3xY + d_4XY) \\ \qquad\qquad - E(e_1yz + e_2Yz + e_3yZ + e_4YZ) \\ \dfrac{Z-z}{h} = -F(a_1Z + a_2z) + G(b_3Zy + b_4zy + b_1ZY + b_2zY), \end{cases} \tag{7.2.8}$$

where

$$\begin{cases} a_1 + a_2 = 1 \\ b_1 + b_2 + b_3 + b_4 = 1 \\ c_1 + c_2 = 1 \\ d_1 + d_2 + d_3 + d_4 = 1 \\ e_1 + e_2 + e_3 + e_4 = 1. \end{cases} \tag{7.2.9}$$

We can now state the main result of this section, which gives the conditions on the parameters so that the scheme (7.2.8) preserves the form (7.1.20).

Theorem 7.2.2 *Let*

$$\boldsymbol{v_1} = \begin{pmatrix} d_1 \\ d_3 \\ e_3 \\ e_4 \end{pmatrix} \quad \text{and} \quad \boldsymbol{v_2} = \begin{pmatrix} d_2 \\ d_4 \\ e_1 \\ e_2 \end{pmatrix}.$$

If $A, B, C, D, E, F, G, a_i, b_i, c_i, d_i$, and e_i are real constants, the conditions (7.2.9) are satisfied, and

$$b_1\boldsymbol{v_1} = b_2\boldsymbol{v_1} = b_3\boldsymbol{v_2} = b_4\boldsymbol{v_2} = \begin{pmatrix} 0 \\ 0 \\ 0 \\ 0 \end{pmatrix}, \tag{7.2.10}$$

then the scheme (7.2.8) preserves the form (7.1.20).

Proof:

We require

$$\frac{1}{xyz}dx \wedge dy \wedge dz = \frac{1}{XYZ}dX \wedge dY \wedge dZ,$$

and so we need two functions $S(x, y, z, X, Y, Z)$ and $T(x, y, z, X, Y, Z)$ which satisfy the two equalities

$$S(x, y, z, X, Y, Z)dX \wedge dY \wedge dZ = T(x, y, z, X, Y, Z)dx \wedge dy \wedge dz$$

$$S(x, y, z, X, Y, Z)XYZ = T(x, y, z, X, Y, Z)xyz.$$

To begin, rearrange the equations (7.2.8) to obtain

$$\begin{cases} \overbrace{(1 - Aa_2h + Bb_2hy + Bb_4hY)}^{L_1} X \\ \qquad = \overbrace{(1 + Aa_1h - Bb_1hy - Bb_3hY)}^{R_1} x \\ \overbrace{(1 + Cc_2h - Dd_3hx - Dd_4hX + Ee_2hz + Ee_4hZ)}^{L_2} Y \\ \qquad = \overbrace{(1 - Cc_1h + Dd_1hx + Dd_2hX - Ee_1hz - Ee_3hZ)}^{R_2} y \\ \overbrace{(1 + Fa_1h - Gb_3hy - Gb_1hY)}^{L_3} Z \\ \qquad = \overbrace{(1 - Fa_2h + Gb_4hy + Gb_2hY)}^{R_3} z. \end{cases} \tag{7.2.11}$$

Multiplying these three equations, we obtain

$$S(x, y, z, X, Y, Z) = L_1L_2L_3 \quad \text{and} \quad T(x, y, z, X, Y, Z) = R_1R_2R_3. \tag{7.2.12}$$

Now, differentiate and rearrange the equations (7.2.8) to obtain

$$\begin{cases} \overbrace{(1-Aa_2h+Bb_2hy+Bb_4hY)}^{\alpha_x}\,dX+\overbrace{(Bb_3hx+Bb_4hX)}^{\alpha_y}\,dY+\overbrace{(0)}^{\alpha_z}\,dZ \\ \qquad=\overbrace{(1+Aa_1h-Bb_1hy-Bb_3hY)}^{\overline{\alpha}_x}\,dx+\overbrace{(-Bb_1hx-Bb_2hX)}^{\overline{\alpha}_y}\,dy+\overbrace{(0)}^{\overline{\alpha}_z}\,dz \\ \overbrace{(-Dd_2hy-Dd_4hY)}^{\beta_x}\,dX+\overbrace{(1+Cc_2h-Dd_3hx-Dd_4hX+Ee_2hz+Ee_4hZ)}^{\beta_y}\,dY \\ \qquad+\overbrace{(Ee_3hy+Ee_4hY)}^{\beta_z}\,dZ \\ \qquad=\overbrace{(Dd_1hy+Dd_3hY)}^{\overline{\beta}_x}\,dx+\overbrace{(1-Cc_1h+Dd_1hx+Dd_2hX-Ee_1hz-Ee_3hZ)}^{\overline{\beta}_y}\,dy \\ \qquad+\overbrace{(-Ee_1hy-Ee_2hY)}^{\overline{\beta}_z}\,dz \\ \overbrace{(0)}^{\gamma_x}\,dX+\overbrace{(-Gb_1hZ-Gb_2hz)}^{\gamma_y}\,dY+\overbrace{(1+Fa_1h-Gb_3hy-Gb_1hY)}^{\gamma_z}\,dZ \\ \qquad=\overbrace{(0)}^{\overline{\gamma}_x}\,dx+\overbrace{(Gb_3hZ+Gb_4hz)}^{\overline{\gamma}_y}\,dy+\overbrace{(1-Fa_2h+Gb_4hy+Gb_2hY)}^{\overline{\gamma}_z}\,dz. \end{cases} \tag{7.2.13}$$

We can write this compactly as

$$\begin{pmatrix}\alpha_x & \alpha_y & \alpha_z\\ \beta_x & \beta_y & \beta_z\\ \gamma_x & \gamma_y & \gamma_z\end{pmatrix}\begin{pmatrix}dX\\ dY\\ dZ\end{pmatrix}=\begin{pmatrix}\overline{\alpha}_x & \overline{\alpha}_y & \overline{\alpha}_z\\ \overline{\beta}_x & \overline{\beta}_y & \overline{\beta}_z\\ \overline{\gamma}_x & \overline{\gamma}_y & \overline{\gamma}_z\end{pmatrix}\begin{pmatrix}dx\\ dy\\ dz\end{pmatrix}. \tag{7.2.14}$$

Taking the wedge product of these three equations gives

$$\begin{vmatrix}\alpha_x & \alpha_y & \alpha_z\\ \beta_x & \beta_y & \beta_z\\ \gamma_x & \gamma_y & \gamma_z\end{vmatrix}dX\wedge dY\wedge dZ=\begin{vmatrix}\overline{\alpha}_x & \overline{\alpha}_y & \overline{\alpha}_z\\ \overline{\beta}_x & \overline{\beta}_y & \overline{\beta}_z\\ \overline{\gamma}_x & \overline{\gamma}_y & \overline{\gamma}_z\end{vmatrix}dx\wedge dy\wedge dz, \tag{7.2.15}$$

so that

$$\begin{aligned} S(x,y,z,X,Y,Z)&=\begin{vmatrix}\alpha_x & \alpha_y & \alpha_z\\ \beta_x & \beta_y & \beta_z\\ \gamma_x & \gamma_y & \gamma_z\end{vmatrix}\\ T(x,y,z,X,Y,Z)&=\begin{vmatrix}\overline{\alpha}_x & \overline{\alpha}_y & \overline{\alpha}_z\\ \overline{\beta}_x & \overline{\beta}_y & \overline{\beta}_z\\ \overline{\gamma}_x & \overline{\gamma}_y & \overline{\gamma}_z\end{vmatrix}. \end{aligned} \tag{7.2.16}$$

Comparing (7.2.12) and (7.2.16), we must have

$$L_1L_2L_3 = \begin{vmatrix} \alpha_x & \alpha_y & \alpha_z \\ \beta_x & \beta_y & \beta_z \\ \gamma_x & \gamma_y & \gamma_z \end{vmatrix}, \tag{7.2.17}$$

and

$$R_1R_2R_3 = \begin{vmatrix} \overline{\alpha}_x & \overline{\alpha}_y & \overline{\alpha}_z \\ \overline{\beta}_x & \overline{\beta}_y & \overline{\beta}_z \\ \overline{\gamma}_x & \overline{\gamma}_y & \overline{\gamma}_z \end{vmatrix}, \tag{7.2.18}$$

or equivalently,

$$L_1L_2L_3 - \begin{vmatrix} \alpha_x & \alpha_y & \alpha_z \\ \beta_x & \beta_y & \beta_z \\ \gamma_x & \gamma_y & \gamma_z \end{vmatrix} = 0, \tag{7.2.19}$$

and

$$R_1R_2R_3 - \begin{vmatrix} \overline{\alpha}_x & \overline{\alpha}_y & \overline{\alpha}_z \\ \overline{\beta}_x & \overline{\beta}_y & \overline{\beta}_z \\ \overline{\gamma}_x & \overline{\gamma}_y & \overline{\gamma}_z \end{vmatrix} = 0. \tag{7.2.20}$$

After simplification using *Mathematica*, (7.2.19) reduces to

$$\begin{aligned} 0 = {} & b_3d_2(BDh^2xy + BDFa_1h^3xy - BDGb_3h^3xy^2 - BDGb_1h^3xyY) \\ & + b_4d_2(BDh^2Xy + BDFa_1h^3Xy - BDGb_1h^3XyY) \\ & + b_3d_4(BDh^2xY + BDFa_1h^3xY - BDGb_3h^3xyY - BDGb_1h^3xY^2) \\ & + b_4d_4(BDh^2XY + BDFa_1h^3XY - BDGb_1h^3XY^2) \\ & - b_3b_4d_2(BDGh^3Xy^2) - b_3b_4d_4(DGh^3XyY) \\ & + b_2e_3(EGh^2yz - AEGa_2h^3yz + BEGb_2h^3y^2z + BEGb_4h^3yYz) \\ & + b_2e_4(EGh^2Yz - AEGa_2h^3Yz + BEGb_2h^3yYz + BEGb_4h^3Y^2z) \\ & + b_1e_3(EGh^2yZ - AEGa_2h^3yZ + BEGb_4h^3yYZ) \\ & + b_1e_4(EGh^2YZ - AEGa_2h^3YZ + BEGb_4h^3Y^2Z) \\ & + b_1b_2e_3(BEGh^3y^2Z) + b_1b_2e_4(BEGh^3yYZ), \end{aligned} \tag{7.2.21}$$

which will be true if

$$b_3d_2 = b_4d_2 = b_3d_4 = b_4d_4 = b_2e_3 = b_2e_4 = b_1e_3 = b_1e_4 = 0.$$

Similarly, after simplification with *Mathematica*, (7.2.20) reduces to

$$\begin{aligned}
0 = {} & b_1d_1(BDh^2xy - BDFa_2h^3xy + BDGb_4h^3xy^2) \\
& + b_2d_1(BDh^2Xy - BDFa_2h^3Xy + BDGb_4h^3Xy^2 + BDGb_2h^3XyY) \\
& + b_1d_3(BDh^2xY - BDFa_2h^3xY + BDGb_4h^3xyY) \\
& + b_2d_3(BDh^2XY - BDFa_2h^3XY + BDGb_4h^3XyY + BDGb_2h^3XY^2) \\
& + b_1b_2d_1(BDGh^3xyY) + b_1b_2d_3(BDGh^3xY^2) \\
& + b_4e_1(EGh^2yz + AEGa_1h^3yz - BEGb_1h^3y^2z) \\
& + b_4e_2(EGh^2Yz + AEGa_1h^3Yz - BEGb_1h^3yYz) \\
& + b_3e_1(EGh^2yZ + AEGa_1h^3yZ - BEGb_1h^3y^2Z - BEGb_3h^3yYZ) \\
& + b_3e_2(EGh^2YZ + AEGa_1h^3YZ - BEGb_1h^3yYZ - BEGb_3h^3Y^2Z) \\
& - b_3b_4e_1(BEGh^3yYz) - b_3b_4e_2(BEGh^3Y^2z),
\end{aligned} \tag{7.2.22}$$

which will hold if

$$b_1d_1 = b_2d_1 = b_1d_3 = b_2d_3 = b_4e_1 = b_4e_2 = b_3e_1 = b_3e_2 = 0,$$

and the result is proven. ■

At this point, we have given a general class of NSFD integrators for the three-dimensional Lotka-Volterra predator-prey model which preserve the differential form (7.1.20), and hence should preserve the periodicity of the solutions. We can show that the conditions (7.2.9) and (7.2.10) give the following result:

Proposition 7.2.3 *Any scheme (7.2.8) satisfying the conditions (7.2.9) and (7.2.10) must be explicit.*

Proof:

There are two possible cases to consider. First, suppose that at least one of b_3 and b_4 is non-zero. Then from (7.2.10), we have

$$d_2 = d_4 = e_1 = e_2 = 0$$

and (7.2.9) gives

$$\begin{cases} d_1 + d_3 = 1 \\ \\ e_3 + e_4 = 1. \end{cases}$$

Combining this with (7.2.10) we obtain

$$0 = b_1 d_1 = b_1(1 - d_3) = b_1 - b_1 d_3 = b_1$$

and

$$0 = b_2 d_1 = b_2(1 - d_3) = b_2 - b_2 d_3 = b_2$$

so that

$$b_3 + b_4 = 1.$$

Summarizing, we have

$$\begin{cases} a_1 + a_2 = b_3 + b_4 = c_1 + c_2 = d_1 + d_3 = e_3 + e_4 = 1 \\ \\ b_1 = b_2 = d_2 = d_4 = e_1 = e_2 = 0, \end{cases} \tag{7.2.23}$$

and the scheme (7.2.8) reads

$$\begin{cases} X = \dfrac{1 + Aa_1 h - Bb_3 hY}{1 - A(1 - a_1)h + B(1 - b_3)hY} x \\ Y = \dfrac{1 - Cc_1 h + Dd_1 hx - Ee_3 hZ}{1 + C(1 - c_1)h - D(1 - d_1)hx + E(1 - e_3)hZ} y \\ Z = \dfrac{1 - F(1 - a_1)h + G(1 - b_3)hy}{1 + Fa_1 h - Gb_3 hy} z. \end{cases} \tag{7.2.24}$$

The third equation of (7.2.24) does not contain the terms X or Y, and the second equation of (7.2.24) does not contain the term X so that the scheme is explicit.

Alternatively, suppose that both $b_3 = b_4 = 0$. Then by (7.2.9) we have

$$b_1 + b_2 = 1$$

so that from (7.2.10) we obtain

$$\begin{cases} 0 = b_1 d_1 = (1 - b_2) d_1 = d_1 - b_2 d_1 = d_1 \\ 0 = b_1 d_3 = (1 - b_2) d_3 = d_3 - b_2 d_3 = d_3 \\ 0 = b_1 e_3 = (1 - b_2) e_3 = e_3 - b_2 e_3 = e_3 \\ 0 = b_1 e_4 = (1 - b_2) e_4 = e_4 - b_2 e_4 = e_4. \end{cases}$$

Summarizing, we have

$$\begin{cases} a_1 + a_2 = b_1 + b_2 = c_1 + c_2 = d_2 + d_4 = e_1 + e_2 = 1 \\ b_3 = b_4 = d_1 = d_3 = e_3 = e_4 = 0, \end{cases} \tag{7.2.25}$$

and the scheme (7.2.8) reads

$$\begin{cases} X = \dfrac{1 + A a_1 h - B b_1 h y}{1 - A(1 - a_1) h + B(1 - b_1) h y} x \\ Y = \dfrac{1 - C c_1 h + D d_2 h X - E e_1 h z}{1 + C(1 - c_1) h - D(1 - d_2) h X + E(1 - e_1) h z} y \\ Z = \dfrac{1 - F(1 - a_1) h + G(1 - b_1) h Y}{1 + F a_1 h - G b_1 h Y} z. \end{cases} \tag{7.2.26}$$

The first equation of (7.2.26) does not contain the terms Y or Z, and the second equation of (7.2.26) does not contain the term Z so that the scheme is explicit. ■

For the remainder of this thesis, we will work with the explicit scheme (7.2.26) for simplicity. Analogous calculations show that the following results hold for the scheme (7.2.24) as well.

7.3 Dynamic Consistency of the Integrators and the Model

Recall that at the conclusion of §7.1, a list of important properties regarding system (7.1.1) was given. Ideally, these properties would be preserved by a discretization of

the model. In this section, we investigate which of these properties are preserved by the explicit scheme (7.2.26) developed in the previous section. To begin, note that the scheme preserves the weighted differential-form (7.1.20), as it was constructed to do so. As a result, solutions given by the discretization should be periodic, which will be seen in the next section. Now, the system (7.1.1) is also Poisson, and possesses two first integrals H_1 and H_2. While these properties are not preserved exactly, we can show that when the step-size is small, they are preserved approximately. To make this more precise, we introduce several definitions.

Definition 7.3.1 *The numerical method $\psi_h(u_n) = u_{n+1}$ preserves the perturbed function $H(u)$ if*

$$H(u_{n+1}) = H(u_n) + G(u_n, u_{n+1}),$$

where

$$\lim_{h\to 0} G(u_n, u_{n+1}) = 0.$$

Equivalently, we have

$$\lim_{h\to 0} \left(H(u_{n+1}) - H(u_n)\right) = 0.$$

Now since the system (7.1.1) was shown to be Poisson, by Theorem 5.3.13, its flow must be a Poisson map which respects the Casimir function H_1. The discrete analogy to a Poisson map is a Poisson integrator, defined in Definition 5.3.14. Here, we give the corresponding perturbed Poisson integrator definition:

Definition 7.3.2 *The numerical method $\psi_h(u_n) = u_{n+1}$ is a perturbed Poisson inte-*

grator for the system $\frac{du}{dt} = B(u)\nabla H(u)$ *if it preserves the perturbed Casimir functions, and if*

$$\lim_{h\to 0}\left(\left[\left(\frac{\partial u_{n+1}}{\partial u_n}\right)B(u_n)\left(\frac{\partial u_{n+1}}{\partial u_n}\right)^T\right] - B(u_{n+1})\right) = 0$$

To begin, we consider the two first integrals.

Proposition 7.3.3 *The scheme (7.2.26) preserves the two perturbed first integrals* H_1 *and* H_2 *defined in (7.1.3).*

Proof:

Beginning with H_1, we must show that

$$\lim_{h\to 0}(\ln X + \ln Z - \ln x - \ln z) = 0.$$

From (7.2.26), we have

$$\begin{aligned}\ln X + \ln Z - \ln x - \ln z &= \ln\left(\frac{1 + Aa_1h - Bb_1hy}{1 - A(1-a_1)h + B(1-b_1)hy}x\right)\\ &\quad + \ln\left(\frac{1 - F(1-a_1)h + G(1-b_1)hY}{1 + Fa_1h - Gb_1hY}z\right) - \ln x - \ln z\\ &= \ln(1 + h(Aa_1 - Bb_1y)) - \ln(1 - h(A(1-a_1) - B(1-b_1)y))\\ &\quad + \ln(1 - h(F(1-a_1) - G(1-b_1)Y)) - \ln(1 + h(Fa_1 - Gb_1Y))\\ &\quad + \ln x + \ln z - \ln x - \ln z.\end{aligned}$$

Taking limits, we see

$$\lim_{h\to 0}(\ln(1 + h(Aa_1 - Bb_1y))) = \ln(1) = 0,$$

and similarly for the other three h-containing terms. Hence we obtain

$$\lim_{h\to 0}(\ln X + \ln Z - \ln x - \ln z) = 0.$$

For H_2, we require

$$\lim_{h\to 0}\left(X+Y+Z-\ln X-\ln Y-(x+y+z-\ln x-\ln y)\right)=0.$$

From above, we have $\lim_{h\to 0}(\ln x-\ln X)=0$, and similarly we can show that $\lim_{h\to 0}(\ln y-\ln Y)=0$. Now, from (7.2.26), we see that

$$\begin{aligned}\lim_{h\to 0}(X-x) &= \lim_{h\to 0}\left(\frac{1+h(Aa_1-Bb_1y)}{1-h(A(1-a_1)-B(1-b_1)y)}x-x\right)\\ &= \frac{1+0}{1-0}x-x\\ &= x-x\\ &= 0.\end{aligned}$$

Similarly, we obtain $\lim_{h\to 0}(Y-y)=0$ and $\lim_{h\to 0}(Z-z)=0$, and the result is proven. ■

The implication of this result is that the energy of the discretization should be relatively constant across mesh points, and hence the difference in energy between mesh points should stay bounded near zero. This will be investigated numerically in the following section.

We now turn to the Poisson structure of the discretization, where we have the following result.

Proposition 7.3.4 *The scheme (7.2.26) is a perturbed Poisson integrator for the system (7.1.1).*

Proof:

That the perturbed Casimir function H_1 is conserved was shown in Theorem 7.3.1. To

show that the second requirement of Definition 7.3.2 is satisfied, we must show that

$$\lim_{h\to 0}\left(\left(\frac{\partial\left(X,Y,Z\right)}{\partial\left(x,y,z\right)}\right)\begin{pmatrix}0 & -xy & 0\\ xy & 0 & -yz\\ 0 & yz & 0\end{pmatrix}\left(\frac{\partial\left(X,Y,Z\right)}{\partial\left(x,y,z\right)}\right)^{T}-\begin{pmatrix}0 & -XY & 0\\ XY & 0 & -YZ\\ 0 & YZ & 0\end{pmatrix}\right)=0. \tag{7.3.1}$$

Computing the left-hand side of expression (7.3.1) using *Mathematica*, we obtain

$$\begin{aligned}&\left(\frac{\partial\left(X,Y,Z\right)}{\partial\left(x,y,z\right)}\right)\begin{pmatrix}0 & -xy & 0\\ xy & 0 & -yz\\ 0 & yz & 0\end{pmatrix}\left(\frac{\partial\left(X,Y,Z\right)}{\partial\left(x,y,z\right)}\right)^{T}-\begin{pmatrix}0 & -XY & 0\\ XY & 0 & -YZ\\ 0 & YZ & 0\end{pmatrix}\\ &\quad=\begin{pmatrix}0 & D_{1,2} & D_{1,3}\\ -D_{1,2} & 0 & D_{2,3}\\ -D_{1,3} & -D_{2,3} & 0\end{pmatrix},\end{aligned} \tag{7.3.2}$$

where $D_{1,2}, D_{1,3}$, and $D_{2,3}$ are defined in Appendix A. From these expressions, we can see that

$$\lim_{h\to 0} D_{1,2}=\lim_{h\to 0} D_{1,3}=\lim_{h\to 0} D_{2,3}=0,$$

and the result is proven. ■

What we have shown is that the schemes developed for the numerical integration of the three-dimensional Lotka-Volterra system are dynamically consistent with the continuous model. As such, they should produce qualitatively accurate simulations of the solutions. These simulations are the topic of the next section.

7.4 Numerical Simulations

In this section, we numerically investigate the dynamic consistency of the schemes developed and the three-dimensional Lotka-Volterra model. As before, we restrict our attention to the explicit scheme (7.2.26). We first give several simulations to show that

the periodicity of the model is preserved by the discrete solutions under a variety of initial conditions and step sizes. Simulated solutions are compared to those obtained from the intersection of the two Hamiltonian functions to confirm their accuracy. We also study the conservation of energy by the schemes developed, and compare the results to the explicit Euler method and the Heun method.

To begin, recall that when $AG = BF$, the three-dimensional Lotka-Volterra model is periodic in x, y, z-space. Our discrete scheme was constructed to replicate this, as it satisfies (7.2.1). First, we choose the following set of simulation parameters for scheme (7.2.26):

$$\begin{cases} A = \ldots = G = 1 \\ \\ a_1 = -1, \quad b_1 = \dfrac{1}{2}, \quad c_1 = \dfrac{1}{2}, \quad d_2 = -1, \quad e_1 = \dfrac{1}{2}. \end{cases} \tag{7.4.1}$$

The following figure shows that periodicity is preserved in phase-space for a variety of initial conditions.

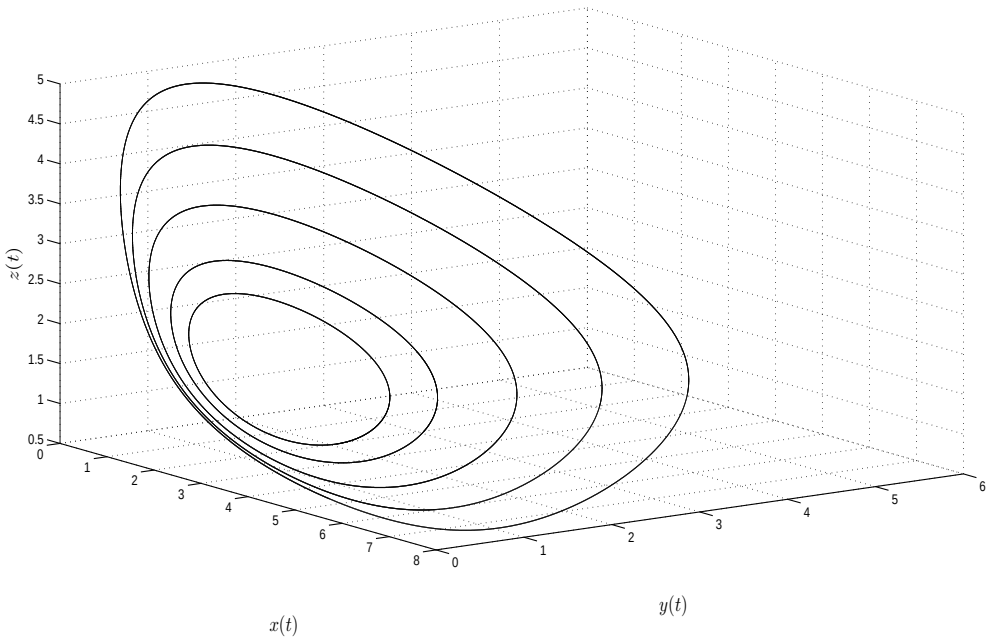

Figure 7.2: Numerical integrations preserve phase-space periodicity for a variety of initial conditions. $(x_0, y_0, z_0) = (4, y, 1)$, where $y = 1$, 2, 3, 4, 5, and $h = .001$.

In contrast, if we try to simulate, for example, the curve with initial condition $(4, 1, 1)$ using the explicit Euler method, we do not obtain a dynamically consistent discretization as above; as expected the simulations spiral away from the initial point.

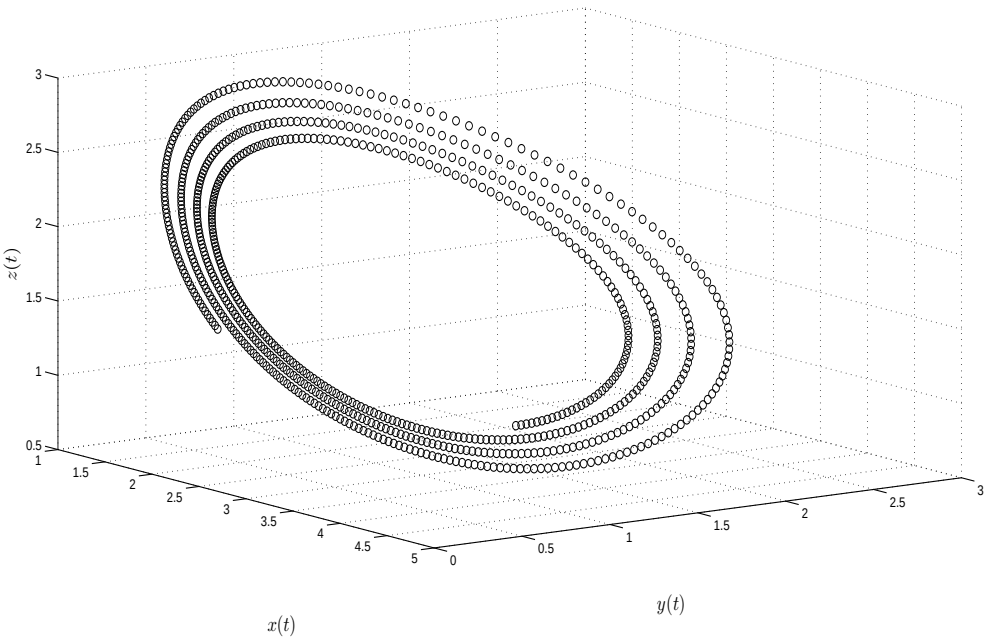

Figure 7.3: The explicit Euler method does not preserve periodicity in phase-space. $(x_0, y_0, z_0) = (4, 1, 1)$ and $h = .001$.

The previous simulation used a relatively small step-size of $h = 0.001$. However, even if the step-size is significantly relaxed, simulations still maintain periodicity.

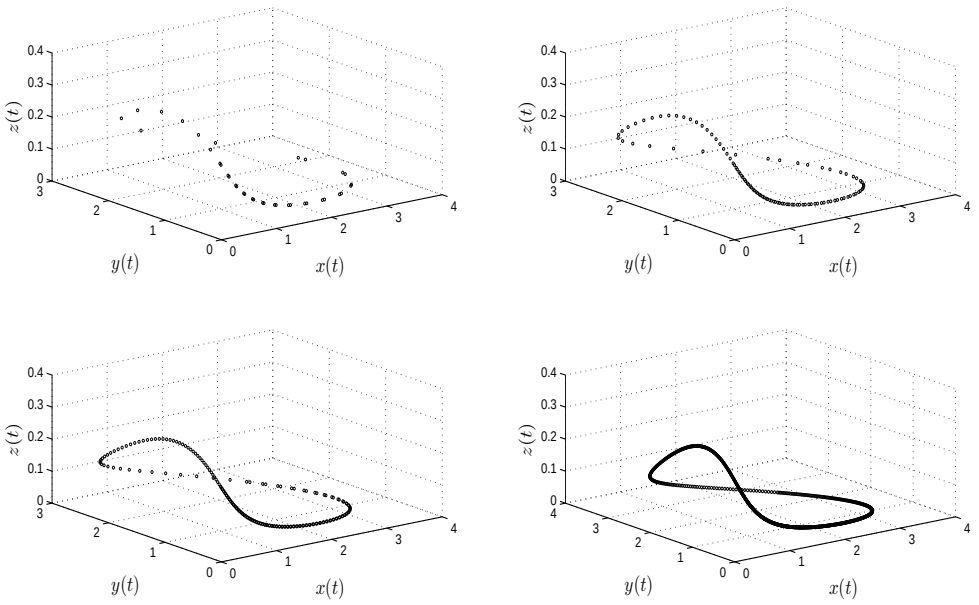

Figure 7.4: Preservation of periodicity under a variety of step-sizes. $(x_0, y_0, z_0) = (0.35, 0.35, 0.20)$ and $h = 0.3$, 0.1, 0.05, 0.01.

We can also demonstrate that the scheme (7.2.26) works in the non-normalized setting as well. Suppose we choose simulation parameters

$$\begin{cases} A = 1, \quad B = 3, \quad C = 0.5, \quad D = 2, \quad E = 3.5, \quad F = 0.75, \quad G = 2.25 \\ \\ a_1 = 1, \quad b_1 = 1, \quad c_1 = -0.5, \quad d_2 = -1.5, \quad e_1 = 0.5. \end{cases} \tag{7.4.2}$$

Again, we can see that periodicity is preserved by the NSFD scheme while the explicit Euler method produces spiraling.

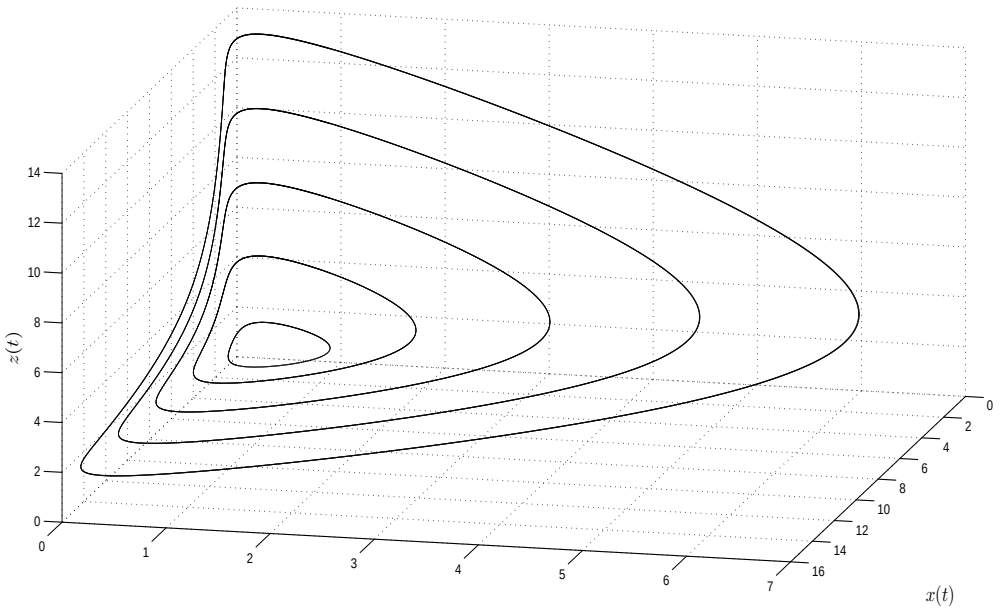

Figure 7.5: Numerical integrations preserve phase-space periodicity for a variety of initial conditions. $(x_0, y_0, z_0) = (1, 1, z)$, where $z = 1$, 4, 7, 10, 13, and $h = .001$.

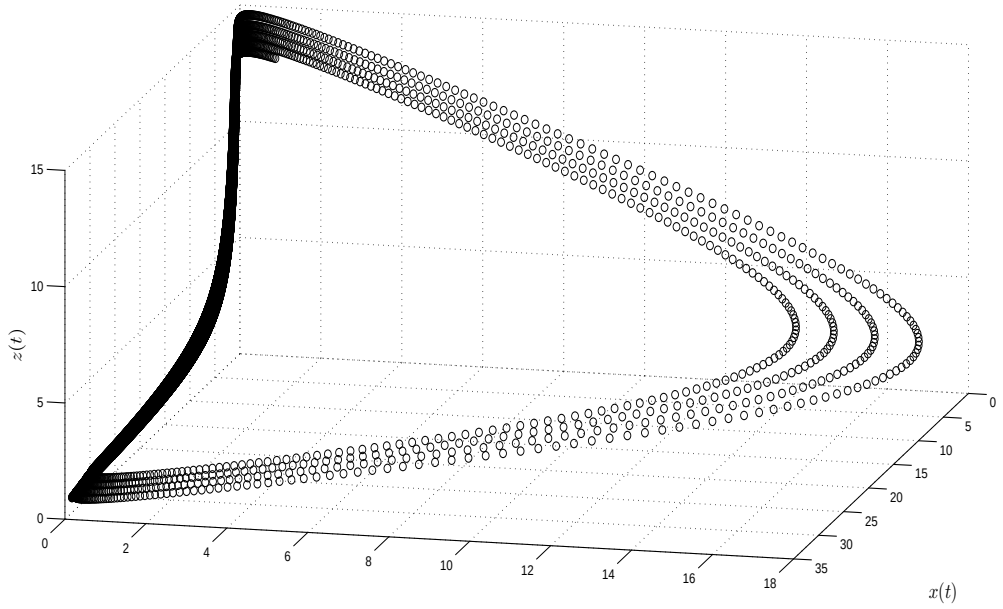

Figure 7.6: The explicit Euler method does not preserve periodicity in phase-space. $(x_0, y_0, z_0) = (1, 1, 13)$ and $h = .001$.

As in the previous example, simulations are still closed in phase-space even if the step-size is significantly relaxed.

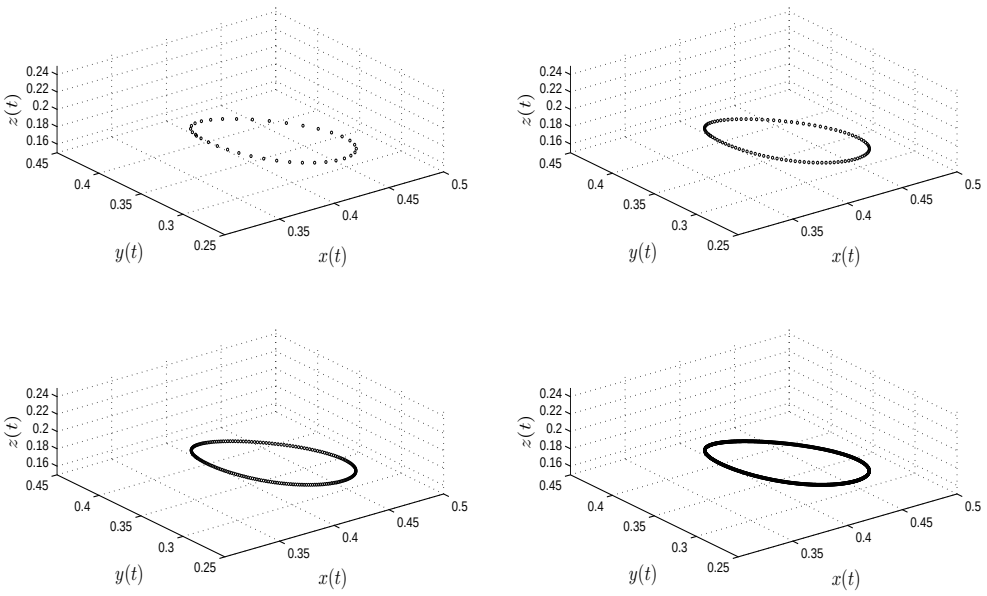

Figure 7.7: Preservation of periodicity under a variety of step-sizes. $(x_0, y_0, z_0) = (0.35, 0.35, 0.20)$ and $h = 0.1$, 0.05, 0.01, 0.001.

It is worth mentioning that, in addition to showing that the simulations preserve periodicity, we can show that they are in fact accurate representations of the true solution. Recall from §7.1 that solutions are confined to the intersection of the surfaces defined by the two Hamiltonian functions. Hence, for any set of initial conditions (x_0, y_0, z_0), we can compare the simulation to the curve obtained by intersecting the two surfaces

$$\begin{cases} C_1 = \ln x_0 + \ln z_0 = H_1(x, y, z) \\ \\ C_2 = x_0 + y_0 + z_0 - \ln x_0 - \ln z_0 = H_2(x, y, z). \end{cases}$$

We do this for $(x_0, y_0, z_0) = (0.5, 0.5, 0.6)$ and $h = 0.001$, so that we have the two

surfaces defined by

$$\begin{cases} H_1(x, y, z) = \ln 0.5 + \ln 0.6 \approx -1.204 \\ \\ H_2(x, y, z) = 1.6 - \ln 0.5 - \ln 0.6 \approx 2.986. \end{cases}$$

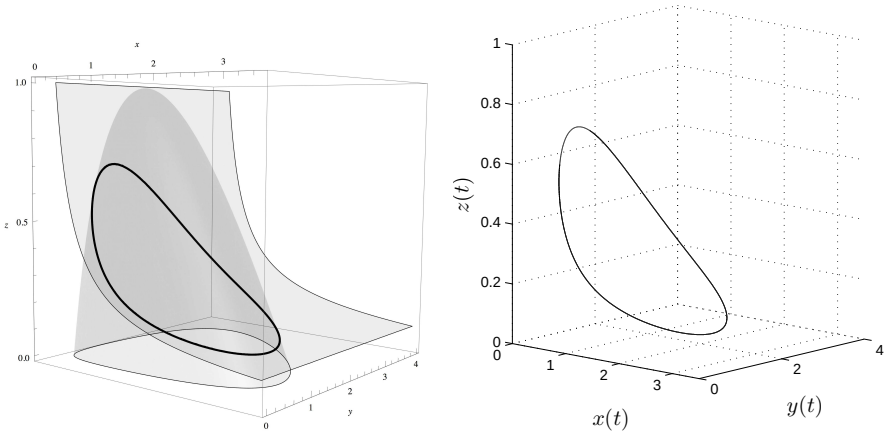

(a) Intersection of Hamiltonians (b) Numerical integration

Figure 7.8: Comparison of solutions obtained through the intersection of Hamiltonian functions and numerical integration.

It is clear that the solution produced through numerical integration accurately models the true solution.

Next, we examine the preservation of the two Hamiltonian functions $H_1(x(t), y(t), z(t))$ and $H_2(x(t), y(t), z(t))$. Recall that these functions should remain constant along solutions of the system. Hence, for all $t \geq 0$, $H_i(t) - H_i(0) = 0$ $(i = 1, 2)$. This energy difference can be plotted as a function of time to investigate the preservation of the first integrals by the numerical methods. Note that in Proposition 7.3.3, we showed that the NSFD schemes developed preserve the two perturbed first integrals, so that energy difference should stay bounded near zero. We compare the results to those obtained by the explicit Euler method.

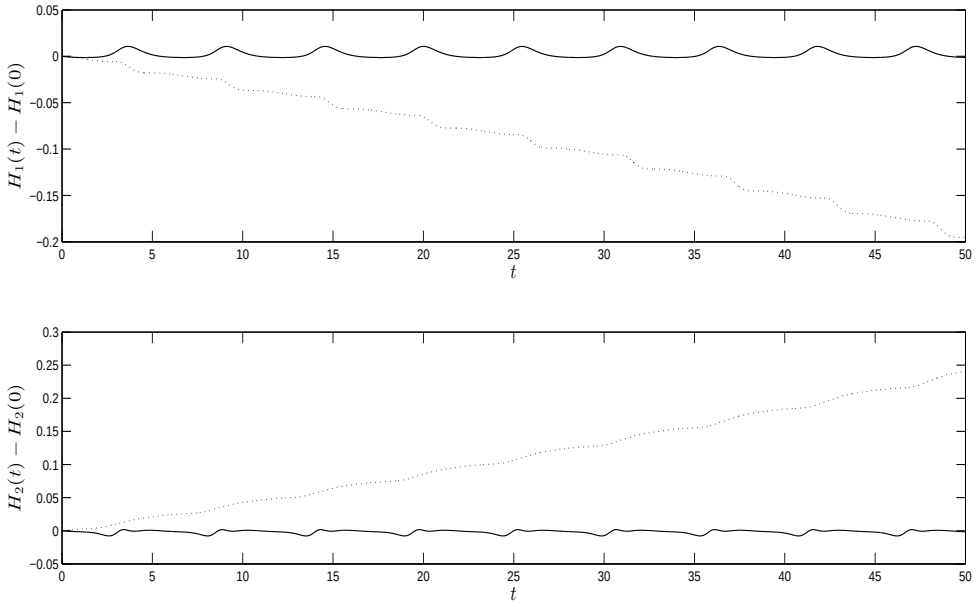

Figure 7.9: Energy difference as a function of time for the NSFD method (solid line) and explicit Euler method (dotted line). $(x_0, y_0, z_0) = (0.5, 0.5, 0.5)$ and $h = 0.005$.

As expected, the NSFD method nearly preserves the two first integrals, as the energy difference is bounded near zero. In contrast, the explicit Euler method does not preserve the first integrals. Instead, the energy $H_1(t)$ decreases while the energy $H_2(t)$ increases.

We can repeat this analysis using a more accurate second-order integrator such as the Heun method. Applying (5.2.11) to the system (7.1.1), we obtain the scheme for

the Heun method:

$$\begin{cases} X = x + hx + (h^2x)(1/2) - hxy - (1/2)h^2xy + (1/2)h^3xy - (1/2)h^2x^2y - (1/2)h^3x^2y \\ \qquad + (1/2)h^2xy^2 - (1/2)h^3xy^2 + (1/2)h^3x^2y^2 + (1/2)h^2xyz \\ \qquad\quad + (1/2)h^3xy(i)z - (1/2)h^3xy^2z \\ Y = y - hy + (h^2y)(1/2) + hxy - (1/2)h^2xy - (1/2)h^3xy + (1/2)h^2x^2y + (1/2)h^3x^2y \\ \qquad - (1/2)h^2xy^2 + (1/2)h^3xy^2 - (1/2)h^3x^2y^2 - hyz + (3/2)h^2yz \\ \qquad\quad - (1/2)h^3yz - h^2xyz - (1/2)h^2y^2z + (1/2)h^3y^2z \\ \qquad\qquad + (1/2)h^2yz^2 - (1/2)h^3yz^2 + (1/2)h^3y^2z^2 \\ Z = z - hz + (h^2z)(1/2) + hyz - (3/2)h^2yz + (1/2)h^3yz + (1/2)h^2xyz - (1/2)h^3xyz \\ \qquad + (1/2)h^2y^2z - (1/2)h^3y^2z + (1/2)h^3xy^2z - (1/2)h^2yz^2 \\ \qquad\quad + (1/2)h^3yz^2 - (1/2)h^3y^2z^2. \end{cases} \tag{7.4.3}$$

If we perform the simulation for only a small time interval and plot the energy difference, it appears that the Heun method better preserves the two first integrals. Note the difference in magnitude of the scale of the vertical axis between the two methods.

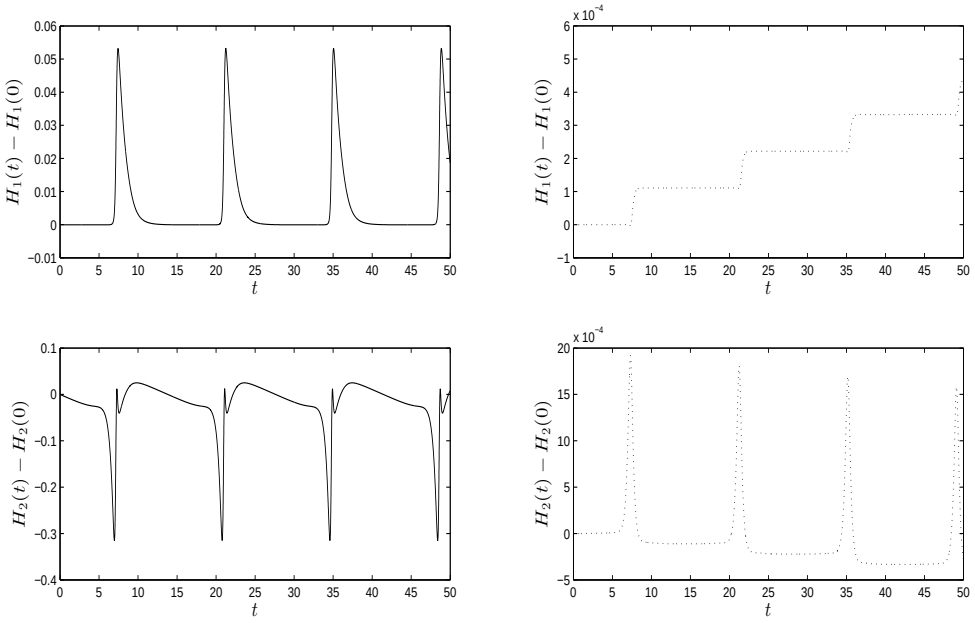

Figure 7.10: Energy difference as a function of time for the NSFD method (solid line) and Heun method (dotted line) over a small time interval. $(x_0, y_0, z_0) = (0.01, 0.01, 0.01)$ and $h = 0.005$.

The difference in magnitude of the energy difference is more clearly illustrated when both methods are plotted on the same set of axes.

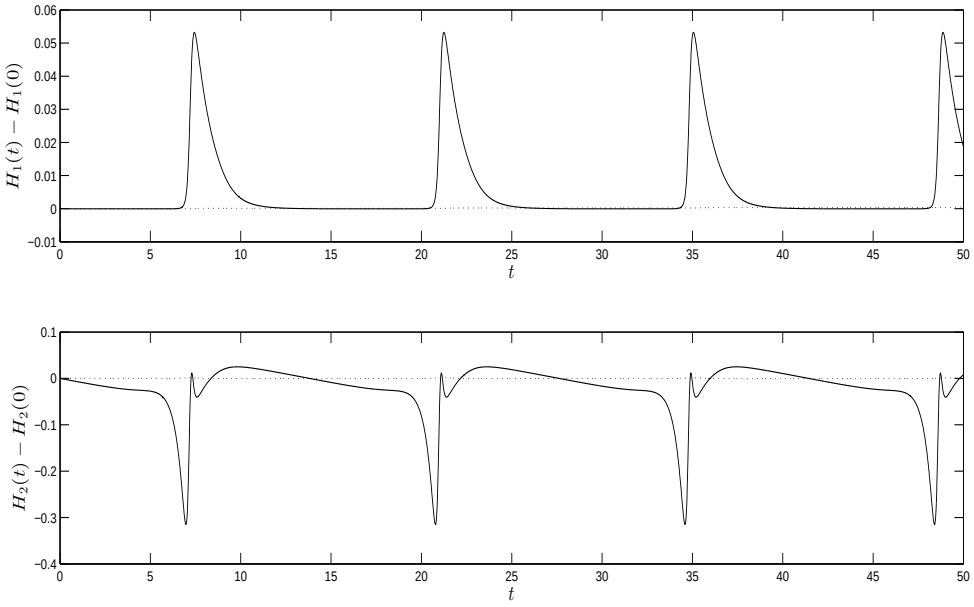

Figure 7.11: Energy difference as a function of time for the NSFD method (solid line) and Heun method (dotted line) over a small time interval. $(x_0, y_0, z_0) = (0.01, 0.01, 0.01)$ and $h = 0.005$.

As a measure of how effectively each numerical method preserves the first integrals, we can compute the metric

$$L = |\max(H_i) - \min(H_i)|\,, \qquad (i = 1, 2). \tag{7.4.4}$$

Clearly, the smaller the magnitude of L, the more effectively that numerical method preserves the Hamiltonian function. For the above small time interval simulations, we have the following values for L:

Hamiltonian Function	NSFD Method	Heun Method
H_1	0.0533	0.00044
H_2	0.3400	0.0023

The above results favour the Heun method. However, we can see from Figure 7.7 that while the energy difference for the volume-preserving method is bounded around zero, the energy difference for Heun method appears to have a trend. If the simulation is performed over a larger time interval, then this is made clear.

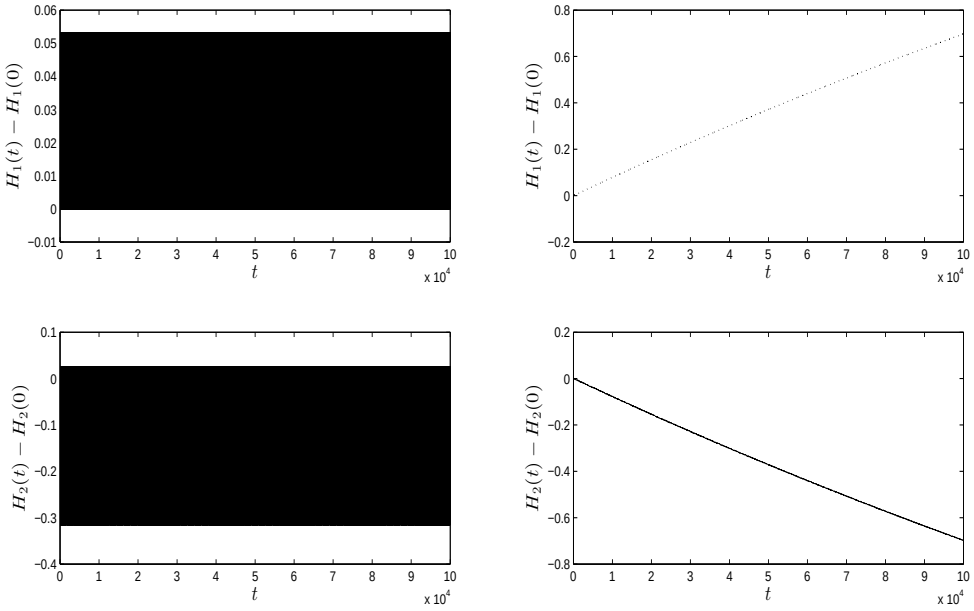

Figure 7.12: Energy difference as a function of time for the NSFD method (solid line, left) and Heun method (dotted line, right) over a large time interval. $(x_0, y_0, z_0) = (0.01, 0.01, 0.01)$ and $h = 0.005$.

Plotting both methods on the same axes clarifies that the NSFD method more effectively conserves the Hamiltonian energy.

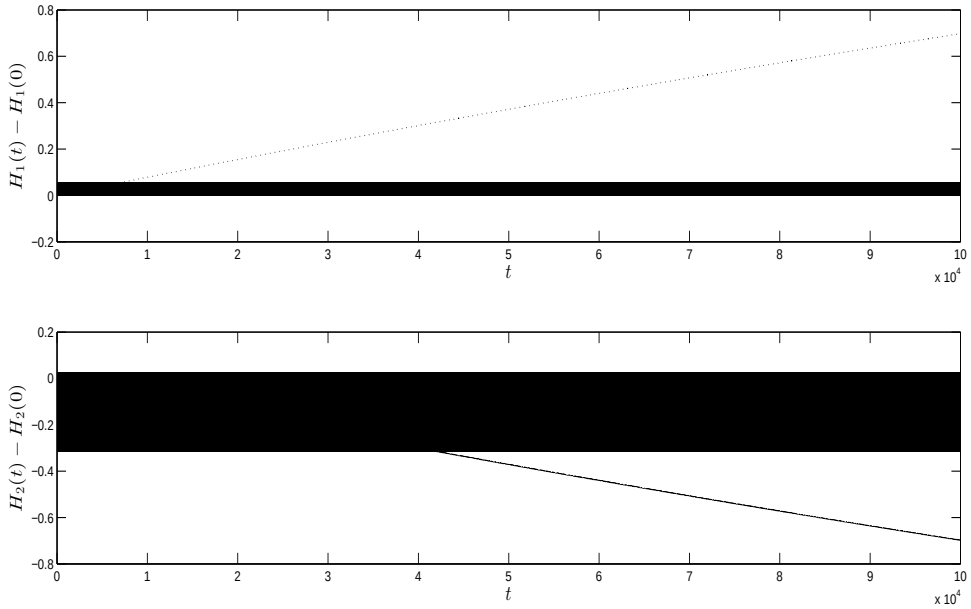

Figure 7.13: Energy difference as a function of time for the NSFD method (solid line) and Heun method (dotted line) over a large time interval. $(x_0, y_0, z_0) = (0.01, 0.01, 0.01)$ and $h = 0.005$.

In this case, we have the following values of L:

Hamiltonian Function	NSFD Method	Heun Method
H_1	0.0533	0.6975
H_2	0.3400	0.7009

The results indicate that for a larger time interval, the volume-preserving method better preserves the Hamiltonian functions.

These simulations highlight the advantage of the geometric numerical integration approach. The volume-preserving schemes developed preserve the periodicity and the perturbed first integrals of the continuous system. Standard integration approaches typically fail to preserve either of these properties. The benefits of incorporating

the underlying geometry of the continuous system are particularly apparent when simulations are required over long-time intervals.

7.5 Concluding Remarks

In Part II of this thesis, we gave a description of the three-species Lotka-Volterra model through the framework of Poisson dynamics. In contrast to the two-species model, the three-dimensional equations possess a bi-Poisson structure with two independent first integrals. Moreover, we showed that this system is integrable, and this imparts a regularity to the behavior of its solutions. In particular, the flow of solutions preserves the weighted volume-form (7.1.20), as through a change of coordinates, the system can be transformed into one which is volume-preserving. We then gave a class of numerical integration schemes and derived a set of conditions so that these schemes preserve the form (7.1.20), and hence the periodicity of the model. It was demonstrated that these schemes also preserve the perturbed first integrals and Poisson bracket.

This work highlights the issue with the naive application of a general numerical method to a particular system, as these methods can often produce incorrect qualitative behavior. For instance, when applied to the Lotka-Volterra model, the explicit Euler method produces simulations which spiral away from the initial conditions. To avoid errors such as this, it is crucial to incorporate the underlying structure of the continuous model into a discretization scheme. In this thesis, we gave a general class

of integrators which effectively and accurately model the correct behavior of the three-species Lotka-Volterra model. With these schemes, simulations can be performed for long time intervals without loss of accuracy and the with energy remaining nearly constant. In summary, we have demonstrated a number of new properties of the three-species model, and utilized this information to produce simulations which outperform traditional methods.

Chapter 8

Conclusion

The focus of this thesis was the two-species and three-species Lotka-Volterra predator-prey models. For a particular case of the two-species model, we gave a new derivation of an analytic formula for the solutions and determined expressions for some of the models parameters. Ultimately, the significance of this work is a further understanding of the mathematics underlying the Lotka-Volterra system, as well as its connection to the Lambert W function.

In the case of the three-species model, we described the geometric properties which must be preserved by a numerical integration method in order to produce an accurate simulation of solutions. We then proposed a class of integration schemes and demonstrated their dynamical consistency with the continuous model, as well as illustrating their excellent performance as compared to standard methods. In addition to producing superior simulations, another benefit of geometric numerical integrators is that they often require less computational effort than standard methods [8]. This is likely because they automatically preserve the structure of the continuous system, whereas

a standard method must be set with a very low error tolerance to achieve a similarly accurate simulation, thereby increasing computational cost. In summary, these integrators are typically more accurate and less expensive, and are thus extremely useful, especially for long time-interval simulations.

The main limitation of the work of Part I is of course the hypothesis that $a = c$. Ideally, a closed parametric solution to the general system (2.1.1) could be obtained. However, the method used in this thesis will not work in this case, as the equations no longer possess the same symmetry. It appears unlikely that the problem could be approached by some generalization of the method of Part I; likely, new techniques are required.

In Part II, we studied the three-species predator-prey system (6.3.1). However, there are other ways to generalize the two-species model to three dimensions. For instance, one could include an interaction between species x and z, in which species x is consumed by species z. In this case, the model would be

$$\begin{cases} \dfrac{dx}{dt} = Ax - Bxy - Cxz \\ \dfrac{dy}{dt} = -Dy + Exy - Fyz \\ \dfrac{dz}{dt} = -Gz + Hyz + Ixz. \end{cases}$$

Likely, this model would possess entirely different dynamics than (6.3.1), and new approaches would be required for the construction of suitable integrators. Ultimately, the final goal would be a general theory of geometric numerical integration of n-species Lotka-Volterra models.

As a final note, we discuss a technical detail somewhat assumed in this thesis. When studying the two-species model, we stated that if a numerical method preserves the differential form $\frac{1}{xy}dx \wedge dy$, then the numerical solutions will not spiral. This is not a trivial implication. For the two-species model, this is guaranteed by the well-known Kolmogorov-Arnold-Moser Theorem [38], or simply the KAM-Theorem. In fact, this theorem applies to the trajectories of any integrable Hamiltonian system. However, Hamiltonian systems are even-dimensional, while the three-species Lotka-Volterra system is not. Hence, it remains to develop a theory which will guarantee that if an integrator preserves the form (7.1.20), then the numerical solutions will be periodic in phase space. Several results of KAM type have been developed [25] which do apply to odd-dimensional systems. However, work is required to clarify whether or not these results can be applied to the model considered in this thesis.

References

[1] M. A. Abdelkader, Exact solutions of Lotka-Volterra equations, *Math. Biosci.* **20** (1974) 293–297.

[2] M. Abramowitz and I. A. Stegun, *Handbook of Mathematical Functions with Formulas, Graphs, and Mathematical Tables* (Dover, 1964).

[3] V. I. Arnold, *Mathematical Methods of Classical Mechanics* (Springer, 1997).

[4] V. I. Arnold, *Ordinary Differential Equations* (The MIT Press, 1973).

[5] M. Arrigoni and A. Steiner, Die losung gewisser rauber-beute-systeme, *Studia Biophysica* **123** (1988) 125–134.

[6] S. K. Bhowmik, Nonstandard numerical integrations of a Lotka-Volterra system, *Int. J. Open Problems Compt. Math.* **2** (2009) 332-341.

[7] R. L. Bishop and S. I. Goldberg, *Tensor Analysis on Manifolds* (Dover, 1980).

[8] S. Blanes and F. Casas, *A Concise Introduction to Geometric Numerical Integration* (CRC Press, 2016).

[9] H. Boudjellaba and T. Sari, Dynamic transcritical bifurcations in a class of slow-fast predator-prey models, *J. Differential Equations* **246** (2009) 2205–2225.

[10] M. Calvo and J. M. Sanz-Serna, *Numerical Hamiltonian Problems* (Chapman and Hall, 1994).

[11] E. Chauvet, J. E. Paullet, J. P. Previte and Z. Walls, A Lotka-Volterra three-species food chain, *Math. Mag.* **75** (2002) 243-255.

[12] T. Y. Chow, What is a closed-form number?, *Am. Math. Monthly* **106** (1999) 440-448.

[13] C. W. Clark, *Mathematical Bioeconomics: The Optimal Management of Renewable Resources* (Wiley-Interscience, 1976).

[14] R. M. Corless, G. H. Gonnet, D. E. G. Hare, D. J. Jeffrey and D. E. Knuth, On the Lambert W function, *Adv. Comput. Math.* **5** (1996) 329–359.

[15] R. Devoglaere, Methods of integration which preserve the contact transformation property of the Hamilton equations, *Unpublished* (1956).

[16] J. R. Dormand and P. J. Prince, A family of embedded Runge-Kutta formulae, *J. Comput. Appl. Math.* **6** (1980) 19–26.

[17] H. I. Freedman, *Deterministic Mathematical Models in Population Ecology* (Marcel Dekker, 1980).

[18] M. J. Gander and R. Meyer-Spasche, An introduction to numerical integrators preserving physical properties, In R. E. Mickens (Ed.) *Applications of Nonstandard Finite Difference Schemes* (pp. 181-243) (World Scientific, 2000).

[19] G. F. Gause, *The Struggle for Existence* (Williams and Wilkins, 1934).

[20] E. Hairer, C. Lubich and G. Wanner, *Geometric Numerical Integration: Structure-Preserving Algorithms for Ordinary Differential Equations* (Springer-Verlag, 2010).

[21] Y. He, Y. Sun and Z. Shang, Integrable discretisation of the Lotka-Volterra system, *J. Comput. Math.* **33** (2015) 468-494.

[22] S. B. Hsu, A remark on the period of the periodic solution in the Lotka-Volterra system, *J. Math. Anal. Appl.* **95** (1983) 428–436.

[23] W. Kahan, Unconventional numerical methods for trajectory calculations, *Lecture Notes* (CS Division, Department of EECS, University of California at Berkeley, 1993).

[24] C. Laurent-Gengoux, E. Miranda and P. Vanhaecke, Action-angle coordinates for integrable systems on Poisson manifolds, *Int. Math. Res. Not. IMRN* **8** (2011) 1839-1869.

[25] Y. Li and Y. Yi, Persistence of invariant tori in generalized Hamiltonian systems, *Ergodic Theory Dynam. Systems* **22** (2002) 1233-1261.

[26] A. J. Lotka, Analytical note on certain rhythmic relations in organic systems, *Proc. Natl. Acad. Sci. USA* **6** (1920) 410–415.

[27] A. J. Lotka, Undamped oscillations derived from the law of mass action, *J. Am. Chem. Soc.* **42** (1920) 1595–1599.

[28] R. E. Mickens, A nonstandard finite-difference scheme for the Lotka-Volterra system, *Appl. Numer. Math.* **45** (2003) 309-314.

[29] R. E. Mickens (Ed.), *Advances in the Applications of Nonstandard Finite Difference Schemes* (World Scientific, 2005).

[30] A. S. Mounim and B. de Dormale, A note on Mickens's finite-difference scheme for the Lotka-Volterra system, *Appl. Numer. Math.* **51** (2004) 341-344.

[31] J. D. Murray, *Mathematical Biology I: An Introduction* (Springer, 2002).

[32] Y. Nambu, Generalized Hamiltonian dynamics, *Phys. Rev. D*, **7** (1973) 2405-2412.

[33] M. Plank, *Hamiltonische Systeme und Lotka-Volterra Gleichungen* (Diplomarbeit, University of Vienna, 1993).

[34] M. Plank, Bi-hamiltonian systems and Lotka-Volterra equations: A three-dimensional classification, *Nonlinearity* **9** (1996) 887-896.

[35] L.-I. W. Roeger, Nonstandard finite-difference schemes for the Lotka-Volterra systems: Generalization of Mickens's method, J. Difference Equ. Appl. **12** (2006) 937-948.

[36] F. Rothe, The periods of the Volterra-Lotka system, *J. Reine Angew. Math.* **355** (1985) 129–138.

[37] J. M. Sanz-Serna, An unconventional symplectic integrator of W. Kahan, *Appl. Numer. Math.* **16** (1994) 245-250.

[38] J. M. Sanz-Serna, Two topics on nonlinear stability, In *Advances in Numerical Analysis, Vol. 1* (pp. 147-174) (Oxford University Press, 1991).

[39] S. D. Shih, The period of a Lotka-Volterra system, *Taiwanese J. Math.* **1** (1997) 451–470.

[40] P. Turchin, *Complex Population Dynamics: A Theoretical/Empirical Synthesis* (Princeton University Press, 2003).

[41] V. Volterra, Variazioni e fluttuazioni del numero dindividui in specei animali conviventi, *Mem. R. Acad. Naz. dei Lincei* **2** (1926) 31–113.

[42] J. Waldvogel, The period in the Volterra-Lotka predator-prey model, *SIAM J. Numer. Anal.* **20** (1983) 1264–1272.

[43] J. Waldvogel, The period in the Volterra-Lotka system is monotonic, *J. Math. Anal. Appl.* **114** (1986) 178–184.

Appendix A

Expressions for $D_{1,2}$, $D_{1,3}$, and $D_{2,3}$

$$D_{1,2} =$$

$$\left(h^2\,x\,y^2\,z\,(a\,h-b\,h+1)\left(h^2\,(c\,(a-b\,y+y-1)+d\,x\,(b\,y-a)+e\,(a\,(x-1)+y\,(b\,(-x)+b-1)+1))-\right.\right.$$
$$\left.h\,(a-b\,y-c+d\,x-e\,x+e+y-1)-1)\right)\Big/\left((h\,(a-b\,y+y-1)+1)\right.$$
$$\left(a\,h\,(h\,(c-d\,x+e\,z+x-z-1)-1)-c\,h\,(b\,h\,y-h\,y+h-1)+b\,d\,h^2\,x\,y-b\,e\,h^2\,y\,z-b\,h^2\,x\,y+b\,h^2\,y\,z+\right.$$
$$\left.\left.b\,h^2\,y+b\,h\,y-d\,h\,x+e\,h^2\,y\,z-e\,h^2\,z+e\,h\,z-h^2\,y\,z-h^2\,y+h^2\,z+h^2+h\,x-h\,y-h\,z-1\right)^2\right)$$

$$D_{1,3} =$$

$$\frac{1}{((a-b\,y+y-1)\,h+1)^2}h\,x\,y\left(1\Big/\left(a\,h-\frac{b\,y\left(-c\,h+\frac{(a\,h-b\,y\,h+1)\,d\,x\,h}{(a-b\,y+y-1)\,h+1}-e\,z\,h+1\right)h}{-c\,h+\frac{(d-1)\,(a\,h-b\,y\,h+1)\,x\,h}{(a-b\,y+y-1)\,h+1}-(e-1)\,z\,h+h+1}+1\right)^2(a\,h-b\,h+1)\,z\right.$$

$$\left(\left(-\frac{(1-b)\,e\,y\,z\,h^2}{-c\,h+\frac{(d-1)\,(a\,h-b\,y\,h+1)\,x\,h}{(a-b\,y+y-1)\,h+1}-(e-1)\,z\,h+h+1}-\frac{(1-b)\,(1-e)\,y\,z\left(-c\,h+\frac{(a\,h-b\,y\,h+1)\,d\,x\,h}{(a-b\,y+y-1)\,h+1}-e\,z\,h+1\right)h^2}{\left(-c\,h+\frac{(d-1)\,(a\,h-b\,y\,h+1)\,x\,h}{(a-b\,y+y-1)\,h+1}-(e-1)\,z\,h+h+1\right)^2}+\right.\right.$$

$$\left.\left.(a-1)\,h+\frac{\left(-c\,h+\frac{(a\,h-b\,y\,h+1)\,d\,x\,h}{(a-b\,y+y-1)\,h+1}-e\,z\,h+1\right)(1-b)\,y\,h}{-c\,h+\frac{(d-1)\,(a\,h-b\,y\,h+1)\,x\,h}{(a-b\,y+y-1)\,h+1}-(e-1)\,z\,h+h+1}+1\right)\right.$$

$$\left(a\,h-\frac{b\,y\left(-c\,h+\frac{(a\,h-b\,y\,h+1)\,d\,x\,h}{(a-b\,y+y-1)\,h+1}-e\,z\,h+1\right)h}{-c\,h+\frac{(d-1)\,(a\,h-b\,y\,h+1)\,x\,h}{(a-b\,y+y-1)\,h+1}-(e-1)\,z\,h+h+1}+1\right)+$$

$$\left(b\,h^2\,y\left(((a-b\,y+y-1)\,c+((x-1)\,a+(-x\,b+b-1)\,y+1)\,e+(b\,y-a)\,d\,x)\,h^2-(a-c+e+d\,x-\right.\right.$$

$$\left.\left.e\,x-b\,y+y-1)\,h-1\right)\left((a-1)\,h\,z+\frac{\left(-c\,h+\frac{(a\,h-b\,y\,h+1)\,d\,x\,h}{(a-b\,y+y-1)\,h+1}-e\,z\,h+1\right)(1-b)\,h\,y\,z}{-c\,h+\frac{(d-1)\,(a\,h-b\,y\,h+1)\,x\,h}{(a-b\,y+y-1)\,h+1}-(e-1)\,z\,h+h+1}+z\right)\right)\Big/$$

$$\left.\left.\left((a-b\,y+y-1)\,h+1\right)\left(-c\,h+\frac{(d-1)\,(a\,h-b\,y\,h+1)\,x\,h}{(a-b\,y+y-1)\,h+1}-(e-1)\,z\,h+h+1\right)^2\right)\right)+$$

$$\left(h^2\,(a\,h-b\,h+1)^2\,x\,y\,(a\,h-b\,y\,h+1)\,((a-b\,y+y-1)\,h+1)\,z\,(-d\,(z+1)\,h+c\,h+e\,z\,h-1)\right)\Big/$$
$$\left(-b^2\,d\,x\,y^2\,h^3+b^2\,e\,y^2\,z\,h^3-b\,e\,y^2\,z\,h^3+b\,e\,y\,z\,h^3+(h\,(c-d\,x+x+e\,z-z-1)-1)\,a^2\,h^2-b^2\,y^2\,h^2+\right.$$
$$b\,y^2\,h^2-b\,x\,y\,h^2+2\,b\,d\,x\,y\,h^2-y\,h^2-e\,z\,h^2+b\,y\,z\,h^2-2\,b\,e\,y\,z\,h^2+e\,y\,z\,h^2-y\,z\,h^2+z\,h^2+$$
$$h^2-a\left((((2\,b-1)\,y+1)\,c+((-2\,d\,x+x+2\,e\,z-z-1)\,b-e\,z+z+1)\,y+e\,z-z-1)\,h^2+\right.$$
$$\left.(-2\,c+2\,(d-1)\,x-2\,b\,y+y-2\,e\,z+2\,z+1)\,h+2\right)h+$$
$$\left(((b-1)\,y+1)\,b\,y\,h^2+(-2\,b\,y+y-1)\,h+1\right)c\,h-d\,x\,h+x\,h+2\,b\,y\,h-y\,h+e\,z\,h-z\,h-1\Big)^2-$$

$$\left(\left(a\,h-b\,y\,h+1\right)((a-b\,y+y-1)\,h+1)\left((1-b)\,z\left(a\,h-\frac{b\,y\left(-c\,h+\frac{(a\,h-b\,y\,h+1)\,d\,x\,h}{(a-b\,y+y-1)\,h+1}-e\,z\,h+1\right)h}{-c\,h+\frac{(d-1)\,(a\,h-b\,y\,h+1)\,x\,h}{(a-b\,y+y-1)\,h+1}-(e-1)\,z\,h+h+1}+1\right)\right.\right.$$

$$\left(\left((d-1)\left(\left(-(a-b\,y+y-1)\,c+a\,d\,x-b\,d\,y\,x-a\,e\,z+e\,z+b\,e\,y\,z-e\,y\,z\right)h^2+\right.\right.\right.$$

$$\left.\left.\left.(a-c+d\,x-b\,y+y-e\,z-1)\,h+1\right)(a\,h-b\,h+1)\,x\,y\,h^2\right)\Big/((a-b\,y+y-1)\,h+1)^3+\right.$$

$$\left(-\frac{b\,d\,x\,y\,h^2}{(a-b\,y+y-1)\,h+1}-\frac{(b-1)\,d\,x\,y\,(-a\,h+b\,y\,h-1)\,h^2}{((a-b\,y+y-1)\,h+1)^2}-c\,h+\frac{(a\,h-b\,y\,h+1)\,d\,x\,h}{(a-b\,y+y-1)\,h+1}-\right.$$
$$\left.e\,z\,h+1\right)\left(-c\,h+\frac{(d-1)\,(a\,h-b\,y\,h+1)\,x\,h}{(a-b\,y+y-1)\,h+1}-(e-1)\,z\,h+h+1\right)\Bigg)-$$
$$b\left((a-1)\,h\,z+\frac{\left(-c\,h+\frac{(a\,h-b\,y\,h+1)\,d\,x\,h}{(a-b\,y+y-1)\,h+1}-e\,z\,h+1\right)(1-b)\,h\,y\,z}{-c\,h+\frac{(d-1)\,(a\,h-b\,y\,h+1)\,x\,h}{(a-b\,y+y-1)\,h+1}-(e-1)\,z\,h+h+1}+z\right)$$
$$\left(-\Big((d-1)\,(a\,h-b\,h+1)\,x\,y\,\big(\big(-(a-b\,y+y-1)\,c+a\,d\,x-b\,d\,y\,x-a\,e\,z+e\,z+b\,e\,y\,z-e\,y\,z\big)\,h^2+\right.$$
$$\left.(a-c+d\,x-b\,y+y-e\,z-1)\,h+1\big)\,h^2\Big)\Big/((a-b\,y+y-1)\,h+1)^3-$$
$$\left(-c\,h+\frac{(d-1)\,(a\,h-b\,y\,h+1)\,x\,h}{(a-b\,y+y-1)\,h+1}-(e-1)\,z\,h+h+1\right)\left(-\frac{b\,d\,x\,y\,h^2}{(a-b\,y+y-1)\,h+1}-\right.$$
$$\left.\left.\left.\frac{(b-1)\,d\,x\,y\,(-a\,h+b\,y\,h-1)\,h^2}{((a-b\,y+y-1)\,h+1)^2}-c\,h+\frac{(a\,h-b\,y\,h+1)\,d\,x\,h}{(a-b\,y+y-1)\,h+1}-e\,z\,h+1\right)\right)\right)\Bigg/$$
$$\left(\left(-c\,h+\frac{(d-1)\,(a\,h-b\,y\,h+1)\,x\,h}{(a-b\,y+y-1)\,h+1}-(e-1)\,z\,h+h+1\right)^2\right.$$
$$\left.\left(a\,h-\frac{b\,y\left(-c\,h+\frac{(a\,h-b\,y\,h+1)\,d\,x\,h}{(a-b\,y+y-1)\,h+1}-e\,z\,h+1\right)h}{-c\,h+\frac{(d-1)\,(a\,h-b\,y\,h+1)\,x\,h}{(a-b\,y+y-1)\,h+1}-(e-1)\,z\,h+h+1}+1\right)^2\right)\Bigg)$$

$\mathbf{D_{2,3}}$ =

$$\Big(h^2\,(a\,h-b\,h+1)\,x\,y^2\,z\,(-d\,(z+1)\,h+c\,h+e\,z\,h-1)$$
$$\Big(-\big(c\,((b-1)\,y+1)^2+(c-d\,x+x+e\,z-z-1)\,a^2-b^2\,d\,x\,y^2+b\,d\,x\,y^2-(2\,((b-1)\,y+1)\,c+$$
$$((-2\,b\,y+y-1)\,d+b\,y+1)\,x-b\,y-b\,z\,y-2\,e\,z\,y+y+2\,e\,z+2\,b\,e\,y\,z+y\,z-2\,z-2)\,a-b\,y+$$
$$b\,x\,y-b\,d\,x\,y+y+b^2\,e\,y^2\,z-2\,b\,e\,y^2\,z+e\,y^2\,z+e\,z-b\,y\,z+2\,b\,e\,y\,z-2\,e\,y\,z+y\,z-z-1\big)\,h^3+$$
$$\big(a^2-2\,(c-d\,x+x+b\,y-y+e\,z-z)\,a+b^2\,y^2-2\,b\,y^2+y^2+2\,((b-1)\,y+1)\,c-d\,x+x+$$
$$b\,y+b\,x\,y-2\,b\,d\,x\,y+d\,x\,y-y+2\,e\,z-b\,y\,z+2\,b\,e\,y\,z-2\,e\,y\,z+y\,z-2\,z-1\big)$$
$$h^2+(2\,a-c+d\,x-x-2\,b\,y+2\,y-e\,z+z-1)\,h+1\big)\Big)\Big/$$
$$\Big(\big(b\,y\,h^2-b\,x\,y\,h^2+b\,d\,x\,y\,h^2-y\,h^2-e\,z\,h^2+b\,y\,z\,h^2-b\,e\,y\,z\,h^2+e\,y\,z\,h^2-y\,z\,h^2+z\,h^2+h^2-$$
$$c\,(b\,y\,h-y\,h+h-1)\,h+(h\,(c-d\,x+x+e\,z-z-1)-1)\,a\,h-d\,x\,h+x\,h+b\,y\,h-y\,h+e\,z\,h-z\,h-1\big)^2$$
$$\big(-b^2\,d\,x\,y^2\,h^3+b^2\,e\,y^2\,z\,h^3-b\,e\,y^2\,z\,h^3+b\,e\,y\,z\,h^3+(h\,(c-d\,x+x+e\,z-z-1)-1)\,a^2\,h^2-b^2\,y^2\,h^2+$$
$$b\,y^2\,h^2-b\,x\,y\,h^2+2\,b\,d\,x\,y\,h^2-y\,h^2-e\,z\,h^2+b\,y\,z\,h^2-2\,b\,e\,y\,z\,h^2+e\,y\,z\,h^2-y\,z\,h^2+z\,h^2+$$
$$h^2-a\,\big((((2\,b-1)\,y+1)\,c+((-2\,d\,x+x+2\,e\,z-z-1)\,b-e\,z+z+1)\,y+e\,z-z-1)\,h^2+$$
$$(-2\,c+2\,(d-1)\,x-2\,b\,y+y-2\,e\,z+2\,z+1)\,h+2\big)\,h+$$
$$\big(((b-1)\,y+1)\,b\,y\,h^2+(-2\,b\,y+y-1)\,h+1\big)\,c\,h-d\,x\,h+x\,h+2\,b\,y\,h-y\,h+e\,z\,h-z\,h-1\big)\Big)$$